Student Theses and Dissertations

2018

Neural Circuit Mechanisms Underlying Behavioral Evolution in Drosophila

Laura Fairbanks Seeholzer

NEURAL CIRCUIT MECHANISMS UNDERLYING BEHAVIORAL EVOLUTION IN *DROSOPHILA*

A Thesis Presented to the Faculty of

The Rockefeller University

in Partial Fulfillment of the Requirements for

the degree of Doctor of Philosophy

by

Laura Fairbanks Seeholzer

June 2018

NEURAL CIRCUIT MECHANISMS UNDERLYING

BEHAVIORAL EVOLUTION IN *DROSOPHILA*

Laura Fairbanks Seeholzer, Ph.D.

The Rockefeller University 2018

Courtship rituals serve to reinforce reproductive barriers between closely related species. Several species in the *Drosophila melanogaster* subgroup exhibit pre-mating isolation due, in part, to the fact that *D. melanogaster* females produce 7,11-heptacosadiene (7,11-HD), a pheromone that promotes courtship in *D. melanogaster* males but suppresses it in *D. simulans*, *D. yakuba,* and *D. erecta* males. Here we compare pheromone-processing pathways across species to define how males endow 7,11-HD with the opposite behavioral valence to underlie species discrimination.

We first show that *D. melanogaster* and *D. simulans* males detect 7,11-HD using the homologous peripheral sensory neurons, but this signal is differentially propagated to the P1 neurons that control courtship behavior. A change in the balance of excitation and inhibition onto courtship-promoting neurons transforms an excitatory pheromonal cue in *D. melanogaster* into an inhibitory one in *D. simulans*. Our results reveal how species-specific pheromone responses can emerge from conservation of peripheral detection mechanisms and diversification of central circuitry and suggest how evolution can exploit flexible circuit nodes to generate behavioral variation.

To investigate if changes in the balance of excitation and inhibition at this node evolved repeatedly, we began characterizing the pheromone processing pathways in *D. yakuba* and *D. erecta*, two species we believe derived their aversion to 7,11-HD independently from *D.*

simulans. This comparison provides a rare opportunity to explore the neural basis for parallel behavioral evolution.

Finally, we observed differences in the olfactory and gustatory pathways *D. melanogaster* and *D. simulans* males use for sex discrimination. In males of both species, the male-specific volatile pheromone, cVA, activates a conserved sensory pathways and suppresses male courtship. However, 7-T, the major cuticular pheromone produced by all males in the *D. melanogaster* subgroup and by *D. simulans* females, plays a differential role in regulating male courtship across species – 7-T suppresses courtship in *D. melanogaster* males, but neither promotes nor inhibits courtship in *D. simulans* males. A difference in either detection of 7-T by peripheral sensory neurons or propagation of this signal to higher brain regions results in this pheromone activating courtship-suppressing mAL neurons in *D. melanogaster* males, but not *D. simulans* males.

Together, these studies represent the first systematic comparison of neural circuits across *Drosophila* species and mark a new advance in the study of behavioral evolution by revealing how changes in central circuitry can alter discrete behaviors.

To my family

Thank you for almost three decades of unconditional love (and counting).

If not for your influence and support, I would not be writing these sentences today.

Acknowledgments

As I prepare to defend my PhD I feel humbled reflecting on all the large and small ways my family and friends have supported me over the last six years, this process would not have been feasible without them.

First and foremost I thank Vanessa Ruta, my advisor, whose passion for science is unique and infectious. During my PhD, she taught me how to identify interesting questions, stay focused while remaining curious and open to new ideas and, ultimately, execute a project from conception to completion. These are lessons I will carry with me into the future, as I hope to have been molded in her image. I also hope to carry forward her scientific approach, which is a mixture of optimism, perfectionism and rigor. I am forever grateful to have had a Ph.D. advisor who is both brilliant and caring.

I would also like to thank all past and current members of the Ruta Lab - I will always feel fortunate to have overlapped with such smart, talented, passionate scientists. In particular, I would like to thank Max Seppo, an extremely talented technician who conducted many experiments described below, and Josie Clowney, a post-doc who in addition to teaching me molecular biology, was also a friend, bay-mate and inspiration. I was also fortunate to work with several talented undergraduate summer students and graduate rotation student.

I would like to thank my thesis committee members, Leslie Vosshall and Shai Shaham, for their engaged and unwavering support of my PhD and career, the Rockefeller Dean's office for all the behind-the-scenes work that made "the bureaucracy" vanish, and the Stern lab at Janelia and the Vosshall lab at Rockefeller for reagents and advice. A National Science Foundation Graduate Research Fellowship, Kavli Neuroscience Graduate Student Fellowship and the David Rockefeller Program supported my graduate studies.

Table of Contents

List of Figures

1 | Introduction

Animals display an extraordinary diversity of behavior both within and between species. While there is increasing insight into how learning and experience modify neural processing to produce variation in individual behavior, far less is known about how evolution shapes neural circuitry to generate species-specific responses. Cross-species comparative studies have identified genetic loci that explain behavioral diversity, but have only rarely examined the neural substrate upon which genetic variation acts. Therefore, how behavioral adaptations are instantiated within the nervous system remains unclear.

1.1   Principles of Morphological Evolution Applied to Behavioral Evolution

A goal of science is to generate organizing principles through comparisons of meticulously described examples. In no field is this truer than evolutionary biology where its very inception was Darwin's unifying theory of evolution. In the 1970s, the development of new technologies like molecular cloning, PCR and Sanger sequencing ushered in a new age of studying the beautiful molecular details of how bodies are formed. Over the course of decades, two general principles of morphological and developmental evolution came into focus. The first principle was that homologous genes and gene regulatory networks mediate the development of similar structures (i.e. a limb or an eye) across disparate organisms[1–3]. The second principle was that diversification of these morphological structures was primarily due to cis-regulatory changes resulting in gene expression differences[3–7].

Below, in the introduction, I will describe how these principles of morphological evolution can

1

inform our understanding of behavioral evolution. Later, in the discussion, I will describe what I believe could be general principles for the neuronal basis of behavioral evolution. Ultimately, however, systematic circuit comparisons across species are rare and more examples are required to derive general principles. I look forward in the coming decades to see how the mechanisms I uncovered during my Ph.D. relate to findings in other species.

1.1.1 A Conserved Genetic Toolkit

The discovery that genes first described as regulating the *Drosophila* body plan had conserved sequence and function in vertebrates was an immense surprise[8,9]. Subsequently, *Pax6* was discovered to mediate the development of both vertebrate and invertebrate eyes[10]. The recurring observation of functional conservation across long time scales inspired Sean Carroll to propose that a genetic 'tool-kit' in evolutionary developmental biology exists, where conserved genes underlie the development of specific aspects of morphologically dissimilar body types[3]. The presence of conserved molecules and signaling pathways across distant phyla suggested that these elements were derived early in animal evolution with strong functional constraints on their diversification[3].

The idea of a conserved 'tool kit' of genes underlying the development of the body can be conceptually extended to the study of behavioral evolution[11,12]. For instance, the kinase *foraging* (protein kinase G family) impacts foraging behavior in flies, honeybees and nematode worms[13] and the transcription factor *FoxP2* is associated with vocal communication in humans, birds, and mice[14–16]. Identifying conserved molecules that orchestrate similar behaviors in distantly related

species can provide a genetic foothold for studying behavioral diversification, as it has for studying morphological diversification. Conserved genes that coordinately regulate behavior could serve as 'tool kit' genes to facilitate the study of behavioral evolution.

There is strong evidence that *fruitless*, a transcription factor necessary for the development of the neural circuitry controlling male courtship behavior in *Drosophila melanogaster*[17,18], is actually highly conserved as the master regulator of species-specific courtship behaviors across insects[19,20]. One study investigated whether species-specific male courtship behaviors are due to changes in either the protein coding and regulatory regions *fruitless* by introducing the entire *D. ananassae* or *D. persimilis fru* locus into *D. melanogaster fru* mutants[21]. These transgenes rescued courtship deficits in the *fru* mutants and, despite being an allele from another species, restored *D. melanogaster* specific courtship behaviors. Therefore, the function of *fruitless* appears to be conserved across species and, presumably, variable behavior arises from species-specific differences in other genetic loci.

Dopamine and vasopressin/oxytocin could also be considered part of a behavioral genetics 'toolkit'[22]. These neuromodulators are highly conserved and influence similar behaviors in distantly related species[23–25]. In both vertebrates and invertebrates, dopamine is associated with learning and memory while vasopressin/oxytocin is associated with social behaviors[23–25]. As with genes in the developmental 'toolkit', while dopamine and oxytocin are associated with categorically similar behaviors, the neural circuits these neuromodulators are influencing are highly dissimilar across species.

1.1.2 Cis-regulatory Changes Underlie Morphological Evolution

Morphological evolution most frequently occurred through changes in cis-regulatory regions, including promoters and enhancers, which impact the timing or localization of gene expression[2–6]. Across longer evolutionary timescales, protein-coding changes following gene duplication is clearly an important process for the expansion of gene families. On shorter evolutionary timescales, however, changing cis-regulatory elements, and not protein-coding sequence, avoids potential pleiotropic effects while maximizing adaptive potential[5]. The adaptive role of cis-regulatory evolution was uncovered both though unbiased genetic mapping of morphological differences and the study of specific candidate genes.

One illustrative example of how an unbiased mapping approach was used to reveal the genetic basis for morphological diversity emerges from studies of the repeated, independent loss of pelvic fins in populations of three-spine stickleback fish that moved from saltwater to freshwater[26,27]. The pelvic fin is speculated to be a defense mechanism against predators that are not present in freshwater environments. Genome-wide linkage mapping identified a genetic locus tightly associated with the presence of this appendage[26]. This region contained a promising candidate gene *Pituitary homeobox 1* (*Pitx1*), which had a conserved protein-coding sequence in pelvic-reduced fish, but was not expressed where the fin grows. Further linkage mapping of this locus identified a 2.5kb cis-regulatory element whose activity was sufficient to drive pelvic fin development in fish[27]. Interestingly, other three-spine stickleback populations that independently moved to freshwater and experienced pelvic spine reduction also had mutations in the *Pitx1* cis-regulatory elements, suggesting this locus serves as a hot-spot for recurrent evolutionary change.

Another example of repeated cis-regulatory adaptations relates to the evolution of *Drosophila* wing spots in males, which females use for species recognition. Instead of an unbiased analysis, these studies began with the candidate gene *yellow*, which is required for melanization and associated with wing spot formation[28]. *D. biramipes* spots develop, in part, due to changes in the cis-regulatory elements of *yellow*[29]. The *yellow* enhancer region contains several binding domains for the homeotic transcription factor *distal-less*, which are necessary and sufficient for the development of wing spots[30]. Combined, these studies in addition to many others, demonstrate that changes in cis-regulatory elements are sufficient to alter morphology and underlie adaptive characteristics[3,5–7,31].

Changes in cis-regulatory elements may also be a driving force of behavioral evolution as they allow for discrete changes in expression of genes that control circuit function or anatomy[22], the fundamental neural substrate for behavior.

1.2   Mechanisms of Behavioral Evolution

Compared to studying morphological evolution where genetic changes underlie anatomical variation, studying behavioral evolution is almost certainly more complex since genetic changes manifest as physical changes in neural circuitry, which then manifest as alterations in behavior. This additional layer of complexity is potentially why there are only two major modes of behavioral evolution that have been described. First, changes in peripheral sensory detection are thought to be an area of the nervous system that is particularly evolvable. Changing tuning or expression of sensory receptors can rapidly generate or eliminate behavioral sensitivity to

specific stimuli. Second, changes in neuromodulation are thought to be a facile way of changing the circuit function while maintaining circuit integrity. However, as I will discuss in the next section, it is speculated that other changes in nervous systems must underlie behavioral evolution.

1.2.1 Changes in Sensory Detection

Changes in sensory detection are proposed to be a major route of behavioral diversification across the tree of life[32–36], even for bacteria. Quorum sensing is a form of bacterial social communication that exists in phylogenetically diverse species[37]. In species that quorum sense, individual bacterium release 'pheromones' known as auto-inducers that at certain concentrations induce the population to undergo a 'behavioral state' change, which can result in the population collectively forming a biofilm or becoming bioluminescent[37]. While not always true, bacteria often specialize in sensing the concentration of conspecific bacteria and thus have evolved species-specific auto-inducers or receptors for auto-inducers[38]. Therefore, one of the more primitive examples of 'behavioral evolution' involves genetic changes in receptor expression and pheromone detection.

Protein coding changes in pheromone receptors can also underlie species distinctions in more complex organisms. Asian and European corn borer moths are reproductively isolated due to their differential response to two conspecific and heterospecific pheromones, despite that these pheromones only differ in the isomerization of a double bond[39]. Male moths of both species detect these pheromones using a homologous olfactory receptor, Or3, that differs only in a single

amino-acid change[39]. Or3 in the European species is tuned to conspecific female pheromones, but also more weakly responds to heterospecific female pheromones. A residue change in Or3 of the Asian species imparted a 14-fold preferential response to his conspecific female pheromone[39]. Therefore, a single point mutation in an olfactory receptor is sufficient to narrow pheromone tuning, which is proposed to mediate mate recognition in these sister species.

Protein coding changes in chemoreceptors can also impart novel chemical sensitivities, instead of eliminating sensitivities[40,41]. A recent study suggested that sequence changes in the *D. sechellia* IR75b receptor confer greater sensitivity to volatiles of the Morinda fruit, a plant *D. sechellia* specializes on[40]. However, introducing the *D. sechellia* IR75b receptor into *D. melanogaster* did not alter their behavioral attraction to Morinda fruit, suggesting this protein coding change on its own may be insufficient for behavioral evolution. This study also described changes in IR75b expression and an expansion of the size of the antennal lobe innervated by the IR75b olfactory sensory neurons, suggesting that other alterations in the sensory periphery may also be required[40]. Therefore, while peripheral adaptations are frequently invoked as a facile mechanism for behavioral evolution, these adaptations might in fact have a complex genetic basis with numerous genetic changes contributing to the evolution of robust, innate behaviors.

Frequently, sensory receptors gain null mutations or no longer expressed as a rapid mechanism to eliminate sensitivity to chemical stimuli. One study found that there was repeated, independent loss of a pheromone receptor in *C. elegans* that facilitated an adaptive behavioral response. When *C. elegans* worms are grown at high density, nematode worms will enter into a non-reproductive quiescent state called the dauer stage, which is induced though detection of

conspecific pheromones. In two independent lineages of *C. elegans* and one independent lineage of *C. briggsae*, a closely related species of *C. elegans*, worms acquired resistance to high-density dauer formation through the deletion of two G-protein-coupled receptors that detect the conspecific pheromone that induces dauer formation[42]. Thus, without sensory detection of pheromones, the broad-ranging morphological and behavioral changes associated with dauer formation did not occur.

Specific gustatory receptors have also been repeatedly lost thorough evolutionary time to facilitate an adaptive behavioral change in a species or genus. For instance, there were loss-of-function mutations in the umami receptor, T1R1, in giant pandas associated with the switch from carnivorous diets of their ancestors to their current bamboo-based diet[43]. Similarly, the sugar receptors were lost at multiple independent events in the evolution of obligate carnivores like cats, dolphins and otters[44].

Changing peripheral sensory detection that inputs into a conserved neural circuit mediating a behavioral response can rapidly shift an animal's sensitivity. Moreover, these types of changes potentially avoid dangerous pleiotropic effects. Many examples of how changes in peripheral sensory detection can rapidly modulate behavioral responses may also exist because these types of changes may be particularly easy to identify.

1.2.2   Changes in Neuromodulation

Another proposed mechanism for behavioral evolution involves changes in neuromodulation,

which can readily alter the functional properties of homologous circuits[22,45–47]. While neuromodulators and their receptors do not appear to be undergoing rapid diversification, likely because of undesired pleiotropic effects, variation in their expression patterns are thought to contribute to species-specific behaviors[22,45–47]. In two examples in rodents, differences in the expression of either the vasopressin receptor 1a (V1aR) or vasopressin peptide mediate changes in social behavior. Differential expression of V1aR in the ventral palladium, which is part of the reward system of the brain, is thought to underlie monogamous and polygamous behaviors between two species of voles[48]. Similarly, in the deer mouse *Peromyscus*, which last shared a common ancestor with voles (*Microtus*) 10 million years ago and mice (*Mus*) 25 million years ago, differences in the expression of the neuropeptide vasopressin are thought to alter the propensity of males of different species to make nests[49].

Changes in neuromodulation have been proposed to cause changes in the threshold of response to external stimuli. For instance, certain populations of Mexican cavefish *Astyanax mexicanus* have independently decreased the amount of time they sleep. This sleep loss is associated with an increased in the number of hypocretin/orexin (HCRT)-positive hypothalamic neurons. Pharmacological inhibition of HCRT results in greater amount of sleep and behavioral manipulations that increase sleep are associated with decreased *hcrt* expression, suggesting that neuromodulation regulates the cavefish sleep behavior.

From these examples, and many others, one might conclude that behavioral evolution generally involves either changes in neuromodulation or peripheral detection of sensory signals in the environment[45–47]. Bendesky and Bargmann (2011) argued that these classes of genes "are

9

disproportionately associated with variation in behavior because of their evolvability."[46] Indeed, neuromodulatory changes can allow for a conserved, multifunctional neural circuit to produce different behavioral states[50] while altered sensory detection can change incrementally due to the modularity of sensory systems[32]. While these types of changes are almost certainly very important, this conclusion is likely biased by limitations in the methods used to study behavioral evolution thus far. If a candidate approach was used, typically the candidate gene studied is either a chemoreceptor or a neuromodulator. If an unbiased genetic approach was used, only behaviors that have a strongly monogenetic basis are studied since polygenetic traits are difficult to characterize. The bias towards understanding behavioral variation with relatively simple genetic underpinnings or the role of specific candidate genes has left us with only a partial understanding of behavioral evolution.

1.3   Studying the Neural Basis of Behavioral Evolution

Understanding how changes at the genetic level result in behavioral differences between species or populations can frequently provide mechanistic clarity for how genetic differences result in changes in both behavior and nervous system function. Relevant genes can either be identified though a targeted approach, which usually results in the characterization of a sensory receptor. Alternatively, relevant genes can be identified using unbiased mapping techniques like genome-wide association studies, which correlate single-nucleotide polymorphisms to variable traits, or quantitative trait locus mapping, which link genetic variation with phenotypic variation. Understanding the genetic basis of a variable behavior works best when unbiased genetic mapping identifies a single genetic locus that underlies a variable behavior. However, aside from several interesting examples, behavioral variation is often found to have a diffuse, complex

10

genetic architecture[51–54], which makes the genetic contributions to a behavioral more difficult to understand. In the descriptions of the genetic basis of behavioral evolution that exist, generally either peripheral detection or neuromodulation is altered[32–36,45–47,55,56].

Studies that directly compare how neural circuitry differences relate to changes in animal behavior suggest that genetic studies of variation potentially do not uncover all types of neural changes underlying behavioral variation. Indeed, cross-species neural circuitry studies have uncovered novel ways neural circuits differ, including physiological differences in homologous interneurons, strength of synaptic connections, anatomical characteristics of individual neurons, and rewiring of neural circuits[57–62]. Typically, these studies either use high-resolution anatomical characterization of a nervous system or focus on neural population whose somata are easily accessible for physiological characterization. Fundamental limitations in many comparative circuit studies are the inability to precisely probe homologous neural circuits or incomplete knowledge about the causal circuit underlying a behavior. Additionally, when comparing neural circuits over distant phyla, there are often too many changes in a circuit to understand how each relates to alternations in behavior.

During my thesis, I proposed to overcome these limitations by comparing well-described, divergent courtship behaviors across closely related *Drosophila* species. I proposed to use CRISPR/Cas9 to label and manipulate specific neural populations in non-model species to gain mechanistic insight into the nature of circuit changes across closely related species. Even in this context, however, two limitations of comparative approaches remain. First, biases exist in what neural populations are studied since it is infeasible for one person to characterize all neurons in a

nervous system. Second, rigorously demonstrating sufficiency of a neural change to cause a behavioral change is difficult without knowing the genetic basis of that neural change. Although my approach could not directly reveal the genetic basis of behavioral variation in *Drosophila*, I believe that understanding how the nervous system is altered in different species could focus the search for expression differences or coding sequence changes in relevant neural populations.

1.4 Evolution of Drosophila Courtship Behaviors

Drosophilids are an ideal model system to study the neural basis of behavioral evolution since there is a wealth of knowledge about both the neural circuitry underlying innate behaviors in *D. melanogaster*[17,18] and the genetic and behavioral underpinnings of speciation in this genus[63].

The last common ancestor of the *Drosophila melanogaster* subgroup was thought to have originated in sub-Saharan Africa where over the course of 10-15 million years, it moved across the continent and diverged into nine species[64,65]. As these species diverged, their reproductive isolation was often reinforced by the development of behavioral differences that signified species identity and discouraged interspecies courtship[63]. As a result, females rarely mate with heterospecific males and when copulation does occur, hybrid progeny often suffer fitness costs by either being sterile or fertile with lower fitness. Therefore, it is beneficial for males to avoid interspecies courtship. The rapid evolution of courtship and mating rituals that facilitate species-recognition thus provides an entry point to examine the neural mechanisms that underlie behavioral divergence between closely related species.
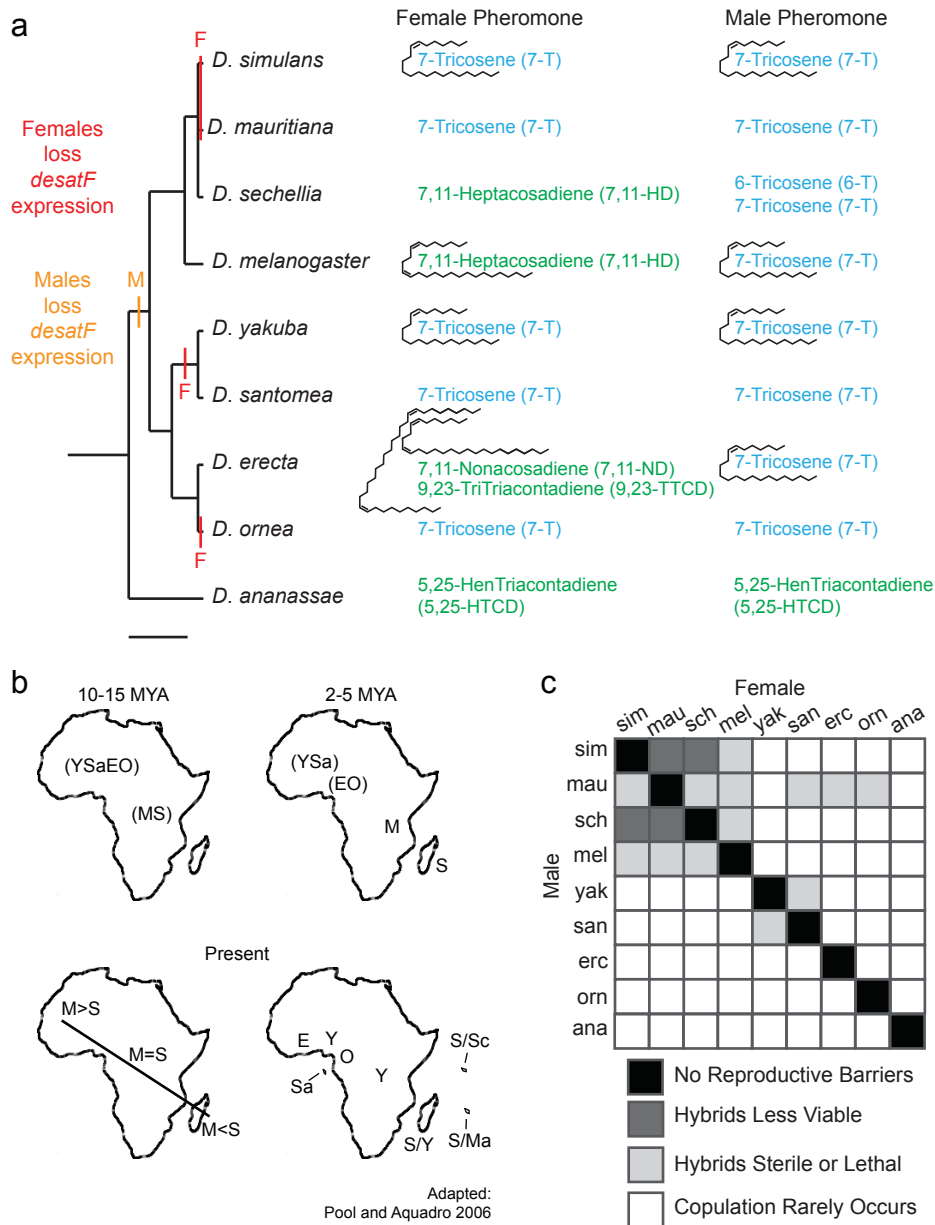
Figure 1.1: Description of species in the _D. melanogaster_ subgroup. a, Pheromone profiles of species in the _D. melanogaster_ subgroup and _D. ananassae_. Pheromones in blue are monoenes and pheromones in green are dienes. Transitions in the expression of _desatF_ are marked on the phylogeny - the orange bar represents male-specific loss of _desatF_ expression and red bars represent further loss of _desatF_ expression in females. **b**, Historical distribution of species in the _D. melanogaster_ subgroup: _D. simulans_ (S), _D. mauritiana_ (Ma), _D. sechellia_ (Sc), _D. melanogaster_ (M), _D. yakuba_ (Y), _D. satomea_ (Sa), _D. erecta_ (E), and _D. ornea_ (O). Flies grouped in brackets represent an ancestral state. Figure adapted from Pool and Aquadro 2006. **c**, Reproductive barriers in the _D. melanogaster_ subgroup.

Diversification of male courtship displays is presumably due to female selection on heritable variation in male courtship behavior. As a result, male courtship displays are perhaps the most distinct behavioral difference between *Drosophila* species and, in my opinion, one of the most charismatic behaviors observed in the animal kingdom. For instance, a *D. virilis* male and female sing a duet with their wings while a *D. elegans* male will extend his spotted wings while shaking his body laterally in an ornate visual display for the female[66]. Within the *D. melanogaster* subgroup males follow a shared series of courtship behaviors – they orient towards the female, tap on her abdomen, chase her as she move, extend one or two wing to sing a courtship song, lick her abdomen and attempt copulation[67]. Females, however, can assess if a male is an appropriate mate by detecting species-specific variations in these behaviors. The most notable differences are in the male's courtship song[68]. Even though *D. melanogaster*, *D. simulans*, *D. sechellia* and *D. mauritiana* males all sing a mixture of low frequency, high amplitude pulse song and high frequency, low amplitude sine song – there are differences in the inter-pulse interval, sine carrier frequency and pulse length[69]. *D. yakuba* and species more closely related to it mainly sing a mixture of sine song and clack song[70]. Understanding the genetic and neural basis for diversification of male song is an active area of study[71,72]. In addition to song, patterns and dynamics of how a male courts a female must be an important component of species discrimination, albeit a potentially less tractable behavior to study.

Males are thought to integrate multimodal sensory cues when discriminating between females. In all studied species, some level of visual discrimination must occur to hone a male's courtship towards flies and not other objects in the environment. However, in some species like *D. melanogaster,* males will mate in the dark suggesting vision is redundant with other sensory

cues. In other species, mating is severely depressed in the dark, like *D. simulans,* or completely absent, like *D. subobscura*. The visual features that regulate courtship, potentially including detection of distinct morphologies or behaviors, are currently not known. Male mate choice could also be mediated by acoustic or female-specific olfactory pheromones, however neither species-specific differences nor the neural mechanisms that process these cues are well characterized. In contrast, we have a wealth of information on how cuticular hydrocarbon pheromones promote species discrimination, which I discuss below.

1.5   Evolution of *Drosophila* Pheromone Preferences

One mechanism for selective courtship is the use of sex- and species-specific pheromones that either promote courtship towards conspecific females or suppress pursuit of inappropriate mates. Multiple evolutionary transitions in pheromone production have occurred across drosophilids, which has resulted in a diversity of cuticular hydrocarbon pheromones on females[73] (Fig. 1.1 a). Pheromone diversification is due, in part, to the rapid evolution of the enzyme *desaturaseF* (*desatF*), which is necessary for the addition of a second double bond to cuticular hydrocarbons[74] (Fig. 1.1 a). In the ancestral state, both male and female flies expressed *desatF* and produced diene hydrocarbons. In the *D. melanogaster* subgroup, however, the expression of *desatF* is controlled by a cis-regulatory *doublesex* (*Dsx*) DNA-bind domain. The female-specific isoform of the Dsx transcription factor, but not the male-specific isoform, binds to this domain to drive female-specific expression of *desatF*, thus resulting in a sexually dimorphic expression pattern of dienes in flies like *D. melanogaster* and *D. erecta*. Three independent losses of *desatF* expression in the *D. melanogaster* subgroup resulted in monomophic expression of dienes in *D. simulans*/*D. mauritiana*, *D. yakuba*/*D. santomea* and *D. orena* (Fig. 1.1 a). These losses are

15

known to be independent based on phylogenetic inference and genomic analysis revealing that all three lineages exhibit distinct mutations in the *desatF* cis-regulatory elements (Fig. 1.1 a)[74]. As a consequence of the evolution of *desatF* and other enzymes controlling the length of cuticular hydrocarbons, *D. melanogaster* and *D. sechellia* produce the diene 7,11-heptacosadiene (7,11-HD), *D. erecta* produces the dienes 7,11-nonacosadiene (7,11-ND) and 9,23-tritriacontadiene (9,23-TTCD), and all other females in the *D. melanogaster* subgroup produce the monoene 7-tricosene (7-T)[73]. All males in the *D. melanogaster* subgroup predominantly produce the monoene 7-T (Fig. 1.1a)[73].

DesatF evolution has been proposed to underlie a pre-zygotic reproductive barrier between the closely related sister species *D. melanogaster* and *D. simulans*[74,75], which form sterile female hybrid progeny when *D. melanogaster* is the parental female (Fig. 1.1 c). *D. melanogaster* males only courted female hybrid progeny expressing dienes and *D. simulans* males only courted female hybrid progeny not expressing dienes[75]. Thus, *desatF* can lead to assortative mating where individuals with similar genotypes preferentially mate. In both cases, even when courtship of hybrid progeny occurred, copulation was severely reduced and second generation hybrids never formed[75], which further underscores the presence strong reproductive barriers that reinforce neural mechanisms underlying species discrimination.

16
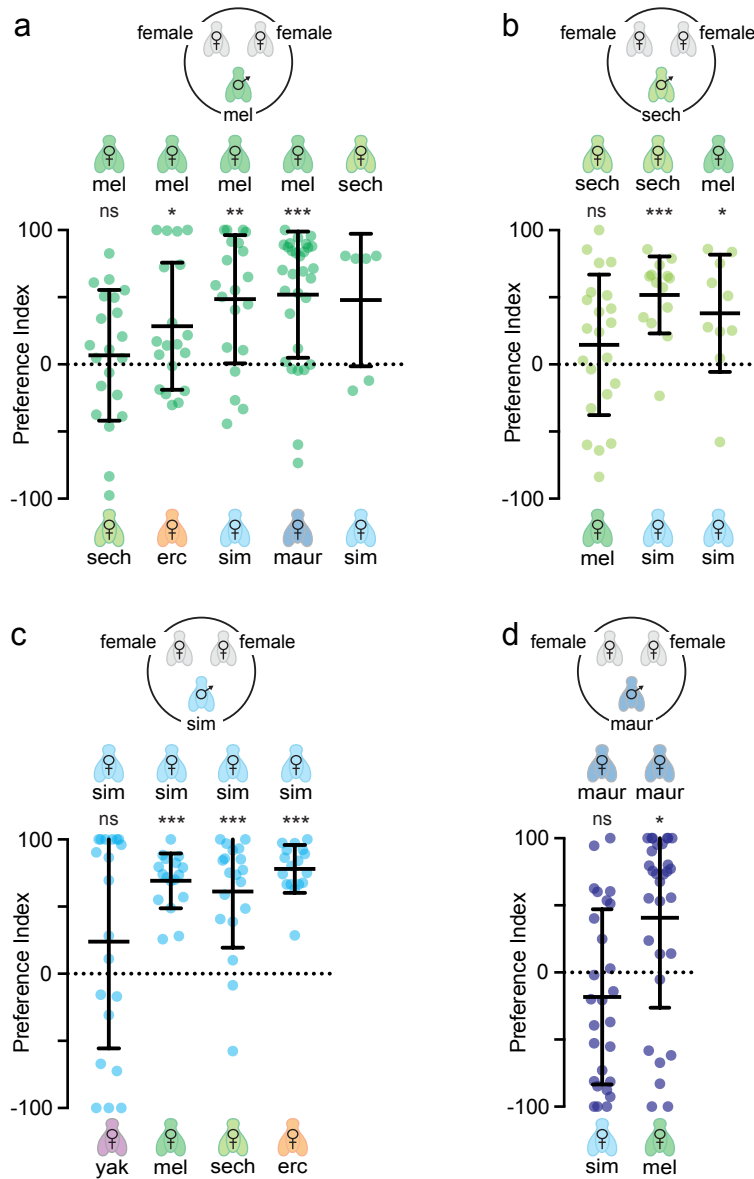
Figure 1.2: Courtship preferences of _D. melanogaster, D. simulans, D. sechellia, D. mauritiana_ males. a-d, Courtship preferences of _D. melanogaster_ (**a**), _D. sechellia_ (**b**), _D. simulans_ (**c**), _D. mauritiana_ (**d**) males with conspecific and heterospecific females. Dots represent the courtship index of an individual and bars represent mean and s.d. Preferences were analyzed using a one-sample t-test with a Bonferroni correction where ns denotes that preference was not significantly different from zero. See methods (pg 157) for sample size and P values.

To study species discrimination by males, frequently single pair assays are used to assess how much a male courts the only female he is offered. This assay provides a wealth of information on the dynamics of a male's "willingness" to court a female, but only permits speculation on his discriminatory abilities. For instance, *D. melanogaster* males are known to promiscuously court heterospecific females that produce dienes[76–78], but it is not known if they can use other cues to discriminate between conspecific and heterospecific females who produce the same pheromone. Further, once a male initiates courtship of conspecific females, it is not known if he can suppress courtship of heterospecific females. In some reports, *D. melanogaster* males exhibit modest courtship of *D. simulans* females[77,79], but *D. simulans* males are always strongly inhibited by *D. melanogaster* females[76–80]. Therefore, we frequently used preference assays where we offer a male the choice of courting two females and analyze his preference (Fig. 1.2). This assay, while infrequently used by others, enables us to directly assess a male's discriminatory capacity. It also more closely replicates natural environments where males and females of many species aggregate on a food source[81]. Thus, males do not just decide if he should court a female, but rather which female he should court.

When a male assesses females of different species, in addition to detecting differences in cuticular hydrocarbons, he could also potentially detect differences in morphological features, volatile pheromones, auditory cues or distinct aspects of female behavior. Given the many potential differences between conspecific and heterospecific females, we were surprised that males could not discriminate between females of two species carrying the same cuticular hydrocarbons (Fig. 1.2). For instance, *D. melanogaster* and *D. sechellia* males exhibited no preference for conspecific or heterospecific females, who produce 7,11-HD (Fig. 1.2 a, b).

18

Similarly, *D. simulans* and *D. mauritiana* males could also not discriminate between conspecific and heterospecific females, who produce 7-T (Fig. 1.2 c, d). These results suggest that males are unlikely to be using non-pheromonal cues to discriminate between closely related species.

Conversely, males could robustly discriminate between females when they differed in their cuticular hydrocarbons. For instance, *D. melanogaster* and *D. sechellia* males both exhibited a strong preference for *D. melanogaster* and *D. sechellia* females over *D. simulans* females (Fig. 1.2 a, b). Interestingly, *D. melanogaster* males exhibited a preference, albeit weaker, for conspecific females over *D. erecta* females who produce a distinct diene (Fig. 1.2 a). Similarly, *D. simulans* and *D. mauritiana* males exhibited a strong preference for conspecific females over females producing dienes (Fig. 1.2 c, d).

The ability of males within the *D. melanogaster* subgroup to discriminate between conspecific and heterospecific females is due in part to the differential behavioral valence of 7,11-HD[77–79], the *D. melanogaster* and *D. sechellia* female pheromone. Perfuming *D. simulans* females with 7,11-HD renders them attractive to *D. melanogaster* males, but unattractive to *D. simulans* males[77]. Similarly, perfuming conspecific females with 7,11-HD is also sufficient to suppress courtship by *D. yakuba* and *D. erecta* males[77]. Thus, 7,11-HD is detected by males of all four species but plays opposing roles in regulating their courtship decisions[77]. Interestingly, given that *D. simulans* and *D. yakuba* males had to independently form reproductive barriers with diene-producing species[74], the neural circuitry mediating aversion to 7,11-HD must also be independently derived. *D. erecta,* on the other hand, had to evolve neural mechanisms to suppress courtship towards 7,11-HD-producing females without inhibiting courtship towards the

distinct dienes carried by its own female. Therefore, these three species establish a paradigm to study the neural basis for parallel behavioral evolution.

Species-specific pheromone responses could reflect evolution of peripheral sensory detection mechanisms through alterations in receptor tuning or expression. Indeed, the rapid diversification of chemoreceptors has been proposed to underlie differences in sensory tuning and mate preferences across many species, although causal genetic evidence is rare. Alternatively, behavioral differences could arise from variation in the anatomy or function of the central circuits that process pheromone signals to regulate courtship decisions, a mechanism that has rarely been invoked to explain behavioral evolution. Moreover, each species could derive behavioral aversion to 7,11-HD using similar or distinct changes in the neural circuits that process pheromones.

To differentiate between these possibilities, we performed a direct comparison between the homologous pheromone circuits that process 7,11-HD in *Drosophila* males of different species. **Chapters 2 and 3** focus on comparisons between *D. simulans* and *D. melanogaster,* as they remain reproductively isolated despite frequently encountering each other in their environments. Our analysis of *D. simulans* and *D. melanogaster* demonstrated that species-specific responses to 7,11-HD emerge from reweighting of excitatory and inhibitory inputs at a central node in the courtship circuit, highlighting how functional adaptations of central sensory processing pathways can lead to divergent behaviors. **Chapter 4** extends upon this analysis to include pheromone circuits in *D. yakuba* and *D. erecta* to gain insight into how 7,11-HD also suppresses courtship in these more distantly related species. Analysis of *D. yakuba* and *D. erecta* pheromone processing

circuits provides a rare opportunity to ask if qualitatively similar, but independently derived behaviors evolve through similar or distinct neural mechanisms. **Chapter 5** focuses on mechanisms for differential responses to 7-T in *D. simulans* and *D. melanogaster* and general strategies for suppression of male-male courtship in many drosophilids. While discrimination between females requires species-specific pheromone assessments, all males need to perform appropriate sex discrimination. **Chapter 6** discusses general strategies for species and sex discrimination in *Drosophila,* the selective pressures that facilitated the evolution of these behaviors and new insights into the neural basis for behavioral evolution.

2 | Conserved peripheral sensory neurons drive opposing courtship responses to 7,11-HD in *D. melanogaster* and *D. simulans*

2.1   Introduction

Gene families mediating chemosensation are rapidly diversifying across all studied classes of organisms and even between closely related species[32–34,82,83]. This is in contrast to gene families that underlie essential biological functions, like potassium channels, which are more conserved across distantly related species[84]. In order for diversification of a gene family to occur, there needs to be genetic heterogeneity within a population that selective pressures can act upon. Compared to potassium channel mutants, chemosensory mutants should have relatively fewer fitness deficits suggesting that there are potentially fewer barriers for the maintenance or development of the prerequisite genetic diversity necessary for rapid diversification. As a result, chemoreceptor gene families like olfactory receptors (ORs) have massively expanded and diversified across closely related orders of insects – there are approximately 60 ORs in dipterans[82] and several hundred ORs in hymenopterans[83]. The expansion of olfactory receptors in hymenoptera is thought to underlie the extreme behavioral diversification in this order and, in particular, the evolution of social behavior[83].

The highly modular nature of the olfactory system of vertebrates and invertebrates is also thought to facilitate peripheral evolution[32,33]. Almost every OSN expresses only a single olfactory receptor and the axons of OSNs that express the same olfactory receptor converge to form discrete glomeruli in the antennal lobe of invertebrates and the olfactory bulb of vertebrates[82,85–87]. While most glomeruli detect a diverse array of chemicals in the environment

that are used for forming flexible associations, a few glomeruli specialize in detecting important odors and activate neural circuits that are hardwired to drive innate behaviors. As such, changing the functional tuning or expression of receptors in these OSNs could cause immediate changes in behavioral response. These hard-wired circuits are probably more prevalent in other sensory detection appendages like the legs, proboscis, wings and genitals. Sensory neurons in these appendages frequently express more than one type of receptor and, thus, could derive novel sensitivities without losing preexisting sensitivities[32]. The rapid evolution of chemosensory receptors combined with modular nature of the olfactory system have inspired the proposal that the sensory periphery is one of the most evolutionary labile parts of the nervous system[32–36,46].

While the rapid diversification of chemosensory receptors likely plays a significant role in the evolution of novel chemical sensitivities[32,33,42,88,89], the overall importance of these peripheral adaptations relative to central circuit adaptations is unclear. One reason peripheral adaptations may be overrepresented in the literature as an explanation for behavioral evolution is because the genetic changes underlying these adaptations are relatively easy to conceptualize, discover, and test. For instance, it is easy to conceptualize how a change in receptor expression or tuning mediates species discrimination between *D. melanogaster* and *D. simulans* – the receptors for 7-T and 7,11-HD could either have protein coding mutations or swapped which sensory neuron they are expressed in.

In the following chapter I directly test whether a change at the sensory periphery mediates species-specific behavioral differences to 7,11-HD by examining the tuning, function and

anatomy of the sensory neurons that process female gustatory pheromones in *D. melanogaster* and *D. simulans*.

2.2 ppk23 plays a conserved role in 7,11-HD detection

A critical step in *Drosophila* mate assessment occurs when a male taps the abdomen of another fly with his foreleg to taste their cuticular pheromones[90]. *D. melanogaster* and *D. simulans* males whose foreleg tarsi have been surgically removed court promiscuously, underscoring the critical role of cuticular pheromones in mate discrimination (Fig. 2.1 a, b). Tarsi-ablated males still court vigorously (Fig. 2.1 a, b), indicating that other sensory cues, such as vision[91,92], serve a redundant role to promote courtship in the absence of any excitatory contact pheromones.

Multiple classes of gustatory sensory neurons on the *D. melanogaster* male foreleg detect pheromones to differentially regulate courtship. One heterogeneous sensory population expresses the ppk23 DEG/ENaC channel: a subset of ppk23+ neurons termed "female cells" detects *D. melanogaster* female pheromones, including 7,11-HD, to promote courtship and another subset termed "male cells" detects male pheromones to inhibit courtship[93–97]. A smaller population of foreleg sensory neurons expresses the Gr32a receptor and detects 7-T to suppress inappropriate pursuit of *D. simulans* females and *D. melanogaster* males[98,99]. Although it is not known whether Gr32a and ppk23 directly bind cuticular hydrocarbons, since neither has been shown to be sufficient to confer pheromone sensitivity when expressed ectopically, they serve as essential components of these pheromone transduction pathways[93–95,98,99]. We therefore investigated how Gr32a and ppk23 shape mate preferences in *D. simulans* by using CRISPR-Cas9 genome

24
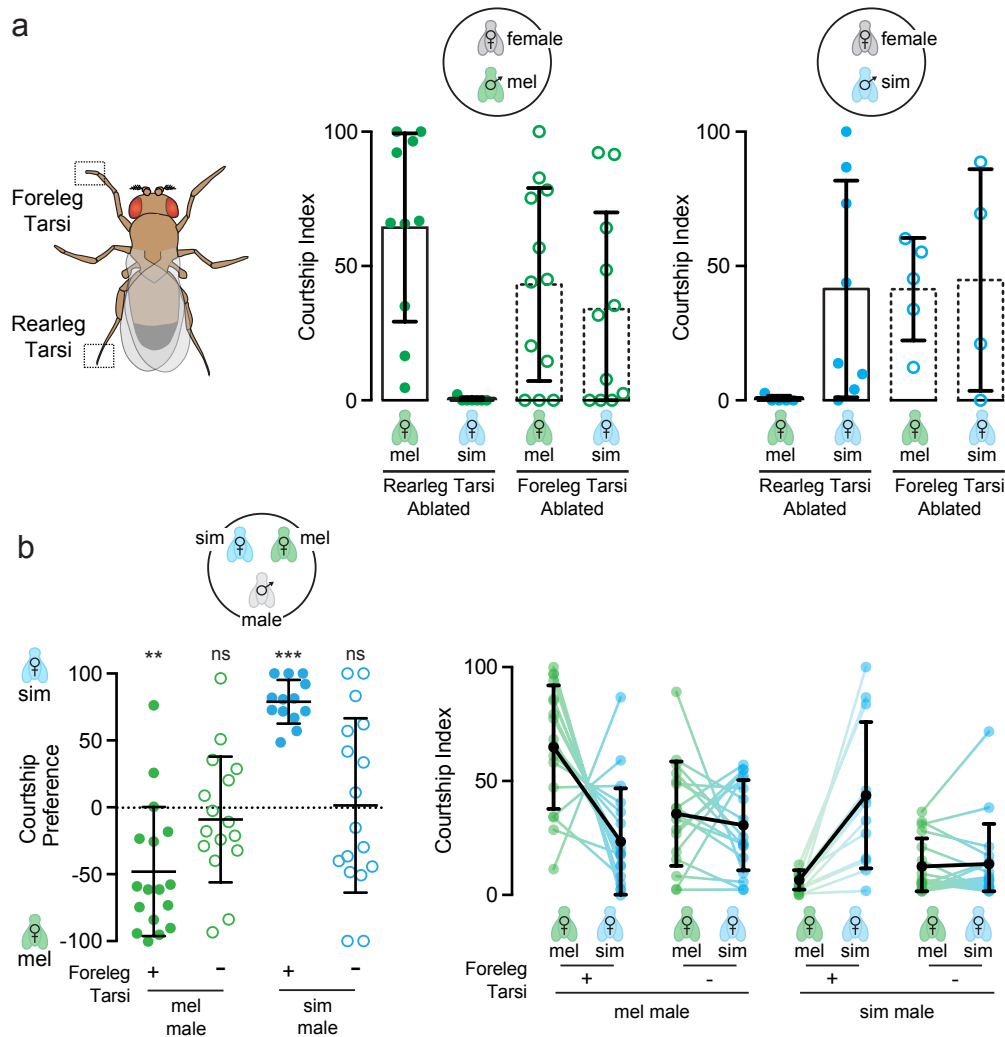
Figure 2.1: Foreleg tarsi are necessary for species discrimination. a, Schematic illustrating location of foreleg and rearleg tarsi (left). Courtship index towards *D. melanogaster* and *D. simulans* females by *D. melanogaster* (left) and *D. simulans* (right) males with either their foreleg tarsi or rearleg tarsi ablated. **b**, Courtship preferences of *D. melanogaster* (green) and *D. simulans* (blue) males with foreleg tarsi intact (+) or surgically ablated (-) when presented with conspecific and heterospecific females (left, n=13-17, one-sample t-test with a Bonferroni correction where ns denotes that preference is not significantly different from zero. P <0.0001, P=0.9303, P=0.0009 and P=0.4521, respectively). Courtship index underlying courtship preference during the choice assay (right). Dots represent courtship by an individual, bars represent mean and s.d and lines connect then courtship indices for an individual.
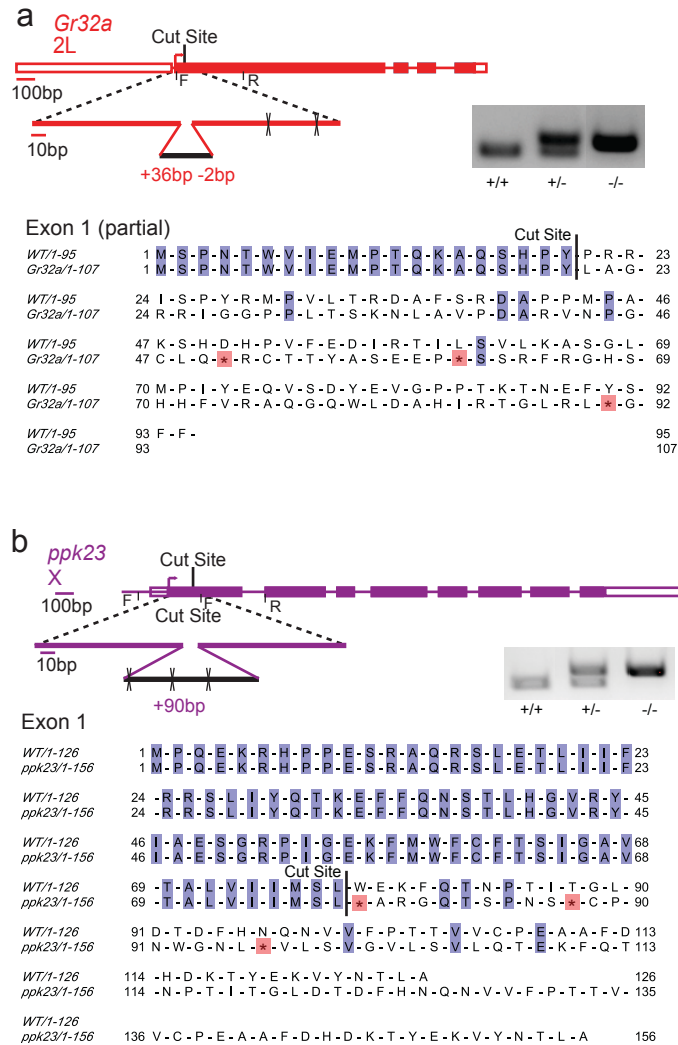
Figure 2.2: Generation of *D. simulans ppk23* and *Gr32a* mutants. **a**, **b**, Detailed schematics of CRISPR/Cas9-induced mutations (top) in *Gr32a* (**a**) and *ppk23* genes (**b**). Cas9 was targeted by CRISPR gRNA to the first exon (cut site) of *Gr32a* or *ppk23*. Cleaved DNA was repaired by non-homologous end-joining, an error prone process that resulted in a 36 bp insertion, 2 bp deletion in the *Gr32a* coding sequence and 90 bp insertion into the *ppk23* coding sequence. Both indels resulted in proximal in-frame stop codons (bottom, * highlighted red in resulting amino acid sequence). Forward (F) and reverse (R) genotyping primers are marked with a line.

editing to introduce multiple stop codons into the first exon of each gene to generate mutant alleles (Fig. 2.2).

In single pair courtship assays, we found that both *Gr32a* and *ppk23* mutant males pursued conspecific females with the same vigor as wild type *D. simulans* males (Fig. 2.3). This result suggests either that Gr32a and ppk23 do not contribute to 7-T detection in *D. simulans* or that 7-T, despite being the predominant cuticular pheromone on *D. simulans* females[73], does not play a prominent role in promoting male courtship[79].

Given that the evolution of pheromone receptors has been proposed as a mechanism to generate species-specific mate preferences[32,33,42,88,89], we considered the possibility that the Gr32a receptor may have acquired altered ligand specificity such that in *D. simulans* it now mediates detection of *D. melanogaster* female pheromones, such as 7,11-HD, and activates a conserved courtship-suppressing circuit. However, *D. simulans* Gr32a mutant males did not court *D. melanogaster* females nor females of three more distant species (Fig. 2.3). Thus, contrary to its role mediating courtship suppression in *D. melanogaster*[98,99], Gr32a appears to convey neither strong excitatory nor inhibitory input to influence mate choices in *D. simulans*.

In contrast to the selective courtship exhibited by *Gr32a* mutants, *ppk23* mutants pursued *D. melanogaster* females and other drosophilids carrying inhibitory diene pheromones with the same intensity as they courted *D. simulans* females (Fig. 2.3). Therefore, *ppk23* is necessary for courtship suppression towards females carrying 7,11-HD in addition to a diversity of other dienes like 9,23-tritriacontadiene present on *D. erecta* females and 5,25-hentiacontadiene present
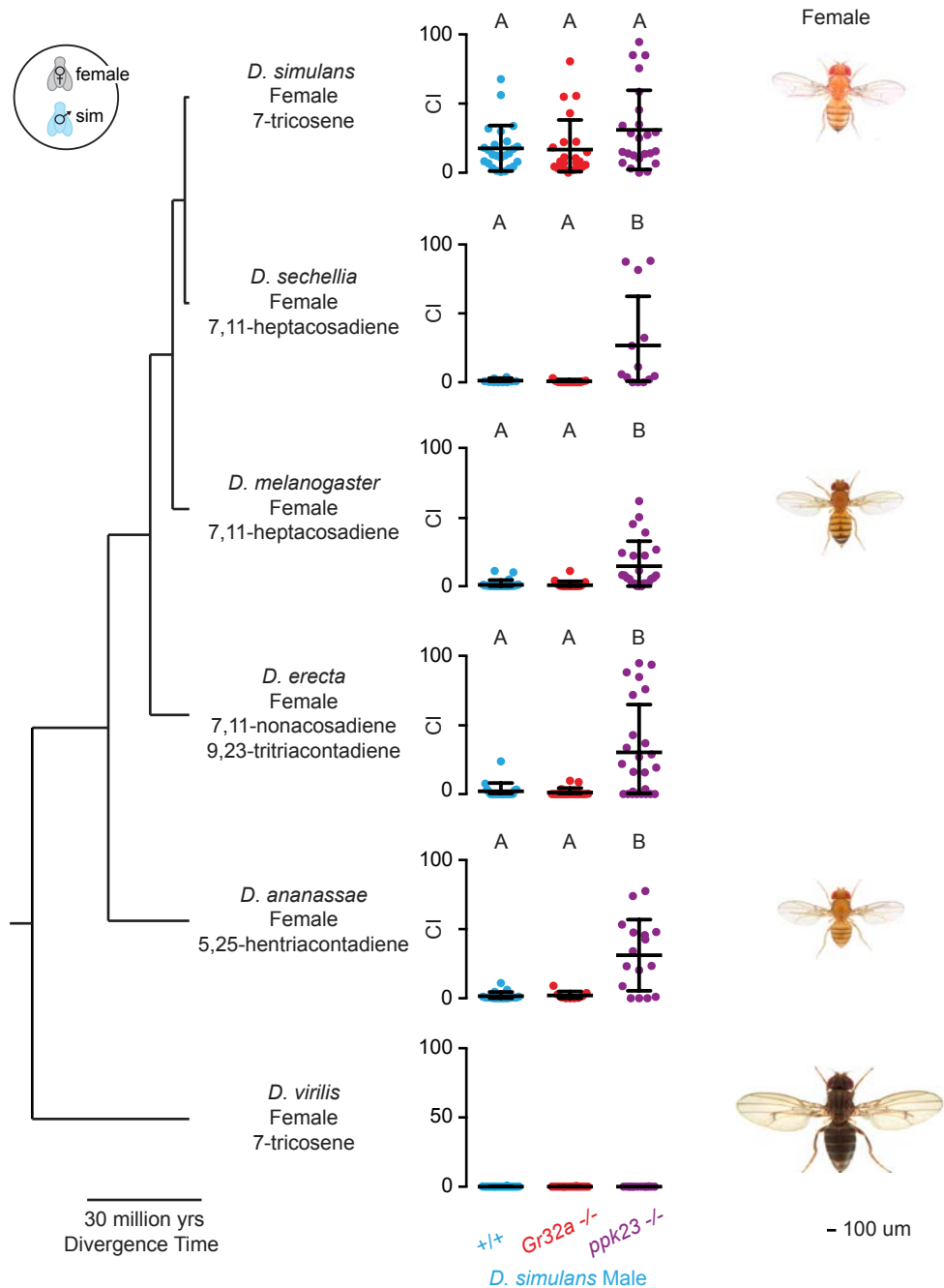
Figure 2.3: Single choice courtship behavior of *D. simulans ppk23* and *Gr32a* mutant males.
Courtship indicies of *D. simulans* wild type (+/+), *Gr32a*, and *ppk23* mutant males with *D. simulans*, *D. sechellia*, *D. melanogaster*, *D. erecta*, *D. ananassae*, and *D. virilis* females (n=16-25, Kruskal-Wallis test, P<0.001, different letters mark significant differences in courtship by Dunn's multiple comparisons test). All females except *D. simulans* and *D. virilis* produce diene hydrocarbons. From left to right: phylogeny, cuticular hydrocarbons, courtship indices and image of female. Dots represent courtship by an individual and bars represent mean and s.d.

on *D. ananassae* females. These data demonstrate that *D. simulans* males can be aroused in the absence of any species-specific excitatory pheromonal cue, implying that other sensory inputs control the initiation of courtship. Given that vision is obligatory for robust courtship in *D. simulans* (but not *D. melanogaste*r) we speculate that there may exist specific visual cues that serve to promote *D. simulans* male's sexual arousal. Interestingly, the only female tested that *D. simulans* wild type or mutant males did not court was *D. virilis*, who produce 7-T but are double the size and significantly darker than *D. simulans* females (Fig. 2.3). Since it was previously reported that *D. melanogaster Gr32a* mutant males would court *D. virilis* females[99], we speculate that *D. simulans* males have a species-specific visual preference for females that resemble conspecifics.

In preference assays, *D. simulans ppk23* mutant males were unable to differentiate between *D. melanogaster* and *D. simulans* females (Fig. 2.4 a), indicating this sensory pathway is essential for erecting a pre-mating barrier between species. This observation also further highlights that males are indiscriminately attracted to any female that does not produce an inhibitory pheromone. To test whether the promiscuous courtship by *ppk23* mutants reflects an inability to detect 7,11-HD, we offered *D. simulans* males the choice of *D. simulans* females perfumed with 7,11-HD or ethanol. While wild type males preferentially courted the ethanol-perfumed female, *ppk23* mutants pursued both females indiscriminately (Fig. 2.4 b). Thus, males of both species rely on *ppk23* to detect 7,11-HD, but detection of this pheromone initiates opposing behaviors in the two species—promoting courtship in *D. melanogaster* while suppressing courtship in *D. simulans*. We therefore developed genetic tools in *D. simulans* to examine the sensory neurons in
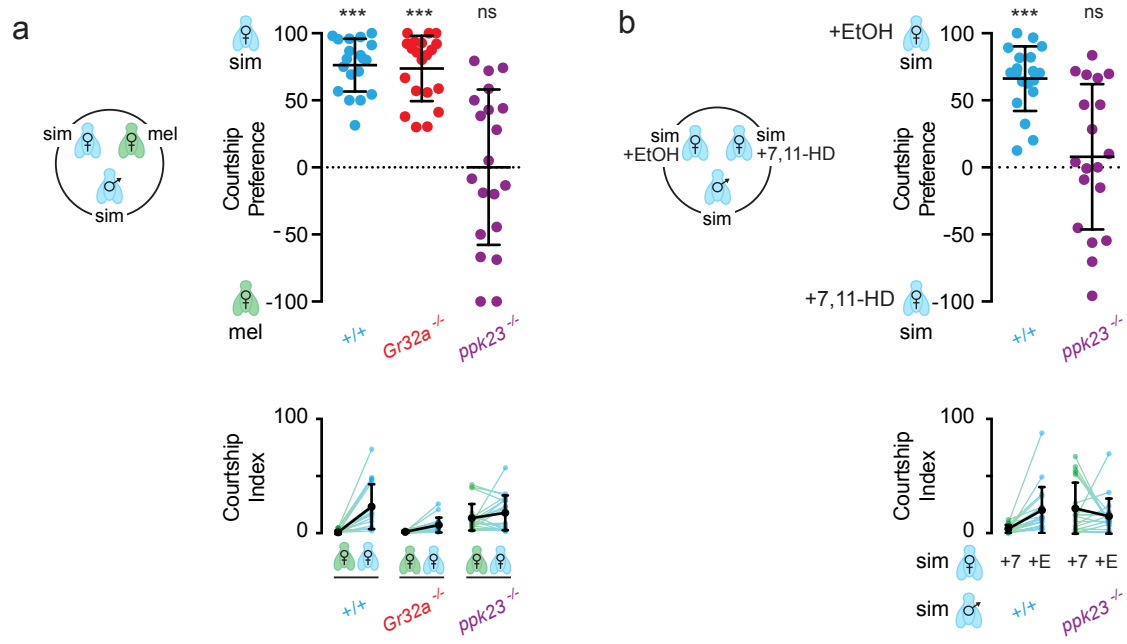
Figure 2.4: Courtship preferences of *D. simulans ppk23* and *Gr32a* mutant males. a, Courtship preferences of *D. simulans* wild type (+/+), *Gr32a*, and *ppk23* mutant males when presented with conspecific and heterospecific females (n=19-20). Courtship index underlying courtship preference during the choice assay (bottom). **b**, Courtship preferences of *D. simulans* wild type (+/+) and *ppk23* mutant males when presented with *D. simulans* females prefumed with ethanol or 7,11-HD (n=19). Courtship index underlying courtship preferences during the choice assay (bottom). Dots represent courtship by an individual and bars represent mean and s.d. Preferences were analyzed using a one-sample t-test with a Bonferroni correction where ns denotes that preference was not significantly different from zero. See methods (pg 157) for sample size and P values.

which ppk23 is expressed and, ultimately, the downstream circuits that process 7,11-HD in order to identify the neural changes that contribute to these species-specific pheromone responses.

2.3   A conserved role for *fruitless* in regulating courtship behavior

In *D. melanogaster*, the male-specific isoform of the Fruitless transcription factor (Fru^M) mediates the development of the neural circuitry underlying male courtship behavior[17,18,100,101]. Labeling the neurons that express Fru^M with Gal4 (henceforth referred to as *fru^{Gal4}*) has enabled dissection of the *D. melanogaster* neural circuits controlling most aspects of male courtship behavior, from sensory detection to motor implementation. As such, *fru^{Gal4}* labels the neurons that process 7,11-HD pheromones to regulate courtship behavior[102] including the majority of ppk23+ gustatory sensory neurons in the male foreleg[93–95].

To gain genetic access to the repertoire of Fru+ neurons including those that detect and process 7,11-HD, we used CRISPR-Cas9-mediated homology-directed repair along with phiC31-mediated recombination to integrate either the GFP or Gal4 coding sequence into the first intron of the *fru* locus (Fig. 2.5 a), which we designed to be in a similar genomic position as the extensively studied *fru^{Gal4}* line in *D. melanogaster*[17] (Fig. 2.5 c). We observed that in both species, *fru* marks a similar ensemble of neurons distributed throughout the male nervous system, with comparable innervation patterns evident in most brain neuropils (Fig. 2.6).

Differences in the innervation patterns of *fru^{Gal4}* likely exist between the two species, which could be due to technical limitations of capturing endogenous expression patterns with Gal4 transgenes. Indeed, there are even differences in the innervation patterns of Gal4 and LexA
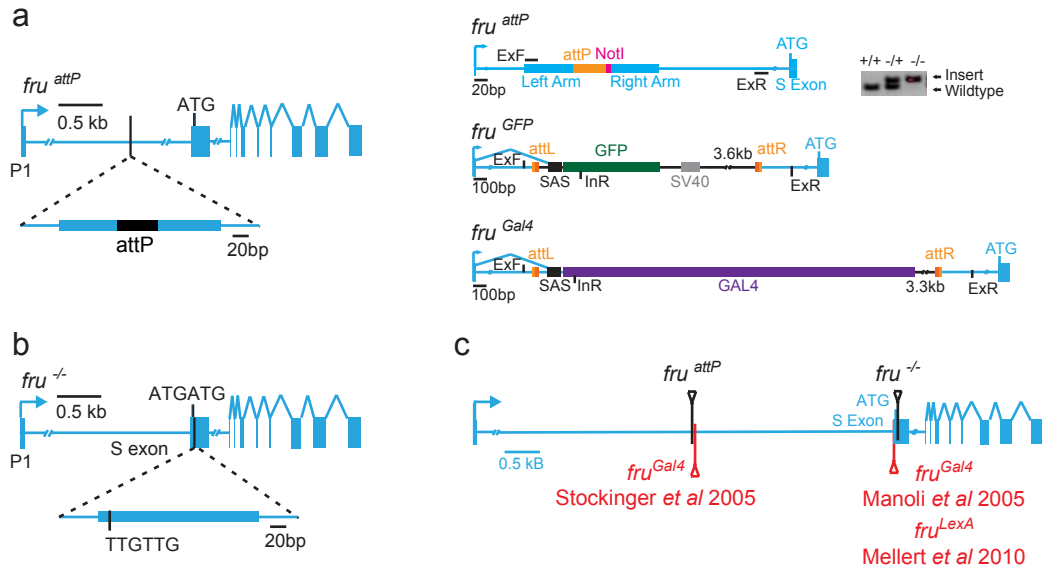
Figure 2.5: Targeted mutagenesis and integration of Gal4 into the _D. simulans fruitless_ locus. Genomic organization and targeted insertion into the _fru_ locus in _D. simulans_ using CRISPR/Cas9 homology directed repair. **a**, _fru_ _attP_ was generated by integrating an attP containing oligo in the first intron. _fru_ _GFP_ and _fru_ _Gal4_ were subsequently generated via PhiC31-mediated recombination into _fru_ _attP_. Lines represent predicted splicing from _fru_ transcription start site (arrowhead) to the splice acceptor site (SAS). ExF and ExR are primers located in the genome and InR is a primer located inside the transgene. **b**, Generation of _fru_ _-/-_ by integrating an oligo that deleted codons 1 and 2 of the first exon, introducing a frameshift mutation. **c**, Schematic of chromosomal location of _fru_ _attP_ and _fru_ _-/-_ integration sites in _D. simulans_ relative to the extensively studied _fru_ _Gal4_ and _fru_ _LexA_ transgenes in _D. melanogaster_.
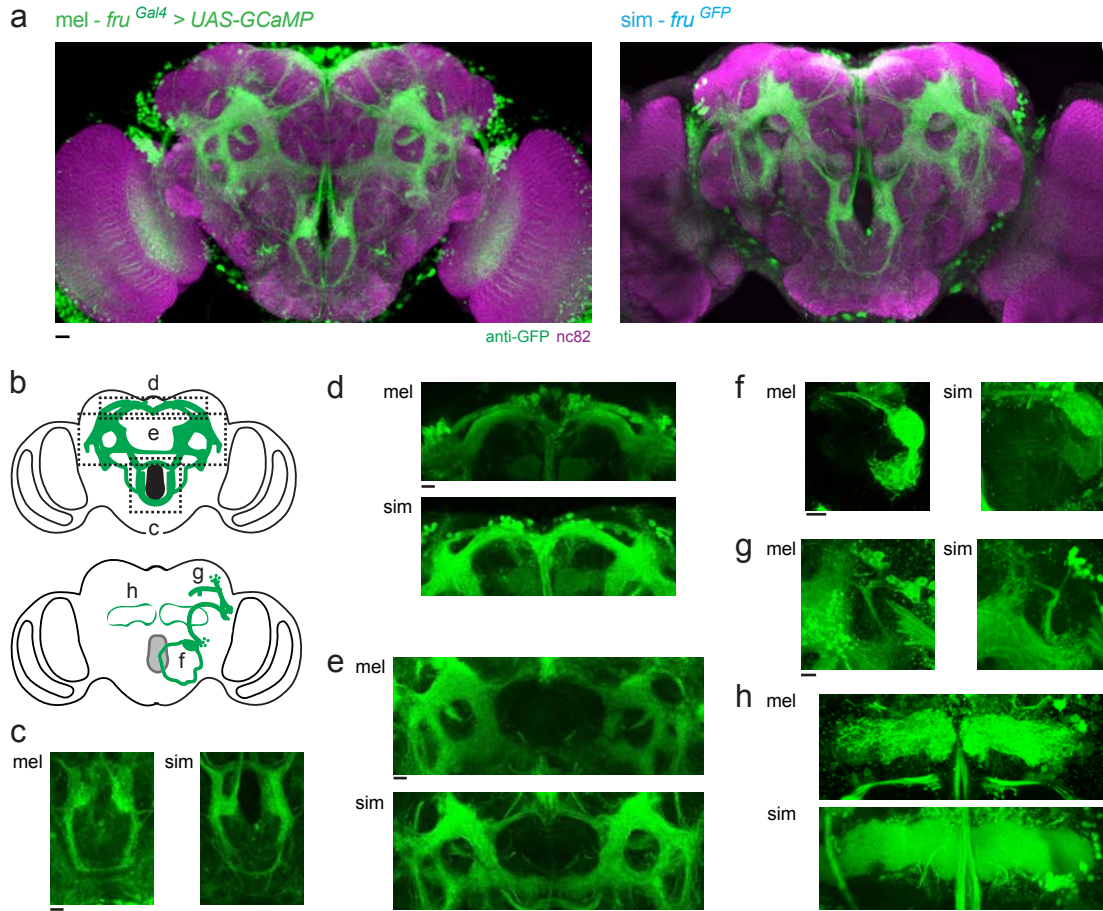
Figure 2.6: Anatomical conservation of Fru+ neurons. a, *D. melanogaster* (left) and *D. simulans* (right) adult male brain expression of Fru+ neurons (green) and neuropil counterstain (magenta). **b-h**, Maximum intensity confocal (**c-e**) and two-photon stacks (**f-h**) of anatomically defined regions of Fru+ neuropil in *D. melanogaster fru* ^{Gal4}>UAS-GCaMP6s and *D. simulans fru* ^{GFP} males: suboesophageal zone (**c**), lateral protocerebral complex (**d**, **e**), antennal lobe (**f**), lateral horn and DC1 neural tract and soma (**g**) and mushroom body γ-lobes (**h**). Scale bars represent 10 μm.

transgenes integrated into various positions in the *D. melanogaster fru* locus with none perfectly representing the endogenous expression pattern of Fru^M. Alternatively, differences in innervation patterns across species could reflect meaningful adaptations. These meaningful differences, however, are likely subtle and best characterized by more careful comparison of specific cell types.

Given the gross anatomical similarity of Fru+ neurons, we wished to confirm that *fru* plays an evolutionarily conserved role as a master regulator of male courtship behaviors[17,18,20,21,103] in *D. simulans*. We used the CRISPR/Cas9 system to mutate the open reading frame of *fru^M* (Fig. 2.5 b), a manipulation that in *D. melanogaster* generates null mutant males with aberrant mate preferences[18]. Likewise, *D. simulans fru^M* mutant males exhibited promiscuous attraction to males and heterospecific females (Fig. 2.7 a, b). Furthermore, we used *fru^{Gal4}* to drive expression of the light-activated ion channel, CsChrimson, in Fru+ neurons and verified that in *D. simulans*, as in *D. melanogaster*[104], activation of this neuronal population in an isolated male was sufficient to trigger multiple components of courtship behavior (Fig. 2.7 c). Therefore, in both species, *fru* marks circuits that specify male courtship towards appropriate sexual partners, providing an inroad to systematically trace and compare the neural pathways that process 7,11-HD and underlie mate discrimination, from the sensory periphery to higher brain centers.
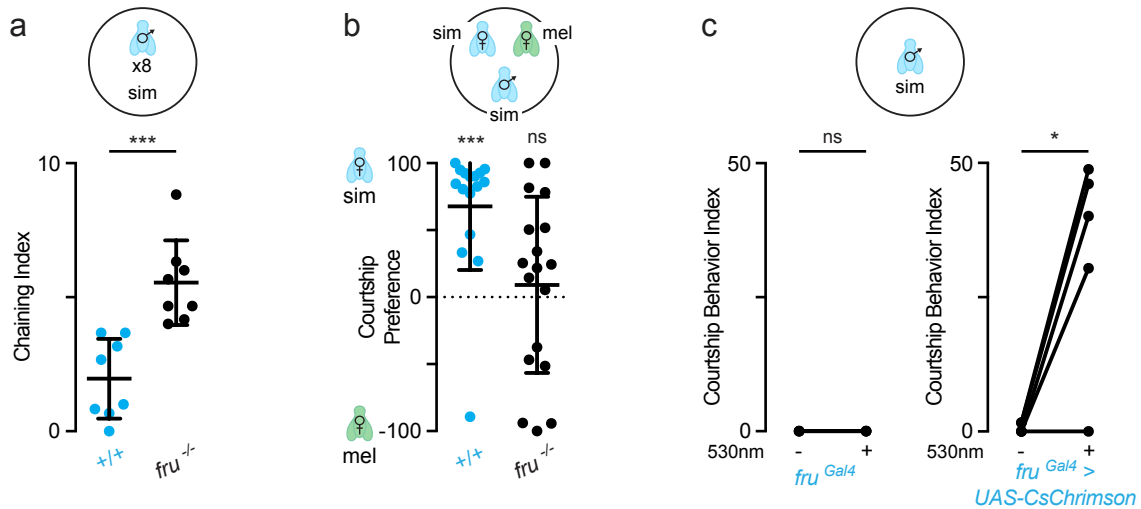
Figure 2.7: Functional conservation of Fru+ neurons. **a**, Male-male chaining index of wild type (+/+) and *fru* [-/-] males (n=8 groups of males, unpaired t-test, P<0.0001). **b**, Courtship preference of *D. simulans* wild type (+/+) and *fru* [-/-] males when presented with conspecific and heterospecific females (n=16-18, one-sample t-test with ns not significantly different than zero, P<0.0001 and P=0.5644, respectively). **c**, Percentage of time isolated *fru* [Gal4] (control) and *fru* [Gal4] > UAS-CsChrimson males displayed courtship behaviors in the presence or absence of 530nm illumination (n=5-6, Wilcoxon matched-pairs signed rank test, P=0.999, P = 0.034, respectively). Dots represent courtship by an individual and bars represent mean and s.d.

2.4   Conserved pheromone responses in peripheral sensory neurons

To compare the pheromone tuning of ppk23+ sensory neurons in *D. melanogaster* and *D. simulans* males, we developed a fictive tapping assay in which we could visualize the aggregate activity of foreleg sensory neurons in response to stimulation with different target flies (Fig. 2.8 a). We drove expression of the Ca^{2+} indicator GCaMP6s in Fru+ neurons and monitored the functional responses of sensory afferents in the ventral nerve cord of a male as his foreleg tarsus contacted the abdomen of a virgin female (Fig. 2.8 a).

We found that the Fru+ foreleg sensory neurons of both *D. melanogaster* and *D. simulans* males exhibited comparable pheromone tuning, responding robustly to the taste of a *D. melanogaster* female and weakly to a *D. simulans* female (Fig. 2.8 b, c). In both species, *ppk23* mutants exhibited strongly attenuated responses to the taste of females from either species (Fig. 2.8 b-e), verifying that ppk23 plays a conserved and essential role in pheromone detection.

While these experiments suggest that the pheromone tuning of peripheral sensory neurons is quantitatively similar between *D. melanogaster* and *D. simulans*, we wanted to further explore if there exist differences in the number or organization of ppk23+ sensory neurons responsive to 7,11-HD. To directly compare ppk23+ sensory neurons between species, we generated a *ppk23-*Gal4 reporter construct in *D. simulans,* taking advantage of the fact that in *D. melanogaster* the *ppk23* promoter faithfully reproduces endogenous channel expression[95].
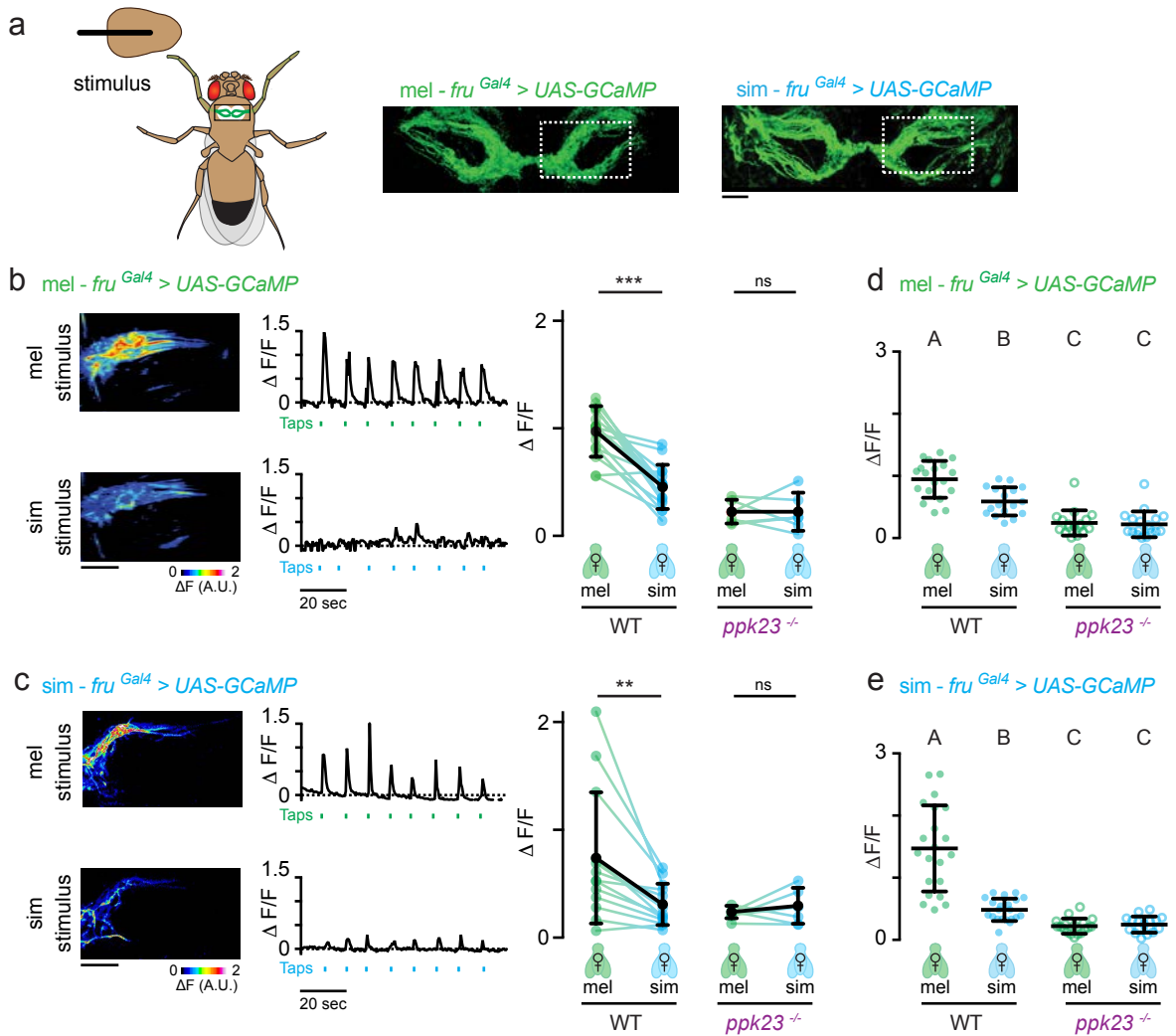
Figure 2.8: Conserved pheromonal tuning of ppk23+ Fruitless+ foreleg sensory neurons. a, Schematic of ventral nerve cord (VNC) imaging preparation (left) and images of the Fru+ foreleg afferents innervating the VNC (right). Box indicates approximate field of view imaged in assay. **b**, **c**, GCaMP imaging of Fru+ foreleg afferents in *D. melanogaster* (**b**) or *D. simulans* (**c**) males in response to the taste of a *D. melanogaster* (green) or *D. simulans* (blue) female. Representative images depict heat map of fluorescence increase (left) and representative traces depicts normalized fluorescence signal (middle). Time of each tap is indicated by a tick mark below the graph. The graphs summarize paired intra-animal averages in wild type and *ppk23* -/- males (right, WT=12-14 and *ppk23* -/- n=6, Wilcoxon matched-pairs test, WT mel P=0.0002, WT sim P=0.005, *ppk23* -/- mel P>0.9999 and *ppk23*-/- sim P=0.6875). **d**, **e**, GCaMP imaging of ppk23+ foreleg afferents in *D. melanogaster* (**d**) and *D. simulans* (**e**) males (n=6, Kruskal-Wallis test with Dunn's multiple comparisons test, mel P=0.0078 and sim P=0.0313). Colored dots represent average ΔF/F for an individual (**b**,**c**) and ΔF/F for taps (**d**,**e**) and black bars and dots represent mean and s.d. Scale bars represent 10 μm.

The *ppk23* promoter from both species drove expression in a comparable number of sensory neurons in the male foreleg, suggesting changes in the overall number of ppk23+ soma cannot explain divergent pheromone preferences (Fig. 2.9 a). Moreover, ppk23+ sensory neurons maintained their characteristic anatomical traits – the soma clustered in pairs under leg sensory bristles, they exhibited sexually dimorphic axonal projections within the VNC and they maintained qualitatively similar axonal projection patterns in the VNC and brain (Fig. 2.9 a-d). In addition, we introduced the *ppk23* promoters from both species into the same chromosomal location of the *D. melanogaster* genome and found they directed expression in identical sensory neuron populations (Fig. 2.9 e). Therefore, the pattern of ppk23 expression in the male foreleg appears to be indistinguishable across species.

The conservation of ppk23+ sensory neuron anatomy was paralleled by functional conservation of pheromone responses. Imaging the aggregate activity of ppk23+ sensory afferents in the ventral nerve cord revealed equivalent pheromone tuning across species, with significantly stronger responses to the taste of a *D. melanogaster* female than a *D. simulans* female (Fig. 2.10 a, b). The responses of individual soma also appear functionally conserved (Fig. 2.10 c). In males of both species the ppk23+ soma are paired beneath a sensory bristle (Fig. 2.9 a). The Scott lab previously demonstrated that when stimulating individual sensory bristles on the *D. melanogaster* male's foreleg with synthetic pheromones, one soma they termed the "female cell" responded to conspecific female pheromones and the other soma they termed the "male cell" responded to male pheromones[95–97]. Similarly, we found that in *D. simulans* only one ppk23+ soma of each pair responded to pure 7,11-HD, with equivalent magnitude across species (Fig. 2.10 c). Responses to synthetic 7-T were negligible in all ppk23+ neurons in both species (data
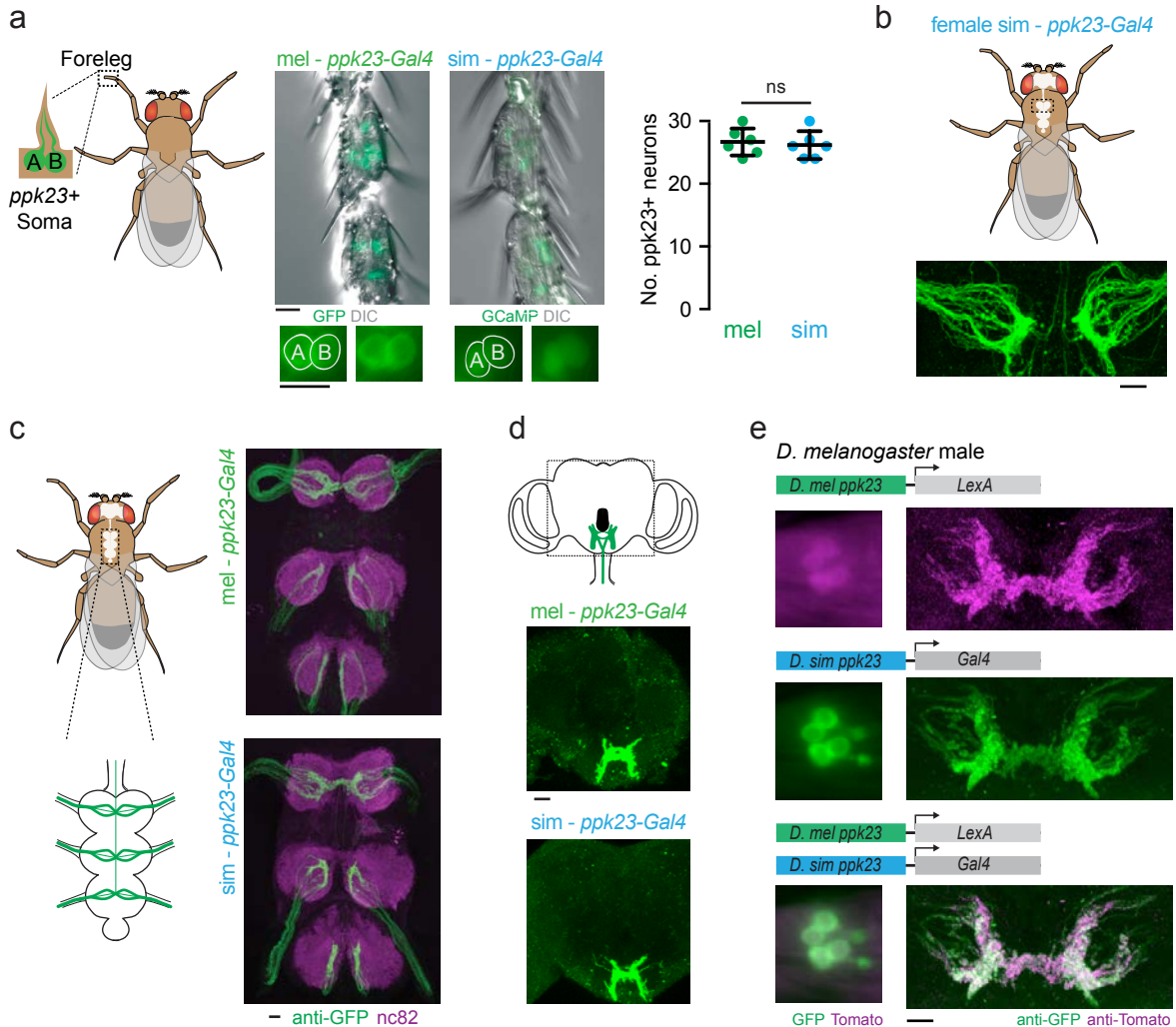
Figure 2.9: Conserved anatomical organization of ppk23+ sensory neurons. a, Schematic (left) and images of *D. melanogaster* and *D. simulans ppk23* promoter expression in the foreleg (middle top) and paired soma of the foreleg (middle bottom), green is GFP or GCaMP expression and grey is DIC. Number of ppk23+ sensory neuron soma in the first three tarsal segments of the foreleg (right) with each dot representing one individual tarsus (n=6, unpaired t-test P=0.7014). **b**, Schematic (top) and image (bottom) of ppk23+ sensory neurons in the VNC of a *D. simulans* females*,* which display a characteristic sexually dimorphic expression pattern in the VNC where they do not cross the midline in females, but do in males. **c**, Schematic of fly VNC (left). *D. melanogaster* and *D. simulans ppk23* promoter expression in the VNC (right), green is anti-GFP staining and magenta is the neuropil counterstain. **d**, Schematic of ppk23+ sensory neuron innervation in the brain (top) and images of the ppk23+ expression in the brain of *D. melanogaster* (middle) and *D. simulans* (bottom) males. **e**, *D. simulans* and *D. melanogaster ppk23*-promoters inserted into the same chromosomal location in the *D. melanogaster* genome drive expression in identical neural populations. *D. melanogaster ppk23-LexA > LexAOP-Tomato* (magenta) and *D. simulans ppk23-Gal4 > UAS-GFP* (green) expression fully overlaps in the male's foreleg soma (left) and axon terminals in the ventral nerve cord (right). Scale bars represent 10 μm.
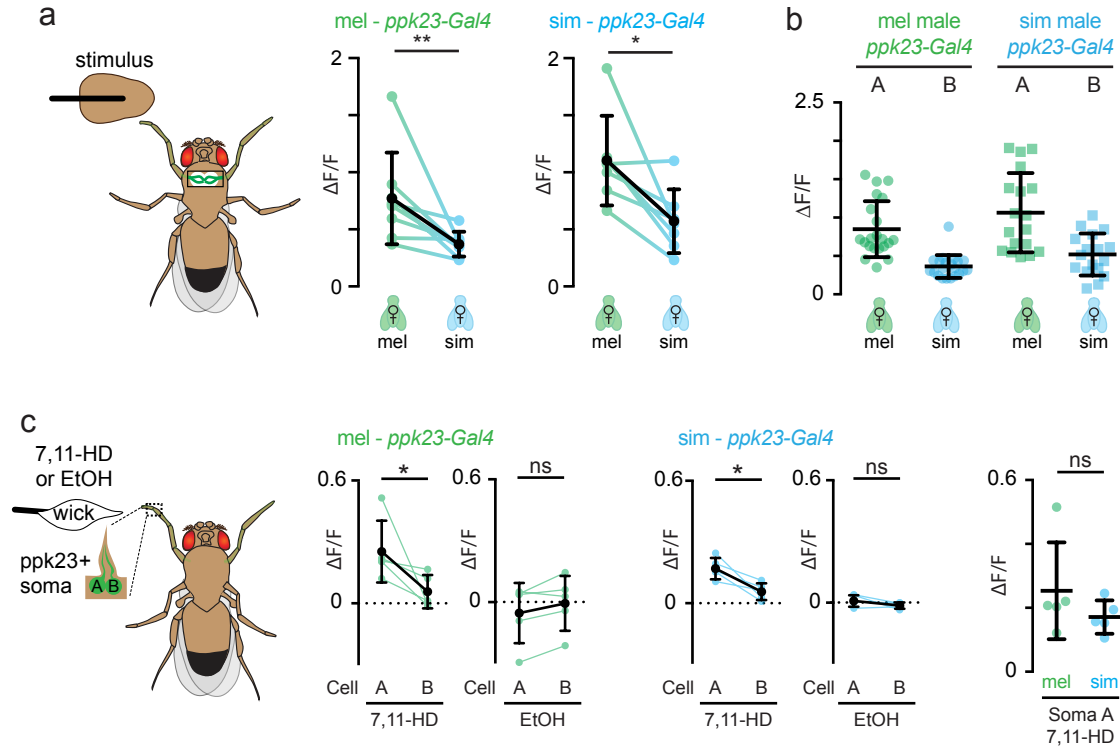
Figure 2.10: Functional conservation of ppk23+ sensory neurons. **a**, Schematic of ventral nerve cord (VNC) imaging preparation and average individual GCaMP responses in ppk23+ fore-leg afferents for *D. melanogaster* and *D. simulans* males when tapping females (n=6, Wilcoxon matched-pairs test mel P=0.0078 and sim P=0.0313). **b**, Tap-evoked GCaMP responses in ppk23+ neurons in the VNC of *D. melanogaster* males and *D. simulans* males (n=15-20 taps per 6 individuals, Kruskal-Wallis test, P<0.0001 for all comparisons, different letters mark significant differences in peak ΔF/F by Dunn's multiple comparisons test). Color dots represent individual taps and black bars and dots represent mean. **c**, Schematic of paired ppk23+ somatic imaging preparation (left) and GCaMP responses when the sensory bristle is stimulated with 7,11-HD or ethanol (right, n=5, Paired t-test, mel 7,11-HD P=0.043, mel EtOH P=0.1250, sim 7,11=HD P=0.022 and sim EtOH P=0.2075). Statistical comparison of 7,11-HD responses in ppk23+ soma across species (left, n=5, unpaired t-test P= 0.2834). Color dots represent individual responses and black bars and dots represent mean and s.d. Lines connect average GCaMP responses in the same male.

not shown), mirroring the weak responses evoked at the population level by the taste of a *D. simulans* female (Fig. 2.10 a).

It is mysterious why both population level and somatic ppk23+ sensory neuron responses were weaker to 7-T than 7,11-HD (Fig. 2.10), considering that the model put forward by the Scott lab was that these soma were always paired in a 1 to 1 ration within the sensory bristle[95–97]. We therefore wanted to examine the aggregate responses of all "female" or "male" ppk23+ sensory neurons using our fictive tapping assay (Fig. 2.11 a). Previous work from the Scott lab suggested that "female" cells are genetically labeled by *ppk25-Gal4*[96,97] (Fig. 2.11 a)*,* as these neurons also express the ENaC channel *ppk25*, which appears necessary for detection of 7,11-HD. "Female" cells also appear to be labeled by vGlut, which is necessary for the packaging of glutamate into presynaptic vesicles for release[105,106], although they are not stained by anti-vGlut antibody (data not shown). Conversely, "male" cells can be genetically labeled using *ppk23-Gal4/vGLUT-Gal80*[97] (Fig. 2.11 a). When we imaged "female" ppk23+ sensory neurons, we observed preferential responses to the taste of a *D. melanogaster* female, consistent with previous behavioral and functional data[96,97,107] (Fig. 2.11 b). However, "male" ppk23+ sensory neurons had equivalently strong responses to the taste of a male and a *D. melanogaster* female with weaker responses to the taste of a *D. simulans* female (Fig. 2.11 c).

Weak responses to *D. simulans* female pheromones in the "male" cells helped clarify why we observed preferential responses to *D. melanogaster* female pheromones in all Fru+/ppk23+ sensory neurons. First, given that "male" cells are actually heterogeneous, there may be overall more ppk23+ sensory neurons tuned to *D. melanogaster* females than tuned to *D. simulans*
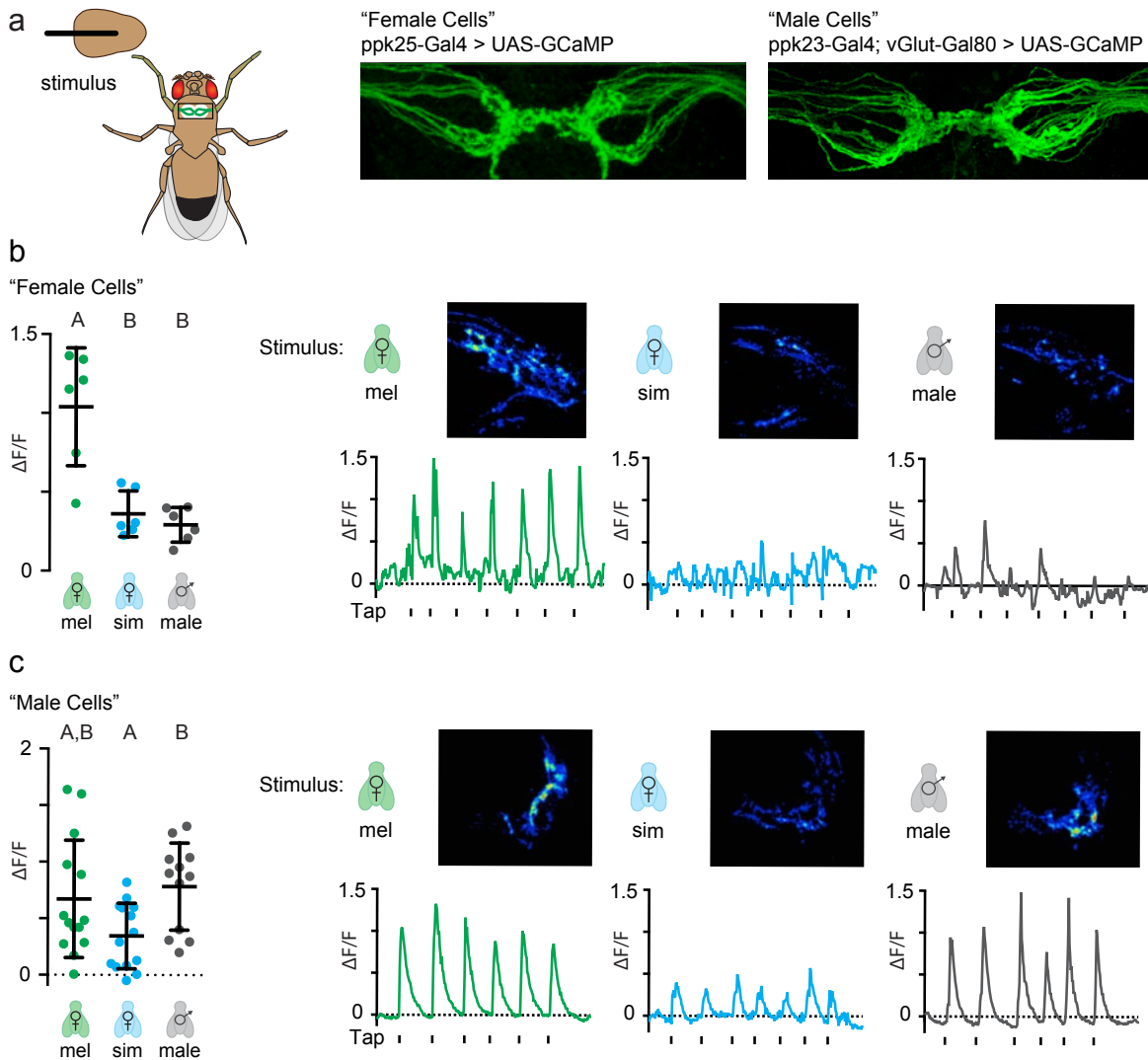
Figure 2.11: Functional heterogenity of *D. melanogaster* ppk23+ sensory neurons. **a**, Schematic of ventral nerve cord (VNC) imaging preparation and innervation pattern of "female" and "male" ppk23+ foreleg afferents in *D. melanogaster* males. **b**, **c**, Tap-evoked GCaMP responses in "female" (**b**) and "male" (**c**) ppk23+ neurons in the VNC of *D. melanogaster* males. Tap-evoked responses (left) with representative examples of ΔF image in the VNC and a ΔF/F response to 6-7 taps (n= taps per individuals, Kruskal-Wallis test, P<0.0001 for all comparisons, different letters mark significant differences in peak ΔF/F by Dunn's multiple comparisons test). Color dots represent individual taps and black bars and dots represent mean.

females, instead of the proposed 1:1 ratio between "male" and "female" cells[95–97]. Second, the "male" cells may only weakly respond to the taste of a *D. simulans* female. This could explain why we did not observe responses in the ppk23+ soma when stimulating with 7-T (data not shown) and why *D. simulans* females suppress *D. melanogaster ppk23* mutant male courtship[99]. Future studies should aim to better understand the genetic identity and functional tuning of the ppk23+ sensory neurons.

2.5   Conserved responses to 7,11-HD in post-synaptic neural population

"Female" and "male" cells can also be defined by the downstream circuitry that they activate. In *D. melanogaster* males, ppk23+ "female" cells respond to 7,11-HD and activate the excitatory ascending Fru+ vAB3 neurons[102] and Fru- PPN1 neurons[97]. However, we found that only vAB3 neurons and not PPN1 neurons respond to the taste of a *D. melanogaster* female (data not shown)[102,108], suggesting that PPN1 may carry non-pheromonal signals. Since there are no easily translatable driver lines labeling vAB3, we modified our *in vivo* preparation to allow us to image an anatomically well-defined and isolated region of vAB3 neurons using fru^{Gal4} (Fig. 2.12 a, b). We validated this preparation first by using *D. melanogaster* AbdB-Gal4, which more selectively labels vAB3 than fru^{Gal4}. In accord with previous results, we found that vAB3 neurons in *D. melanogaster* were only activated by the taste of a *D. melanogaster* female (Fig. 2.12 a). These responses were lost in $ppk23^{-/-}$ mutants (Fig. 2.12 a), which further supports that vAB3 is downstream of *ppk23+* sensory neurons that respond to 7,11-HD. Double-labeling of AbdB+ neurons with Tomato and Fru+ neurons with GCaMP provided additional confidence that we can reproducibly identify and observe responses in vAB3 when it is labeled by fru^{Gal4} (Fig. 2.12 b).
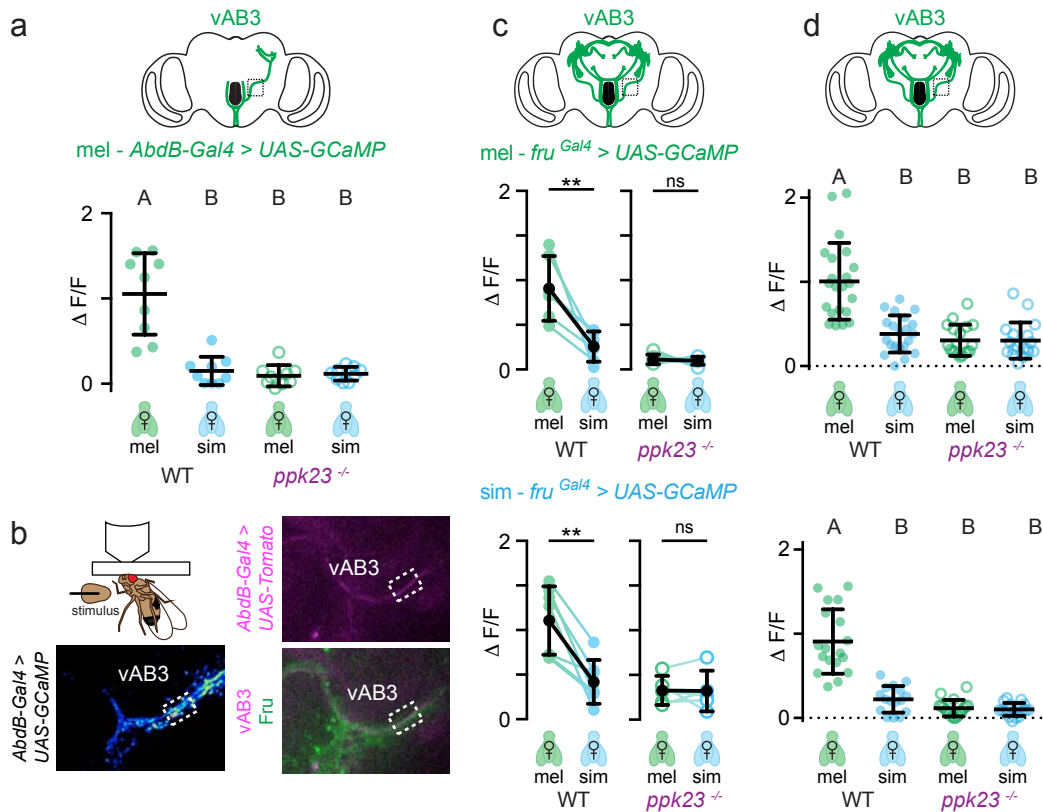
Figure 2.12: Conserved functional responses in vAB3 neurons between species. a, Tap-evoked GCaMP responses to the taste of female pheromones in the fasiculated AbdB+ vAB3 processes of *D. melanogaster* WT and *ppk23⁻/⁻* males (n=9 taps per 3 individuals, Kruskal-Wallis test, P<0.0001). **b**, Schematic of *in vivo* preparation used to measure pheromone responses in vAB3 (top left). Representative multi-plane ΔF image of vAB3 responses in *D. melanogaster* male AbdB+ neurons when tapping a *D. melanogaster* female (bottom left). Anatomy of Fru+ fasiculated vAB3 processes in the *in vivo* preparation. Fru+ neurons shown in green and vAB3 neurons visualized by Tomato expression (right). White box indicates aproximate ROI analyzed. **c**, Intra-animal GCaMP responses visualized in vAB3 using *fru*^Gal4 in *D. melanogaster* (top) and *D. simulans* (bottom) wild type and *ppk23⁻/⁻* males (Paired t-test, n=6-7, mel vAB3 WT P=0.0031 and *ppk23⁻/⁻* P=0.9361, sim vAB3 WT P=0.0093 and *ppk23⁻/⁻* P=0.7189). **d**, Tap-evoked GCaMP responses in the fasiculated vAB3 processes of WT and *ppk23⁻/⁻ D. melanogaster* (top) and *D. simulans* (bottom) males using *fru* ^Gal4 (**d**, n=16-18 taps per 6 individuals, Kruskal-Wallis test, P<0.0001).

One potential circuit change in *D. simulans* could be that the peripheral inputs to vAB3 have been swapped such that this ascending pathway responds to 7-T and not 7,11-HD. However, functional imaging revealed that vAB3 neurons were similarly tuned to pheromones across species, with robust responses elicited by the taste of a *D. melanogaster,* but not a *D. simulans* female (Fig. 2.12 c). Moreover, vAB3 responses to a *D. melanogaster* female were lost in *ppk23* mutants in both species (Fig. 2.12 d). These data suggests that vAB3 retains a conserved role as the post-synaptic partner of 7,11-HD-responsive ppk23+ sensory neurons, providing further support for peripheral conservation of sensory neurons.

2.6   Conserved sensory neuron population drives opposing behaviors

Together, these anatomical, behavioral, and functional experiments all demonstrate that a quantitatively and qualitatively similar ensemble of ppk23+ sensory neurons is tuned to 7,11-HD in both *D. melanogaster* and *D. simulans* males, which implies that there must be changes in the neural circuits downstream of ppk23 and vAB3. To test if activation of ppk23+ sensory neurons could replicate the opposing courtship behaviors elicited by 7,11-HD, we expressed CsChrimson in this sensory neuron population in males of both species and examined how optogenetic activation influenced courtship of a conspecific female. We found that activation of ppk23+ sensory neurons in *D. melanogaster* males drove increased courtship, consistent with previous studies[94,95] (Fig. 2.13 a). In contrast, optogenetic stimulation of the ppk23+ population in *D. simulans* completely inhibited courtship towards an otherwise attractive conspecific female (Fig. 2.13 b), replicating the courtship suppression that results from perfuming a *D. simulans* female with 7,11-HD (Fig. 2.4 b). Activation of the homologous ppk23+ sensory neuron populations is therefore sufficient to drive opposing behavioral responses in *D. melanogaster* and *D. simulans*
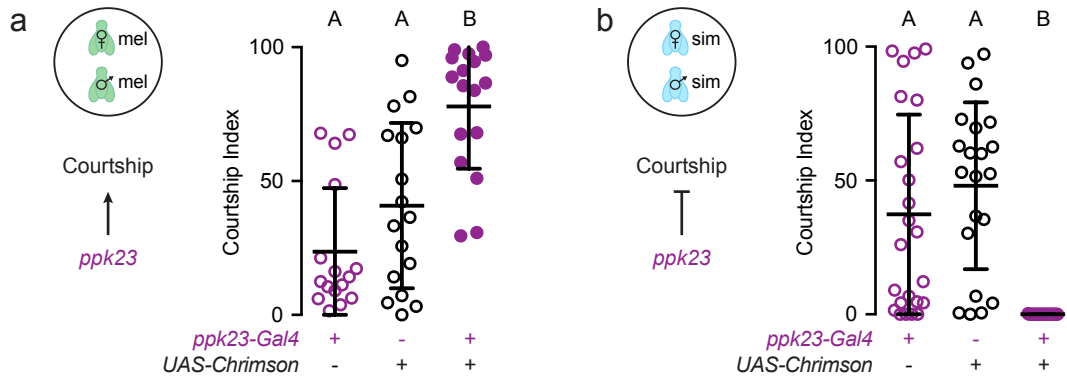
Figure 2.13: Optogenetic activation of ppk23+ sensory neurons drives divergent behaviors between species. a, **b**, Courtship indices of conspecific females during optogenetic activation of parental controls and ppk23+ sensory neurons with CsChrimson in *D. melanogaster* (**a**) and *D. simulans* (**b**) males (n=16-20, Kruskal-Wallis test, P<0.0001, different letters mark significant differences in courtship index by Dunn's multiple comparisons test).

males, suggesting that differences must exist in circuits downstream of vAB3 that link the detection of pheromone cues to courtship decisions.

2.7   Discussion

The sensory periphery has been proposed to be the most evolutionarily labile element of the nervous system[32–36,46], since changes in the expression or tuning of sensory receptors can allow for the emergence of species-specific behaviors without necessitating potentially more complex developmental rewiring of central circuits. However, we found that while ppk23+ sensory neurons drive opposing behavioral responses in *D. melanogaster* and *D. simulans* males (Fig. 2.13), they nevertheless display conserved pheromonal tuning and anatomy (Fig. 2.8, 2.9, 2.10). Moreover, they also equivalently activate the same post-synaptic target that projects into the central brain (Fig. 2.12). Initially, a major criticism of our finding that peripheral sensory responses to 7,11-HD were conserved stemmed from the dogmatic belief the most facile way to alter behavior was by changing the sensory periphery. However, while switches in peripheral expression of sensory receptors are thought to underlie changing responses to sensory cues in many systems, there are very few causal examples.

By all criteria, the sensory neurons that detect 7,11-HD are conserved between *D. melanogaster* and *D. simulans*. The only inter-species difference we could discern was that optogenetic activation of ppk23+ sensory neurons led to divergent behaviors promoting courtship in *D. melanogaster* and suppressing courtship in *D. simulans* (Fig. 2.13). In the absence of characterizing the pheromone tuning of vAB3 neurons, the post-synaptic target of ppk23+ sensory neurons, a reasonable conclusion of our study thus far might have been that conserved

sensory neurons activate different conserved downstream pathways. In *D. simulans,* for instance, 7,11-HD would activate the inhibitory circuit responsive to male pheromones in *D. melanogaster*. However, as I will elaborate upon in the next chapter, we instead find that ppk23+ sensory neurons activate a homologous neural circuit in *D. melanogaster* and *D. simulans*, except a discrete change in the way that circuit processes information has occurred. Although switches in the tuning of sensory neurons may still represent the most facile way to evolve novel sensitivities, my work suggests that alterations to central circuit processing may be more facile for altering the valence of a sensory cue.

3 | Central circuit changes underlie divergent preference for 7,11-HD in *D. melanogaster* and *D. simulans*

3.1 Introduction

While peripheral adaptations are frequently invoked as a facile mechanism for behavioral evolution, there are very few demonstrations of sufficiency of these adaptations. Generation of a robust, innate behavioral change could actually require numerous genetic changes affecting the periphery, not simply swapping receptors.

There is most likely an overrepresentation of peripheral evolution in the literature because changes in peripheral detection have been easier to assess in non-model organisms than central circuitry changes. First, the external sensory periphery is both easier to access and better defined. The well-documented location and morphological characteristics of sensory organs makes homologous structures easier to compare across species. Second, the expansion and diversification of sensory receptors has provided attractive candidate genes for understanding the role of the sensory periphery in behavioral evolution. In central circuits, however, there might never be a single relevant type of gene underlying circuit diversification. Changes in expression of neuropeptides and their receptors are one mechanism for behavioral change[48,49], but unlikely to be the only mechanism. Third, until recently, we have not had the tools to access homologous circuits in other species. Without the ability to carefully compare circuits, there will be a bias in the types of changes described. However, with the advent of CRISPR/Cas9 genome editing, we now have the technical capacity to translate the murine and drosophilid transgenic toolboxes into non-model species.

Below I will describe one the first examples that uses sophisticated *D. melanogaster* transgenic reagents in a non-model species to characterize a central circuit. This study was facilitated by Josie Clowney's detailed description of the neural circuit that processes 7,11-HD in *D. melanogaster*[102] which provided a neuronal blueprint for *D. simulans*.

3.2   Anatomical conservation of excitatory and inhibitory inputs to P1 neurons

In *D. melanogaster* and *D. simulans*, 7,11-HD signals are transmitted from ppk23+ sensory neurons in the foreleg to vAB3 neurons whose dendrites reside in the ventral nerve cord (VNC). In *D. melanogaster*, vAB3 neurons project into the lateral protocerebral complex (LPC) of the higher brain where they provide excitatory drive to the male-specific P1 neurons[102] (Fig. 3.1 a), which integrate input from multisensory pathways and trigger the initiation of courtship in response to a suitable potential mate[97,102,109–113]. vAB3 neurons also extend collaterals into the subesophageal zone (SEZ), where they synapse onto GABAergic mAL interneurons[102] (Fig. 3.1 a). The axons of mAL neurons extensively arborize in the LPC and provide inhibitory input onto P1 neurons, forming a feed-forward inhibitory circuit motif that tempers P1 neuron excitation and stringently regulates the gain of pheromone responses[97,102]. In *D. melanogaster,* P1 neurons thus receive excitatory and inhibitory input even in response to the taste of a conspecific female, with 7,11-HD evoking net excitation to trigger courtship initiation[102]. Anatomical labeling revealed that in both species P1, vAB3 and mAL neurons exhibit rich projections in the lateral protocerebral complex and vAB3 overlaps with mAL neurons in the SEZ (Fig. 3.1, 3.2). Conserved innervation of the LPC by vAB3 and mAL indicates that these inputs remain anatomically poised to synapse onto P1 neurons in both species.

50
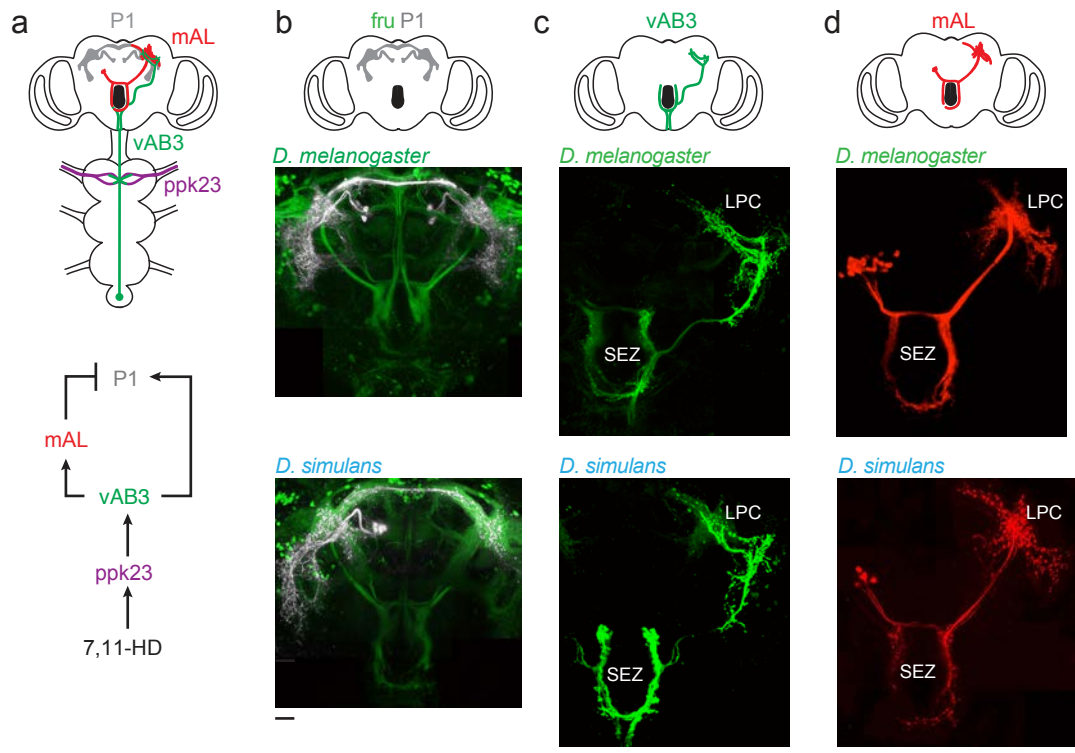
Figure 3.1: Anatomy of Fru+ neurons that process 7,11-HD. a, Schematic summarizing the Fru+ neural circuit that processes 7,11-HD. **b-d**, Schematic (top) and anatomy of P1 (**b**), vAB3 (**c**) and mAL (**d**) neurons as visualized by photoconversion of photoactivatable fluorophores (*D. melanogaster*, middle) or dye-filling with Texas-Red dextran (*D. simulans*, bottom). Scale bars represent 10 μm.

a

P1

D. simulans
fru ^{Gal4}
Texas-Red Dextran

D. simulans
fru ^{Gal4}
Texas-Red Dextran

D. melanogaster
fru ^{Gal4} > UAS-sPAGFP

b

vAB3

c

mAL
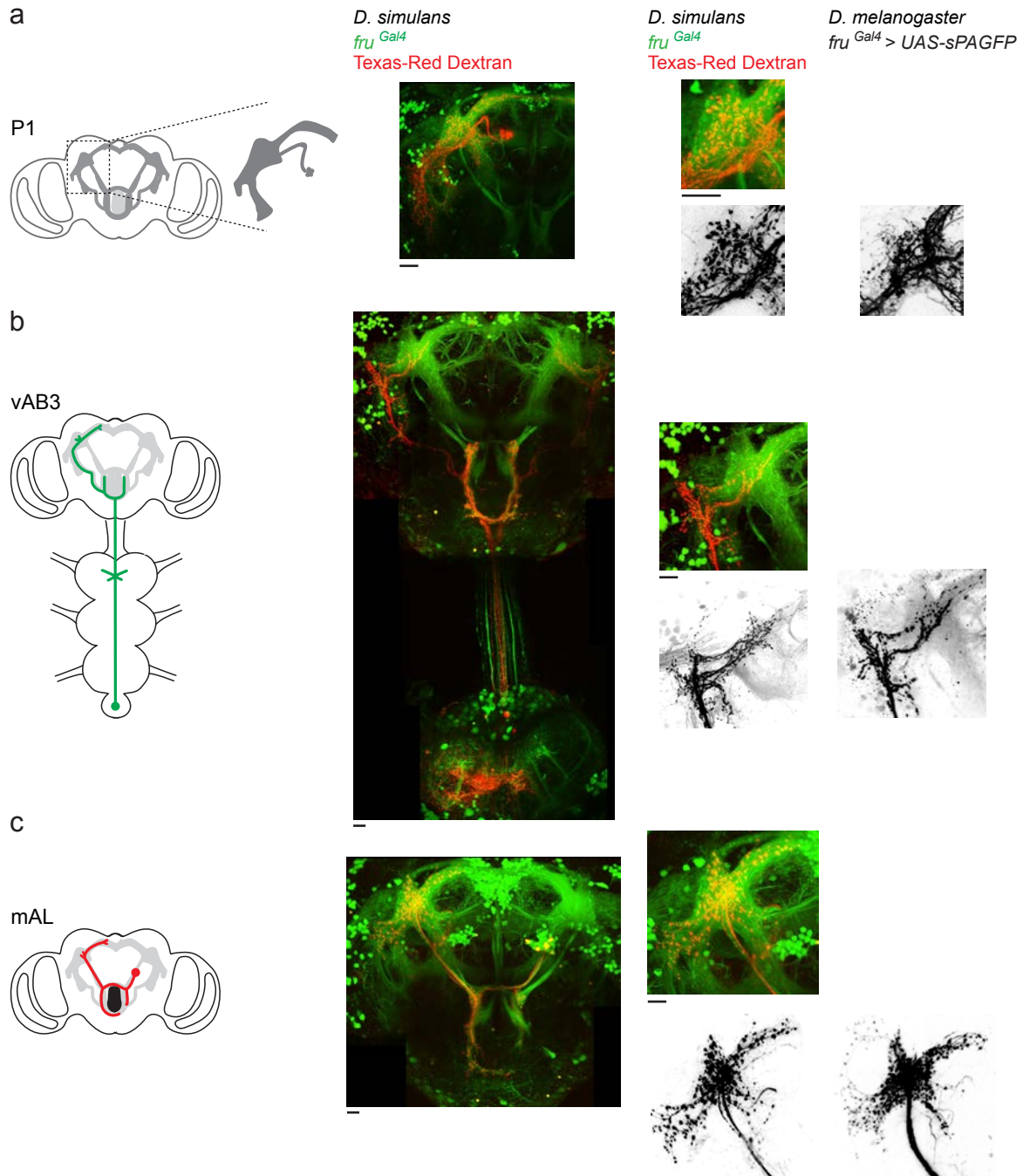
Figure 3.2: Anatomy of *D. simulans* P1, vAB3 and mAL neurons. a-c, Detailed anatomic images of P1 neurons (**a**), vAB3 neurons (**b**) and mAL neurons (**c**). First column has an anatomic cartoon, second column shows Texas-Red dextran dye-fill (red) in *D. simulans fru* ^{GFP} (green) males, third column provides magnified view of the lateral protocerebral complex (LPC) of dye-filled (red) and Fru+ neurons (green) or just dye-filled neuron (black) and fourth column depicts photo-activated neurons in *D. melanogaster* focused on innervation in the LPC (black). Scale bars represent 10 μm.

3.3   P1 neurons are sufficient to drive courtship in *D. melanogaster* and *D. simulans*

Given the anatomic conservation of pheromone pathways across *D. melanogaster* and *D. simulans* males, we considered whether P1 neurons actually play an opposing role in regulating courtship behavior to drive divergent responses to 7,11-HD. In *D. melanogaster,* P1 neurons promote courtship, whereas in *D. simulans,* this neural population may suppress courtship. Thus, in both species vAB3 would excite P1 neurons in response to 7,11-HD, but this would evoke a different behavioral response. To gain genetic access to P1 neurons, our collaborator David Stern (Janelia/HHMI) used phiC-mediated integration to insert the transcriptional enhancer R71G01-Gal4, which labels P1 neurons in *D. melanogaster*[110], into an attP landing site in the *D. simulans* genome. In both species, R71G01-Gal4 labeled P1 neurons (Fig. 3.3 a), which maintained a macroscopically conserved anatomy in which a similar cluster of neurons at the posterior surface of the brain extends a fasiculated axon bundle to the LPC.

To test whether P1 neurons play a conserved role in regulating courtship across species, we expressed CsChrimson in P1 neurons using R71G01-Gal4. As previously demonstrated[102,111,113], optogenetic activation of P1 neurons in *D. melanogaster* was sufficient to drive courtship towards a rotating magnet, an object a male will normally not vigorously court (Fig. 3.3 b). Similarly, optogenetic activation of P1 neurons in *D. simulans* males drove almost incessant courtship of inappropriate targets, including *D. melanogaster* females and a small rotating magnet, and enhanced courtship of conspecific females (Fig. 3.3 c, 3.4). Courtship towards all targets remained elevated after stimulation, indicating that transient P1 activation triggers an enduring state of sexual arousal[102,111,113] (Fig. 3.3 c, d, 3.4). Therefore, the divergent behavioral response in *D. melanogaster* and *D. simulans* to 7,11-HD cannot be attributed to P1 neurons
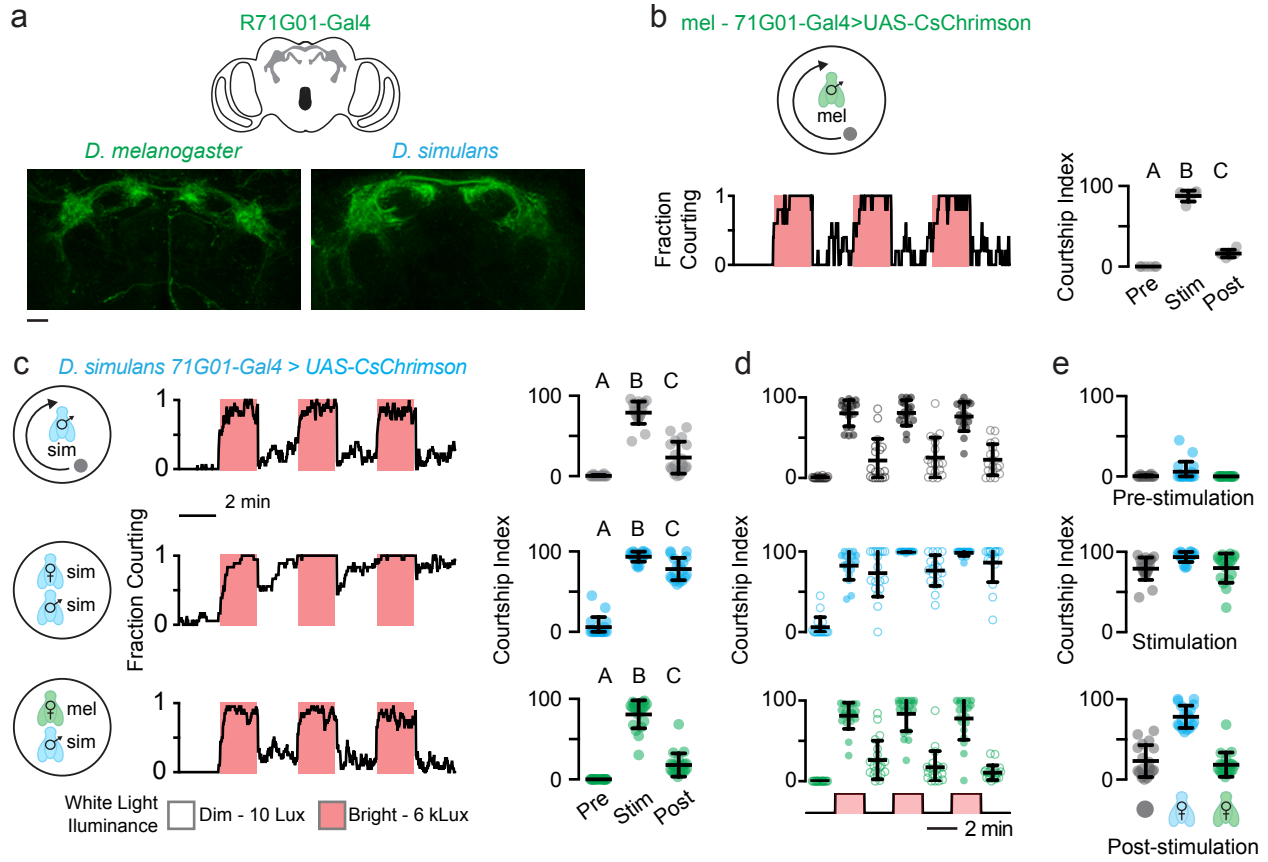
Figure 3.3: P1 neurons drive courtship in *D. melanogaster* and *D. simulans* males. a, The transcriptional enchancer R71G01-Gal4 expresses in both *D. melanogaster* and *D. simulans* male P1 neurons. Scale bar represents 10 μm. **b**, Courtship of a rotating magnet by *D. melanogaster* males expressing CsChrimson in P1 neurons. Fraction of male flies courting a rotating magnet with red boxes denoting time of bright stimulating illumination (left). Courtship index (right) towards a rotating magnet pre-stimulation, during stimulation and after stimulation (n=6, Kruskal-Wallis test, P<0.0001). **c-e**, Courtship by *D. simulans* males expressing CsChrimson in P1 neurons towards a rotating magnet (top), *D. simulans* female (middle), or *D. melanogaster* female (bottom) in dim and bright light. **c**, Fraction of male flies courting with red boxes indicating time of bright stimulating illumination (left). Average courtship index towards different targets pre-stimulation, during stimulation and after stimulation (right, n=18, Kruskal-Wallis test, P<0.0001, different letters mark significant differences in courtship index by Dunn's multiple comparisons test). **d**, Courtship index binned by two-minute sections of the assay. **e**, Courtship index towards different targets before (pre), during (stim) and after (post) stimulation. Colored dots represent an individual's courtship index and black bars represent mean and s.d

54
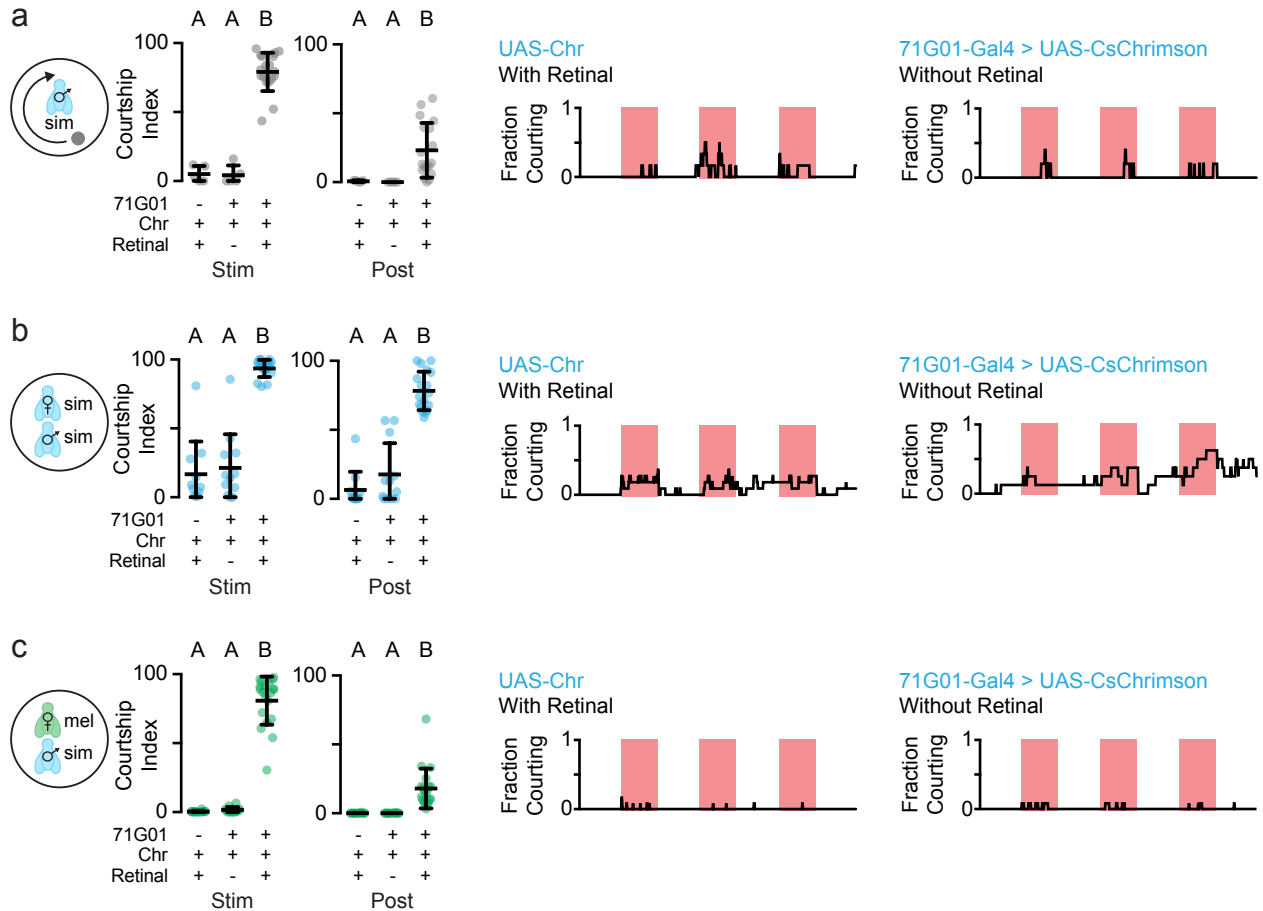
Figure 3.4: Control experiments for *D. simulans* P1 optogenetic activation. a-c, Courtship towards a rotating magnet (**a**), *D. simulans* female (**b**) and *D. melanogaster* female (**c**) by two *D. simulans* control genotypes - males with only the CsChrimson transgene who were fed retinal and males expressing CsChrimson in P1 neurons not fed retinal. Comparison of courtship indicies by *D. simulans* males of control genotypes with males expressing CsChrimson in P1 neurons fed retinal (left) during light stimulation (stim) and after light stimulation (post). Colored dots represent an individual's courtship index and black bars represent mean and s.d. (**a**: n=5-18, **b**: n=12-18, and **c**: n=12-18. Kruskal-Wallis test, P<0.0001 for all ANOVAs, different letters mark significant differences by Dunn's multiple coparisons test for non-parametric data). Fraction of male flies courting with red boxes indicating time of bright stimulating illumination for males of control genotypes (right).

playing distinct roles in controlling male courtship. Rather, in both species, P1 neurons are sufficient to elicit robust and persistent courtship of a moving visual target[71,102,110].

Surprisingly, *D. simulans* wild type males and males carrying just the UAS-CsChrimson allele would occasionally court (for up to 15 seconds) the rotating magnet (Fig. 3.4 a), which did not occur if the magnet was stationary. Sufficiency of visual motion to drive courtship could explain why males of both species robustly court oenocyte-less female flies that lack cuticular pheromones and, further, could explain how courtship in *D. simulans* occurs in the absence of a female-specific contact pheromone. However, since a magnet elicits less courtship than an oenocyte-less female, additional aspects of the fly's appearance, movement, smell or sound must be necessary for eliciting robust courtship behavior. Indeed, wild type *D. simulans* males did not court large, dark *D. virilis* females (Fig. 2.3), who also produce 7-T, suggesting there are probably morphological characteristics of females in the *D. melanogaster* subgroup that *D. simulans* males find attractive. While we are uncertain what visual characteristics are sufficient to initiate robust courtship, motion appears to regulate and promote courtship after P1 neurons have been stimulated. Courtship was significantly reduced when the magnet was stationary or moving slowly, but increased as magnet speed increased (Fig. 3.5). While not statistically significant, courtship was most vigorous when the magnet was at the fastest speed we tested, 20mm/s, which is faster than the average speed of males and females during natural courtship behavior[114]. This observation highlights the importance of motion for vigorous courtship[110,113] and suggests that males are not necessarily tuned to the natural kinematics of female motion.
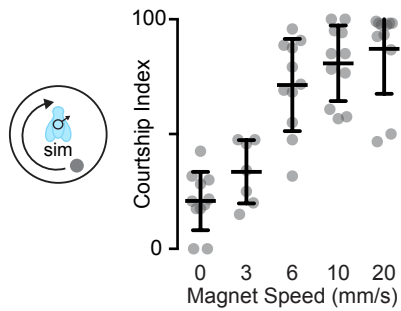
Figure 3.5: Movement of an inherently unattractive target enchanges P1-elicited courtship. Courtship index by *D. simulans* males expressing CsChrimson in P1 neurons towards a magnet rotating at different speeds during bright illumination (n=7-11, One-way ANOVA, P<0.0001. Different letters mark significant differences by Tukey's multiple comparisons test).
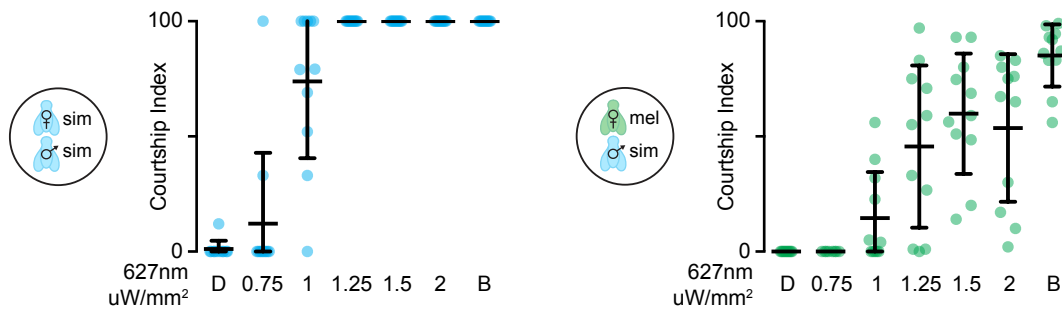
Figure 3.6: Courtship of *D. melanogaster* and *D. simulans* females after P1 neuron stimulation. Courtship towards *D. simulans* females (left) and *D. melanogaster* females (right) as a function of light intensity (n=11) starting with dim white light (D) then adding 627nm light at increasing powers and ending with bright white light (B).

Interestingly, P1 neuron stimulation drove more vigorous courtship towards inappropriate targets like a *D. melanogaster* female or a magnet than we observe for most strains of *D. simulans* when males are paired with a conspecific female (Fig. 3.4). Unlike wild type *D. melanogaster* males, who tend to enter into a persistent state of courtship where males incessantly pursue conspecific females, wild type *D. simulans* males tend to court conspecific females intermittently in short bouts (data not shown). Therefore, it was surprising that brief stimulation of *D. simulans* P1 neurons caused males to shift from short intermittent bouts of courtship to long persistent bouts of courtship (Fig. 3.3 d). This suggests that *D. simulans* males are capable of persistently courting conspecific females with the same vigor as *D. melanogaster* males, but rarely do so naturally. Differences in excitatory input by pheromonal or visual stimuli onto P1 neurons could underlie differences in the inherent vigor or persistence of courtship behavior between *D. melanogaster* and *D. simulans*. For instance, the conspecific female pheromone 7-T may not strongly excite *D. simulans* P1 neurons or P1 neurons may be less excitable in *D. simulans*.

In behavioral assays, while 7-T does not appear to strongly promote courtship[79], 7,11-HD strongly inhibited courtship (Fig. 2.4). Even while directly stimulating P1 neurons, *D. simulans* males still courted a *D. melanogaster* female less than a *D. simulans* female (Fig. 3.3 e). We, thus, wanted to understand if differences exist in the threshold of optogenetically-induced courtship of conspecific and heterospecific females. To modulate the strength of neuronal activation, we increased light intensity every two minutes starting with dim light and ending with bright light. Titrating the stimulating light revealed that evoked courtship in *D. simulans* males was weaker towards *D. melanogaster* females than *D. simulans* females (Fig. 3.6). When courting conspecific females, *D. simulans* males both initiated courtship at lower light intensities

and exhibited higher courtship indices at all light intensities (Fig. 3.6). This observation raises the possibility that 7,11-HD may suppress courtship by countering P1 neuron excitation.

3.4 Divergent pheromone responses within central circuits

Together, these optogenetic experiments reveal that P1 neurons play a conserved role in controlling male courtship in both *D. melanogaster* and *D. simulans* males. To compare how pheromone signals are propagated from the periphery to P1 neurons and other central Fru+ populations, we monitored responses either in the Fru+ neurons of the LPC or in P1 neurons in a tethered male walking on an air-supported ball as he tapped the abdomen of a target fly with his foreleg. To assess pheromone responses specifically in P1 neurons, we attempted to image P1 projections in the LPC using R71G01-Gal4 to drive the expression of GCaMP. In males of both species, the basal fluorescence of GCaMP driven by R71G01-Ga4 was very weak. Nevertheless, we observed robust responses in a *D. melanogaster* male when he tapped a conspecific female (Fig. 3.7 b). P1 neurons in *D. melanogaster ppk23* mutants did not respond to the taste of a *D. melanogaster* female, which further supports the role of ppk23+ sensory neurons in promoting courtship in *D. melanogaster* males (Fig. 3.7 b). In contrast, we observed no response in P1 neurons of *D. simulans* males to the taste of either a *D. melanogaster* or *D. simulans* female (data not shown). While the divergent functional response of P1 neurons in the two species was intriguing, we were concerned that GCaMP expression may be too weak to confidently assess pheromone responses using this genetic reagent. Instead, we imaged the Fru+ fasciulated axons of the P1 neurons as they project into the LPC, which in addition to being anatomically well defined also exhibited higher basal fluorescence than R71G01-Gal4 (Fig. 3.7). Moreover, we could detect equivalent responses to pheromones in other Fru+ neural populations, like ppk23+
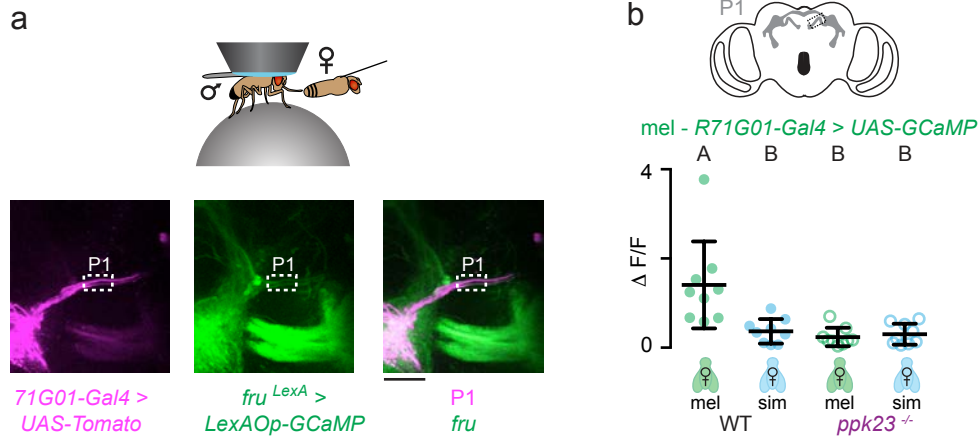
Figure 3.7: Experimental validation for *in vivo* imagaing paradigm of P1 neurons. **a**, Schematic of *in vivo* preparation used to measure pheromone responses (top). Overlay of Fru+ (green) fasiculated P1 processes (magenta) relative to LPC in the *in vivo* preparation (bottom). White box indicates aproximate ROI imaged to measure P1 responses. Scale bar represents 10 μm. **b**, Individual tap-evoked responses in *D. melanogaster* P1 neurons fasiculated processes of WT and *ppk23*^{-/-} males (n=9 taps per 3 individuals, Kruskal-Wallis test, P<0.0001 for both. Different letters mark significant differences by Dunn's multiple coparisons test). Dots represent a tap-evoked GCaMP response and black bars represent mean and s.d.

sensory neurons and vAB3 neurons, suggesting that any differences we observe in P1 neurons are unlikely to be due to differences in GCaMP expression. This preparation also provided an opportunity to assess pheromone responses in the LPC, the neuropil P1 neurons innervate (Fig. 3.8 a, 3.9 a).

The Fru+ neurons in the LPC of *D. melanogaster* males robustly responded to the taste of a *D. melanogaster* female, but not a *D. simulans* female (Fig. 3.8 b), reflecting strong excitation of P1 neurons by the pheromones of an appropriate conspecific mate (Fig. 3.7 b, Fig. 3.9 b)[112,102]. In contrast, in *D. simulans* males neither the P1 neurons or any other Fru+ neural population in the LPC were activated in response to the taste of a *D. simulans* female (Fig. 3.8 c). While initially rather surprising, differential activation of P1 neurons by conspecific females across species is consistent with behavioral evidence that while 7,11-HD promotes courtship in *D. melanogaster* males, 7-T and other pheromones do not promote *D. simulans* courtship[115,79].

The taste of a *D. melanogaster* female weakly activated neurons in the LPC of *D. simulans* males (Fig. 3.8 c). However, these signals failed to propagate to the P1 neurons (Fig. 3.9 c). We speculate that the activity we observed in Fru+ neurons in the LPC to the taste of a *D. melanogaster* female could reflect activation of ascending neurons like vAB3 and mAL, which carry pheromonal information from *ppk23+* sensory periphery to P1 neurons. Responses to the taste of a *D. melanogaster* female in the LPC of both species were lost in *ppk23* mutants verifying that this integrative node relies on ppk23+ sensory pathways for pheromone detection (Fig. 3.10). Opposing behavioral responses to 7,11-HD in the two species, therefore, appear to be mirrored by divergent P1 neuron excitation (Fig. 3.9).
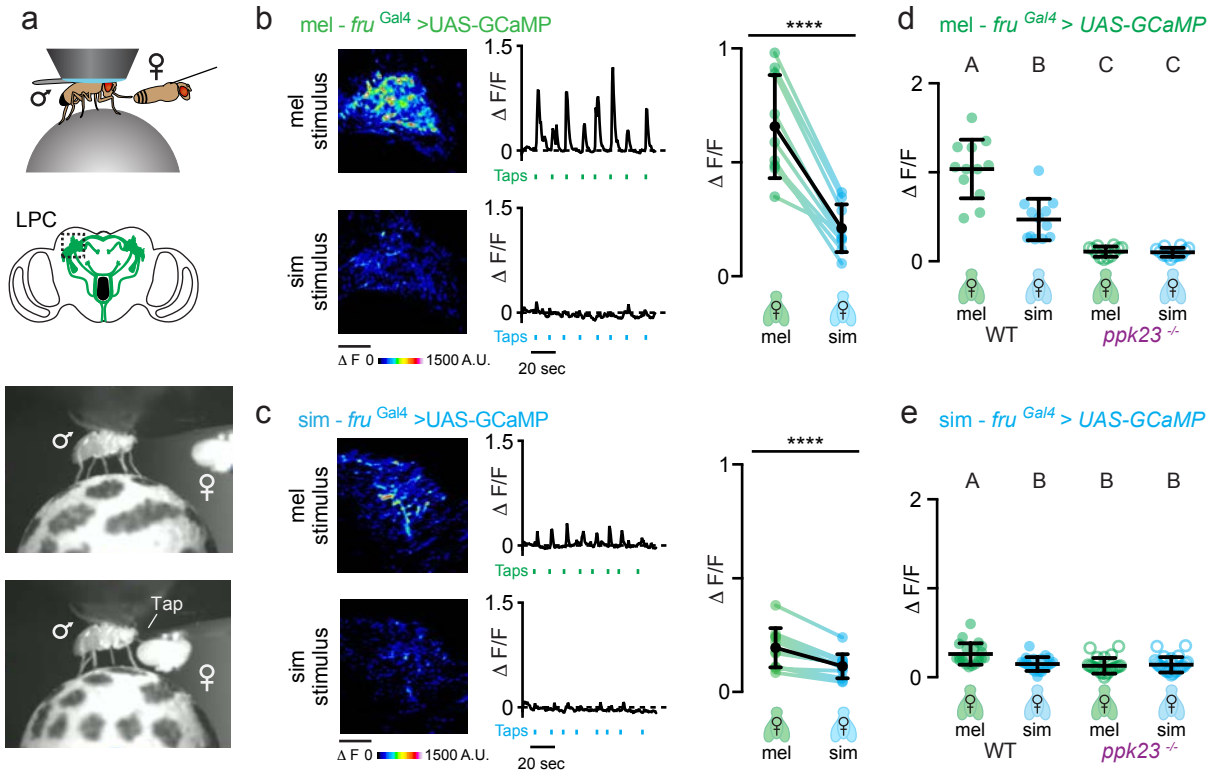
Figure 3.8: Divergent pheromone responses in Fru+ LPC neurons of *D. melanogaster* and *D. simulans* males. **a**, Schematic of *in vivo* preparation used to measure pheromone responses (top), region of Fru+ neurons imaged in the LPC (middle top) and images of the *in vivo* preparation (bottom). **b**, **c**, Functional GCaMP responses visualized in Fru+ neurons in the LPC of *D. melanogaster* males (**b**) and *D. simulans* males (**c**) evoked as a male taps a female abdomen. Representative images depict heat map of fluorescence increase (left) and representative traces depict normalized fluorescence signal for 8 bouts of tapping (middle). Time of each tap indicated by tick mark below graph. Graph summarizes paired intra-animal averages with colored dots representing average individual responses and black bars and dots representing mean and s.d (right, paired t-test. mel n=9, P<0.0001. sim n=12, P<0.0001). **d**, **e**, Individual tap-evoked responses in Fru+ neurons in the LPC of WT and *ppk23⁻/⁻* males (n=15-20 taps per 6 individuals, Kruskal-Wallis test, P<0.0001 for both, different letters mark significant differences by Tukey's multiple comparisons test). Dots represent individual a tap-evoked GCaMP response and black bars represent mean and s.d.
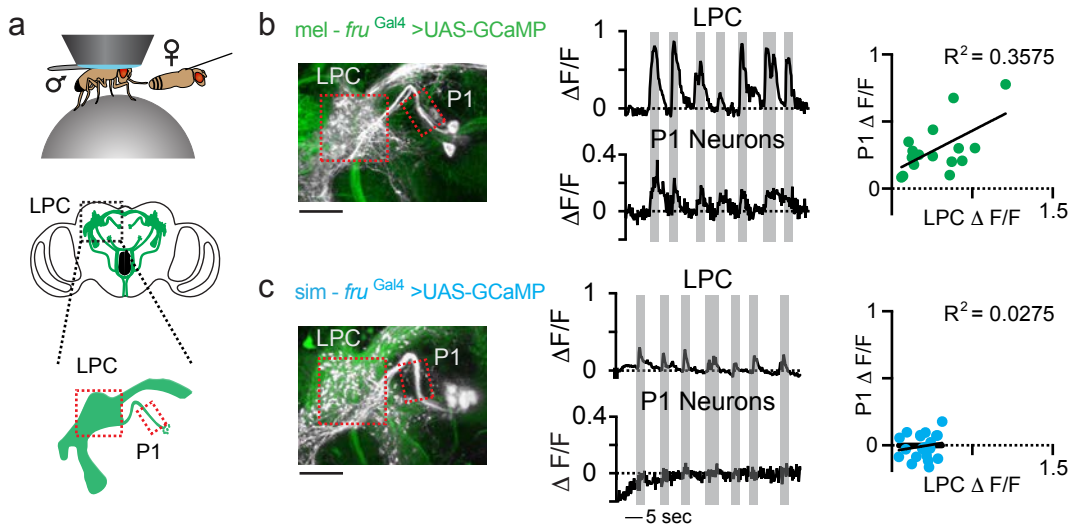
Figure 3.9: Divergent pheromone responses in courtship-promoting P1 neurons of *D. melanogaster* and *D. simulans* males. a, Schematic of *in vivo* preparation used to measure pheromone responses (top) and region of Fru+ neurons imaged in the LPC and P1 axonal tract (bottom, red boxes indicating imaged regions). **b**, **c**, GCaMP responses in LPC and P1 neurons while simultaneously imaging these regions of the brain in response to the taste of a *D. melanogaster* female in *D. melanogaster* (**b**) and *D. simulans* (**c**) males. Zoomed-in view of P1 innervation of Fru+ LPC (left). Representative traces (middle, grey bars indicate taps) and graph (right) depicting the relationship between functional responses in P1 neurons and the LPC (n=6 flies. Linear regression, slope mel=0.4114 and sim= -0.002). Dots represent a tap-evoked GCaMP response and black bars represent mean and s.d. Scale bars represent 10 μm.

3.5 mAL neurons detect 7,11-HD and suppress courtship

Given the structural conservation of vAB3 and mAL neurons, we considered whether there might be functional differences in how pheromone signals are propagated through this circuit to generate divergent P1 neuron responses. For instance, the equivalent responses to 7,11-HD we observed in vAB3 could be differentially propagated to mAL neurons, a GABAergic inhibitory neural population in both species (Fig. 3.10 b). Relatively stronger mAL neuron responses to 7,11-HD in *D. simulans* could alter the balance of excitation and inhibition onto P1 neurons, giving rise to the divergent pheromone responses we observe. This model would point to mAL as an important locus of change in the circuit whereby enhanced mAL excitability or stronger vAB3 input to mAL could produce enhanced 7,11-HD signaling through this inhibitory pathway.

To gain genetic access to mAL neurons, David Stern used PhiC-mediated integration to insert the genetic driver R25E04-Gal4, which labels mAL neurons in *D. melanogaster*, into an attP landing site in the *D. simulans* genome (Fig. 3.10 a). In both species, 25E04-Gal4 labeled mAL neurons with the same characteristic morphology observed when anatomically labeling this Fru+ population in the brain (Fig. 3.1, 3.2). As previously reported in *D. melanogaster*[97,116], optogenetic activation of mAL neurons in *D. simulans* strongly attenuated male courtship towards a conspecific female (Fig. 3.10 c). Therefore, inhibition of neurons in the LPC by this GABAergic population is sufficient to suppress courtship in both species, suggesting that mAL neuron are an essential population for regulating a male's courtship behavior.

64
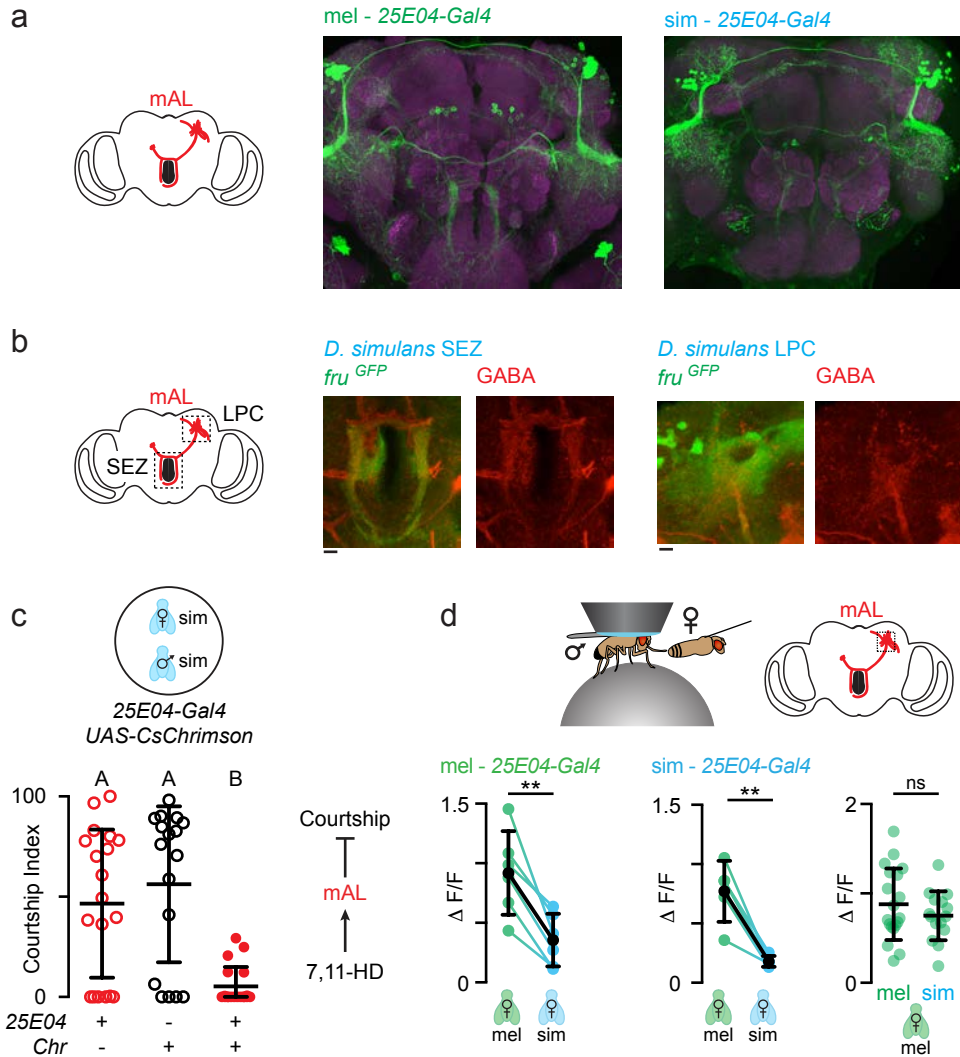
Figure 3.10: Conserved behavioral role and functional tuning of mAL neurons in *D. melanogaster* and *D. simulans* males. **a**, Expression of *25E04-Gal4 > UAS-GCaMP* (green) with neuropil counterstain (magenta) in the brains of *D. melanogaster* (left) and *D. simulans* (right) males **b**, Antibody staining of *D. simulans* Fru+ neurons (anti-GFP, green) with anti-GABA (red) in the SEZ and lateral protocerebral complex shows that mAL neurons are GABAergic and thus inhibitory. Scale bars represent 10 μm. **c**, Courtship index of conspecific females during optogenetic activation of *D. simulans* male mAL neurons with parental controls (n=17-20, Kruskal-Wallis test, P<0.0001. Different letters mark significant differences by Dunn's multiple comparisons test for non-parametric data). **d**, GCaMP imaging of average paired responses in mAL neurons (n=6 individuals, paired t-test, P=0.005 and P=0.0059, respectively) and *D. melanogaster* female tap-evoked responses in mAL neurons (n=6 individuals with 2-3 taps per individual, unpaired t-test, P=0.2981). Colored dots represent average ΔF/F for an individual and black bars represent mean and s.d.

Functional imaging revealed that mAL neurons preferentially responded to the taste of a *D. melanogaster* female over a *D. simulans* female in both species (Fig. 3.10 d). However, the mAL neurons of *D. simulans* and *D. melanogaster* males responded equivalently to the taste of a *D. melanogaster* female (Fig. 3.10 d), suggesting that vAB3 provides similar excitatory drive to this inhibitory neural population in both species. These results, therefore, suggest that divergent P1 neuron responses are not likely mediated by a change in signaling from vAB3 to mAL neurons, but rather arise from alterations in signaling from vAB3 and mAL to P1 neurons.

To explore how mAL mediated inhibition may shape mate preferences, we wished to alter mAL inhibition onto P1 *in vivo*. In *D. melanogaster*, expression of the *Rdl* subunit of the GABA-A receptor in P1 neurons is necessary for male-male courtship suppression[97]. Similarly, we found that expression of the *Rdl* subunit in P1 neurons is also necessary for species discrimination (Fig. 3.11 a). While parental control (*UAS-Rdl-RNAi*) males could robustly discriminate between females, males indiscriminately courted conspecific and heterospecific females when the *Rdl* subunit was knocked-down in *D. melanogaster* P1 neurons (Fig. 3.11 a).

Although we lack the genetic reagents to replicate this experiment in *D. simulans*, we instead tested if pharmacological weakening of inhibition in the LPC changes pheromone responses *in vivo*. Since GABA-A receptors are necessary for mAL inhibition of P1 neurons[97], we locally injected a GABA-A receptor antagonist, picrotoxin, into the LPC. While we do not know which synaptic connections picrotoxin is modulating in the LPC, as it is a complex neuropil innervated by many Fru+ neurons, this pharmacological manipulation could potentially disrupt mAL signaling onto P1. Males of both species exhibited preferential responses to the taste of *D.*
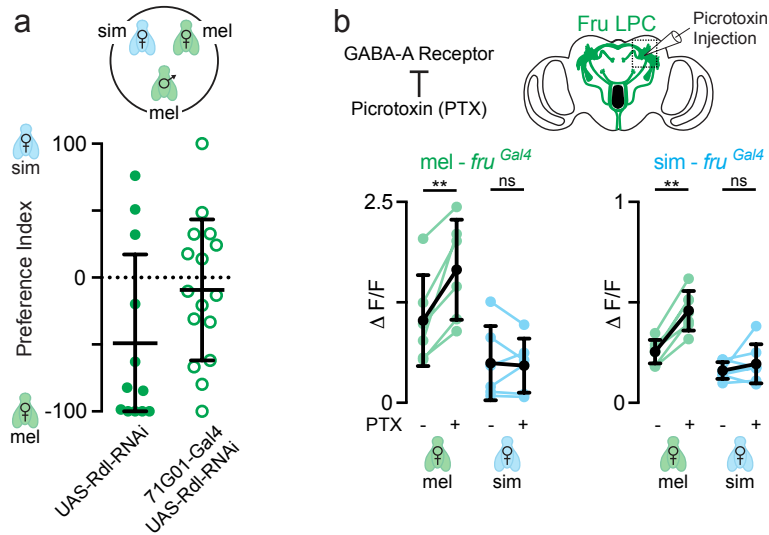
Figure 3.11: Modulating inhibition in the LPC of *D. melanogaster* and *D. simulans* males. a, Courtship preference in control males and males with GABA receptors knocked down in P1 neurons. **b**, Average intra-animal GCaMP responses in Fru+ neurons of the LPC evoked by female pheromones before and after local injection of picrotoxin, a GABA receptor antagonist, into the LPC. In males of both species, application of picrotoxin elicited greater responses only for *D. melanogaster* female stimuli. Lines connect average GCaMP responses in the same male towards the different female targets (n=6-7 individuals, Paired t-test, mel tap mel P=0.0089, mel tap sim P=0.7516, sim tap mel P=0.0001 and sim tap sim P=0.3620). Colored dots represent average ΔF/F for an individual and black bars represent mean and s.d.

melanogaster female pheromones both before and after picrotoxin application (Fig. 3.11 b). However, after picrotoxin application, responses to *D. melanogaster* females, but not *D. simulans* females, significantly increased in males of both species (Fig. 3.11 b), suggesting that picrotoxin is selectively unmasking 7,11-HD-specific excitation in the LPC without altering the overall excitability of this neuropil. These data indicate that in both *D. melanogaster* and *D. simulans* males a structurally and functionally conserved feed-forward inhibitory circuit exists that is tuned to the taste of *D. melanogaster* females.

Together, these experiments raise the possibility that changes in the strength of mAL and vAB3 signaling to P1 neurons might underlie the emergence of species-specific mate preferences, such that 7,11-HD can evoke excitation of P1 neurons only in *D. melanogaster* males to initiate courtship of a *D. melanogaster* female.

3.6 Species differences in excitatory and inhibitory input to P1 neurons

To examine the possibility that changes in the balance of excitation and inhibition onto P1 neurons may explain their divergent pheromone responses across species, we exogenously stimulated vAB3 neurons in the VNC and monitored responses in all Fru+ neurons in the brain. This unbiased technique permitted comparisons of activation patterns in neurons downstream of vAB3. Our *ex vivo* stimulation method relies on local iontophoresis of the excitatory neurotransmitter acetylcholine onto the spatially segregated ppk23 axons and vAB3 dendrites within the VNC (Fig. 3.12 a). Only a sparse population of neurons in *D. melanogaster* are activated (vAB3, mAL and P1 neurons) even if GCaMP is expressed pan-neuronally[102].
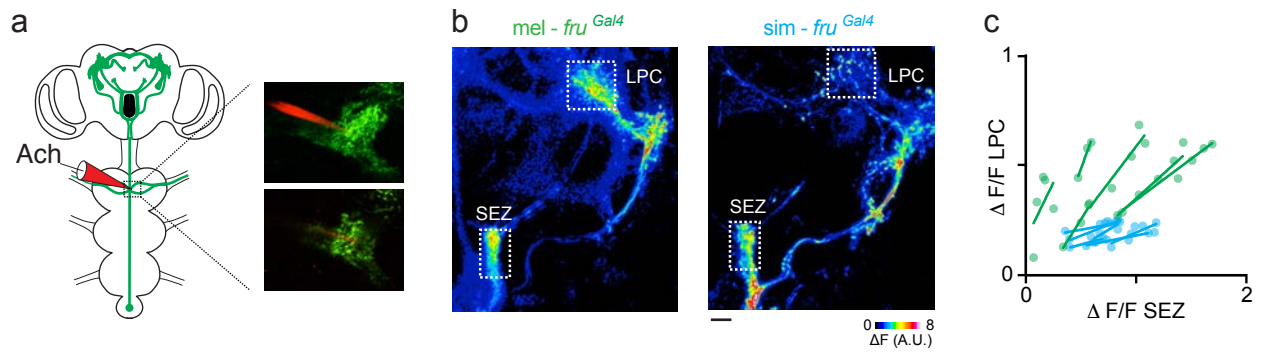
Figure 3.12: Differential propagation of vAB3 stimulation to the LPC. a, Schematic depicting stimulation of vAB3 neurons by acetylcholine iontophoresis in the ventral nerve cord and activated Fru+ neurons in the central brain (top left). **b**, Representative multi-plane image of GCaMP responses in Fru+ neurons in *D. melanogaster* (left) and *D. simulans* (right) males. Boxes highlight suboesophageal zone (SEZ) and lateral protocerebral complex (LPC). **c**, Graph depicts relationship between responses in the SEZ and LPC in *D. melanogaster* (green) and *D. simulans* (blue) males. Dots on graph represent different stimulation intensities and lines connect an individual male (n=6 animals). Scale bar represents 10 μm.
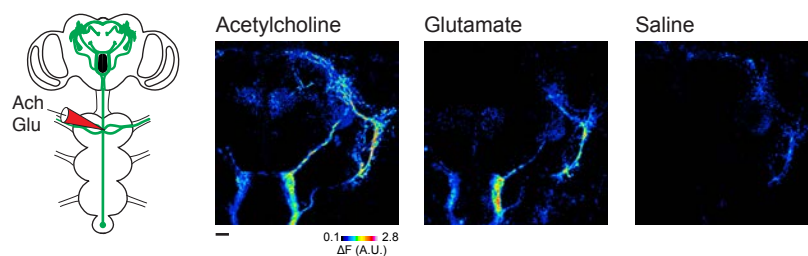
Figure 3.13: Stimulation of vAB3 using different neurotransmitters in *D. simulans* males. Representative multi-plane image of GCaMP responses in Fru+ neurons in *D. simulans* males when the VNC is stimulated with acetylcholine (left), glutamate (middle) and saline (right). Scale bar represents 10 μm.

We performed multi-plane functional imaging of Fru+ neurons in response to stimulation of vAB3 neurons and generated an anatomical map of functionally activated neurons in the brain (Fig. 3.12 b). In *D. melanogaster* males, the vAB3 pathway and its postsynaptic targets in the LPC, including mAL and P1 neurons, were activated[102] (Fig. 3.12 b). In *D. simulans*, a similar pattern of activity was evoked. One notable difference, however, was that the robust excitation of mAL and vAB3 neurons failed to propagate to the LPC (Fig. 3.12 b). While increasing iontophoretic voltages drove progressively greater excitation of the intermingled mAL and vAB3 projections in the SEZ, we observed only marginally increased activity in the LPC in *D. simulans* males (Fig. 3.12 c). In contrast, activity in both the SEZ and LPC increased proportionally with stronger stimulation in *D. melanogaster* males (Fig. 3.12 c).

A similar pattern of activity was evoked in Fru+ neurons in *D. simulans* when either acetylcholine or glutamate, but not saline, was iontophoresed onto vAB3 terminals (Fig. 3.13), as observed in *D. melanogaster* males[102]. In *D. melanogaster,* the subset of "female" ppk23+ sensory neurons is labeled by vGLUT-Gal4[97] suggesting that glutamate is an excitatory neurotransmitter released onto vAB3 neurons. Although an anti-vglut antibody does not label these neurons in *D. melanogaster* (data not shown), complicating the identification of the neurotransmitter they release in *D. simulans*, conservation of glutamate responses between species suggests that in both species ppk23+ sensory neurons may release glutamate to activate vAB3. Preliminary experiments suggested that acetylcholine might either directly activate vAB3 dendrites or activate "female" ppk23+ sensory neurons that are pre-synaptic to vAB3 (data not shown).
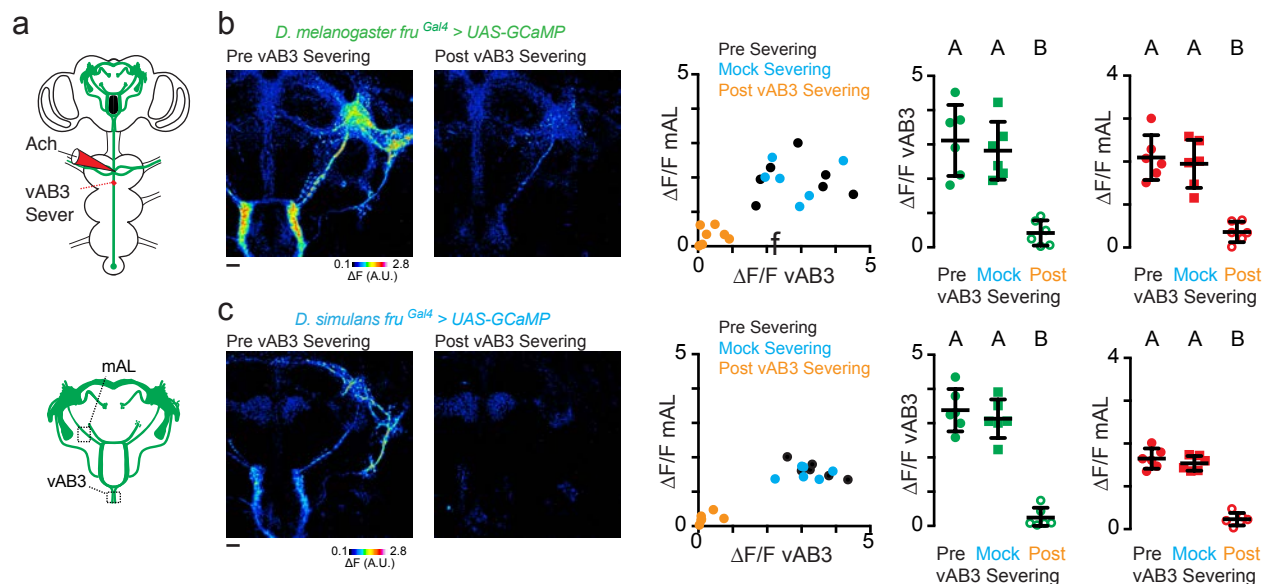
Figure 3.14: Responses evoked by *ex vivo* vAB3 stimulation in *D. melanogaster* and *D. simulans* males. a, Schematic and representative image depicting stimulation of vAB3 neurons by neurotransmitter iontophoresis in the ventral nerve cord. **b**, **c**, To test the necessity of vAB3 in propagating signals from the VNC to the higher brain, we compared response profiles in the brain before severing vAB3 (black), after first severing a nearby Fru+ axon (mock control, blue) and then after severing vAB3 (orange) in *D. melanogaster* males (**b**) and *D. simulans* males (**c**). Representative multi-plane image of GCaMP responses in Fru+ neurons (left) show the loss of signal in the brain after severing vAB3. Graph (middle) depicts relationship between average individual responses in vAB3 and mAL neurons. Average individual responses in vAB3 (green) and mAL (red) were measured before and after severing vAB3 axons. Responses were lost in both neural populations across both species after vAB3 severing but not mock severing (n=6, Kruskal-Wallis test, P<0.0001, different letters mark significant differences in peak ΔF/F by Dunn's multiple comparisons test). Scale bar represents 10 μm.

In both *D. melanogaster* and *D. simulans* males, we observed no responses in Fru+ neurons of the brain after severing the vAB3 axons in the VNC with a two-photon laser to prohibit them from transmitting excitatory signals to the brain (Fig. 3.14). Severing nearby Fru+ ascending fibers in the VNC (mock control) yielded no reduction in activity, confirming the specificity of this manipulation (Fig. 3.14). Therefore, while we cannot determine if acetylcholine iontophoresis exclusively activates vAB3, this result demonstrates that activity in vAB3 and mAL neurons depends on this ascending pathway (Fig. 3.14).

vAB3 neurons, therefore, appear to drive quantitatively distinct activity patterns in the LPC of *D. melanogaster* and *D. simulans* males. To assess if this reflected differential excitation of P1 neurons, we imaged the processes of vAB3, mAL, and P1 neurons in response to vAB3 stimulation (Fig. 3.15 a). We found that while vAB3 and mAL neuron responses were equivalent (Fig. 3.15 b, c), P1 neurons were excited only in *D. melanogaster* and not in *D. simulans* males (Fig. 3.15 d), mirroring the differential *in vivo* propagation of pheromone signals through this pathway (Fig. 3.9).

We therefore considered two alternative models for P1 neuron suppression. First, *D. simulans* vAB3 neurons could no longer be functionally connected to P1 neurons, thus the role of vAB3 is to activate mAL neurons, which in turn suppress P1 neurons. Second, vAB3 neurons could still be functionally connected to P1 neurons with mAL-mediated inhibition countering the excitatory drive of vAB3 inputs. Both models would result in active suppression of P1 neuron responses in *D. simulans*. After severing the fasciculated mAL axonal tract with a two-photon laser, we found

72

that P1 neurons could now be excited by vAB3 stimulation in *D. simulans* males, although to a lower level than in *D. melanogaster* males (Fig. 3.15d, g). These results suggest that vAB3 is still capable of activating P1 neurons and further explain why pharmacological weakening of inhibition in the LPC would lead to increased responses to the taste of a *D. melanogaster* female pheromone (Fig. 3.11 b). Importantly, this experiment demonstrates that mAL-mediated inhibition antagonizes vAB3 excitatory input to fully suppress P1 neuron responses in *D. simulans,* but not *D. melanogaster* males, revealing how alterations in the balance of excitation and inhibition onto P1 neurons may generate divergent responses to the same pheromone cue.
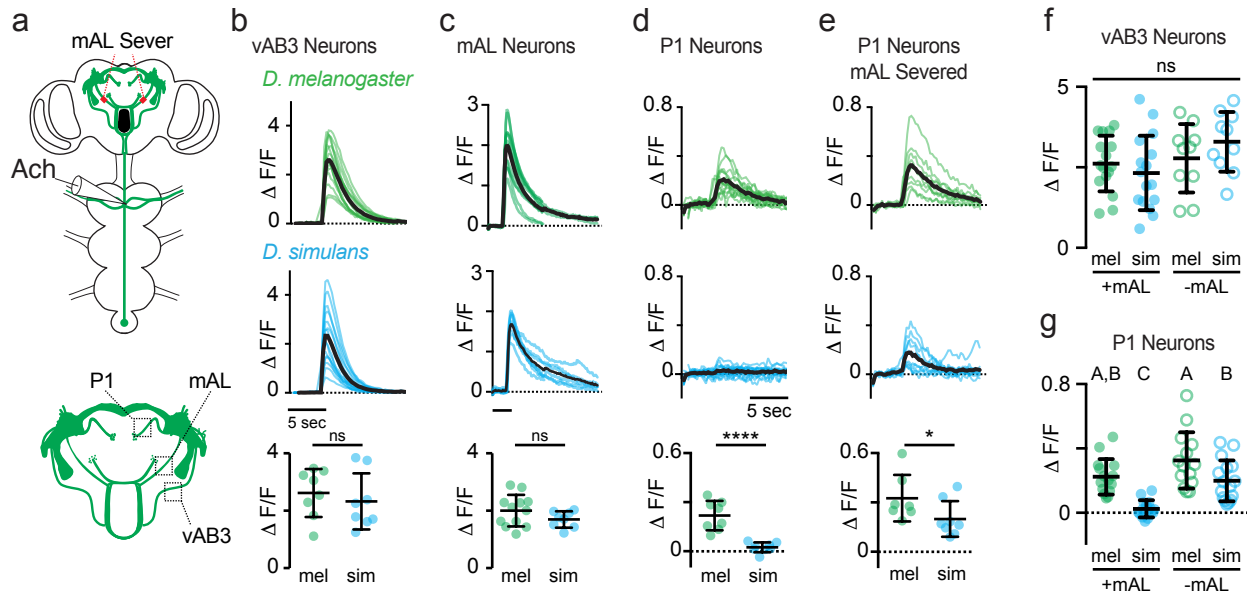
Figure 3.15: Differential propagation of ascending signals to P1 neurons. a, Schematic depicting stimulation of vAB3 neurons in the ventral nerve cord and approximate region of P1, mAL and vAB3 neurons imaged. **b-e**, *D. melanogaster* and *D. simulans* response to vAB3 stimulation measured in vAB3 neurons (**b**), mAL neurons (**c**), and P1 processes before (**d**) and after (**e**) mAL severing. Colored lines (*D. melanogaster* is green and *D. simulans* is blue) represent single stimulations and black line represents the average (n=14-16). Peak ΔF/F plotted on bottom with colored dots representing average response per animal and black bars representing mean and s.d. (n=7-8 animals, unpaired t-test, P = 0.4508, P = 0.1636, P < 0.0001 and P = 0.0318, respectively). **f-g**, Comparison of *D. melanogaster* and *D. simulans* response to vAB3 stimulation measured in vAB3 neurons (**f**) and P1 neurons (**g**) before and after mAL severing (n=14-16 stimulations in 7-8 animals, Kruskal-Wallis test, P = 0.1442 and P<0.0001, different letters mark significant differences in peak ΔF/F by Dunn's multiple comparisons test).

3.7   Discussion and Future Directions

In contrast to the prevailing view that the sensory periphery is the most evolutionary labile component of the nervous system, our data suggest that species-specific behavioral responses to 7,11-HD are mediated by modifications to the central circuits that process pheromone information. In both *D. melanogaster* and *D. simulans* males, we find that 7,11-HD signals are relayed from the foreleg to the P1 neurons through a structurally similar circuit comprised of parallel excitatory and feed-forward inhibitory branches (Fig. 3.1). Despite this anatomical conservation, our data provide evidence for striking differences in circuit function across species such that equivalent mAL and vAB3 activity is transformed into differential P1 neuron excitation in *D. melanogaster* and *D. simulans* males (Fig. 3.9, 3.15).

One argument against behavioral evolution emerging through central circuit changes is that this might necessitate developmental rewiring of complex circuitry. Re-wiring of neural circuits does occur, for instance, in the feeding circuitry of the related nematode worms *C. elegans* and *Pristionchus pacificus,* which last shared a common ancestor 200-300 million years ago[60]. However, our limited understanding of how novel functional connections are formed makes it is difficult to imagine how such changes may occur over short evolutionary time periods. By contrast, the central circuit changes we propose do not require the derivation of novel neural pathways, but rather could be mediated by simple functional changes in the level of excitation and inhibition onto P1 neurons that control courtship. Interestingly, in *D. melanogaster,* P1 neuron excitability is regulated by the social history[111] and sexual satiety of a male[117]. This suggests that circuitry changes mediated evolutionary adaptations could resemble experience-dependent changes that occur in an individual.

Behavioral differences between the two species could rely on a variety of changes in gene expression in vAB3 neurons, mAL neurons or P1 neurons. While not an exhaustive list, below I will highlight a few simple changes that could have occurred in *D. simulans*.

Preliminary evidence suggests that vAB3 releases acetylcholine onto P1 neurons to drive activity. Therefore, if acetylcholine receptors were down regulated in *D. simulans* P1 neurons, net inhibition could occur through weaker vAB3 excitation. Support for this model comes from the observation that directly iontophoresing acetylcholine into the LPC evokes less activity in the *D. simulans* Fru+ neurons (data not shown). The complex nature of the Fru+ LPC makes this observation difficult to interpret, but one explanation is that *D. simulans* P1 neurons are less responsive to acheylcholine. More compellingly, we observed that equivalent vAB3 activation in the absence of mAL inhibition drives less activity in P1 neurons in *D. simulans*. Weaker vAB3 excitation of P1 neurons could also be due to presynaptic changes that cause vAB3 neurons to release less acetylcholine.

Alternatively, the balance of excitation and inhibition onto P1 neurons could also be changed by up-regulation of GABA-A receptors in P1 neurons. A greater concentration of GABA-A receptors could make P1 neurons more sensitive to inhibitory inputs. There could also be presynaptic changes in GABA release by mAL neurons.

In addition to changes in neurotransmitter signaling between pre- and post-synaptic partners, there are numerous other changes that could have occurred in *D. simulans* males. Anatomical

changes we could not readily detect like fine-scale anatomic rewiring or changes in the number of synaptic connections, with either more mAL boutons or less vAB3 boutons could alter functional connectivity. Furthermore, neuromodulatory changes that could alter the balance of excitation and inhibition onto P1 neurons, allowing for anatomically conserved circuits to have distinct output. Ultimately, comparing differences fine-scale anatomy or RNA expression profiles across homologous neural populations in different species could provide insight into molecular mechanism.

Although in principle, functional diversification could have occurred at multiple points within this pathway, our observations suggest that a key node for evolutionary variation is likely at the level of P1 neuron integration itself. However, other neurons within the LPC that control courtship may also receive differential mAL and vAB3 input and contribute to divergent mate preferences. By altering the balance of excitatory vAB3 and inhibitory mAL signaling onto downstream targets, 7,11-HD is transformed from an excitatory signal that promotes courtship in *D. melanogaster* into an inhibitory signal that suppresses courtship in *D. simulans*.

In the future, it will be important to determine if 7,11-HD drives net inhibition of P1 neurons in *D. simulans*. The most direct demonstration of inhibition would be to record electrophysiological currents from P1 neurons as a male taps onto a female's abdomen. We would predict strong hyperpolarization in response to the taste of a male or *D. melanogaster* female and no response to the taste of a *D. simulans* female. Unfortunately, the deep location of P1 soma in the current *in vivo* preparation makes this experiment technically infeasible without considerable reorientation in how the fly is tethered. An alternative way to visualize hyperpolarization is to express a

77

genetically encoded voltage sensor like ASAP2[118] in P1 neurons. To do this experiment, we would need to generate a *D. simulans* UAS-ASAP2 transgenic line and optimize expression in P1 driver lines, as the current R71G01-Gal4 line would probably express too weakly to see fluorescence changes.

A less direct demonstration of P1 inhibition would be to record electrophysiological currents in P1 neurons in response to ppk23 optogenetic stimulation in an *ex vivo* preparation. To do this experiment we would need to generate additional transgenic lines that would allow us to express CsChrimson only in ppk23+ neurons while still fluorescently labeling P1 neurons to facilitate identification. We could alternatively attempt to record from P1 neurons while stimulating vAB3 with acetylcholine. It will also be important to test if P1 inhibition is sufficient to suppress courtship. To do so we could express the light-activated anion channel gtARC in P1 neurons and optogenetically inhibit these neurons during courtship.

Interestingly, detection of inhibitory pheromones during natural courtship does not permanently terminate courtship, but rather transiently suppresses courtship towards the inappropriate mate. This is most obvious when *D. simulans* males have the choice of courting a conspecific or heterospecific female. After courting their conspecific female, frequently males will briefly (<1 second) court the *D. melanogaster* female, but terminate courtship upon tapping her abdomen. Despite courtship termination, the male will reinitiate courtship with shorter latency than it takes him to initiate courtship at the start of the assay. As a result, *D. simulans* males court conspecific females the same fraction of time regardless of the presence or absence of a *D. melanogaster* female (Fig. 2.4 a). Therefore, after a male enters a "courtship" state, inhibitory pheromones will

only transiently suppress courtship rather than permanently stop it. While our model assumes transient P1 inhibition causes transient suppression of courtship, we do not understand how this is implemented at the neural level.

Another interesting question is how an enduring courtship state is triggered or maintained. The stimuli that lead to aroused courtship behavior must be generalized to many species since sensory mutant males, like *D. simulans ppk23* mutants, will vigorously court heterospecific females as distantly related as *D. ananassae* (Fig. 2.3). While visual cues are likely sufficient for a male to initiate courtship, it seems unlikely that they can autonomously induce such a striking behavioral change. Further, the stimuli are most likely non-pheromonal since males without antennae, forelegs and wings can all become sexually aroused[90,99]. I speculate that when males are actively courting, they receive sensory feedback that induces an enduring behavioral state change[113]. The male could potentially be detecting proprioception of self-motion or optic flow over the retina, which could stimulate him to court more. Indeed, both are known to actively modulate courtship behavior[113,114].

The acute state change we observed in males after brief optogenetic activation of P1 neurons, in which a visual object like a magnet becomes an attractive salient target, mirrors the aroused courtship state males naturally enter into. Therefore, the act of courting could provide some sort of sensory feedback, which depolarizes P1 neurons and other central neurons. In this model, if a male initiates courtship towards a visually appropriate target that has an inhibitory pheromone, courtship would be terminated prior to his arousal. However, if a male initiates and continues courting a fly, the act of courting would induce a behavioral state change, which can then only be

briefly terminated when P1 neurons are transiently hyperpolarized by an inhibitory pheromone. While this model is extremely speculative, an exciting future direction will be to understand both the stimuli that potentially excite P1 neurons to induce a behavioral state change and the neural circuitry that maintain arousal even when courtship is transiently suppressed. Further, it will also be interesting to understand how exogenous P1 neuron stimulation induces males to reinitiate courtship more readily.

4| Neural basis for parallel evolution of 7,11-HD-mediated courtship suppression in *D. yakuba* and *D. erecta*

4.1 Introduction

Parallel evolution occurs when a qualitatively similar phenotype was derived independently in two species. In morphological evolution, when the same trait was independently derived between closely related species, in all reported cases the genetic changes occurred at the same locus[6,27,74,119,120]. This is also thought to be true for behavioral evolution, for instance in the case of *FoxP2*, which regulates speech[16]. The most compelling example, however, comes from the observation that high concentrations of conspecific nematode pheromones can induce most, but not all, populations to transition to a longer-lived non-reproductive dauer stage. When grown at high density, two populations of *Caenorhabditis elegans* and one population of *C. briggsae* independently developed mutations in the chemoreceptors that detect these dauer-inducing pheromones rendering them insensitive to the pheromone's effect[42]. Therefore, rapid, population-level adaptation occurred via the same genetic mechanism three independent times in two species[42].

Given the presence of genetic 'hotspots' in morphological and behavioral evolution, we wanted to understand if there were also neuronal 'hotspots.' These genetic and neuronal 'hotspots' could be more 'evolvable' due to minimization of pleiotropic effects[120]. The independent derivation of behavioral aversion to 7,11-HD provided an ideal model system to ask this question (Fig. 1.1 a). In particular, we are curious if the central circuit changes we observed in *D. simulans* also occurred in *D. yakuba*, or if the same behavior was derived using distinct circuit changes.

4.2 Independent evolution of 7,11-HD mediated courtship suppression in *D. simulans* and *D. yakuba*

Similar to *D. simulans*, *D. yakuba* males cannot discriminate between *D. simulans* and *D. yakuba* females as both produce 7-T as their major cuticular hydrocarbon (Fig. 4.1 a). Promiscuous courtship of conspecific and heterospecific females implies that there were weak or non-existent selective pressures for either female pheromone diversification or male discrimination using non-pheromonal cues. In contrast, *D. yakuba* males can robustly discriminate between conspecific females and *D. melanogaster* or *D. erecta* females (Fig. 4.1 a), both of whom produce distinct diene hydrocarbons. The ability of *D. yakuba* males to discriminate between conspecific females and diene-producing females suggests that there was a selective pressure driving this behavioral adaptation. This pressure could be due to *D. yakuba* males needing to discriminate between conspecific and *D. erecta* females as the two species diverged in potentially overlapping environments or males needing to discriminate between conspecific and *D. melanogaster* females as *D. melanogaster* became the dominant species in western Africa. Together, these data further highlight that cuticular pheromones are critical for species discrimination with apparently little role for behavioral or morphological differences between closely related species.

Species discrimination could either be due to *D. yakuba* males finding 7-T attractive or dienes repulsive. While it is difficult to determine if 7-T is attractive or neutral, the *D. melanogaster* female diene 7,11-HD is sufficient to suppress courtship towards an otherwise attractive conspecific *D. yakuba* female[77]. When *D. yakuba* males are presented with the choice of courting a conspecific female perfumed with a solvent control or 7,11-HD, they show a strong preference against the 7,11-HD-perfumed female (Fig. 4.1 b). Additionally, preliminary evidence
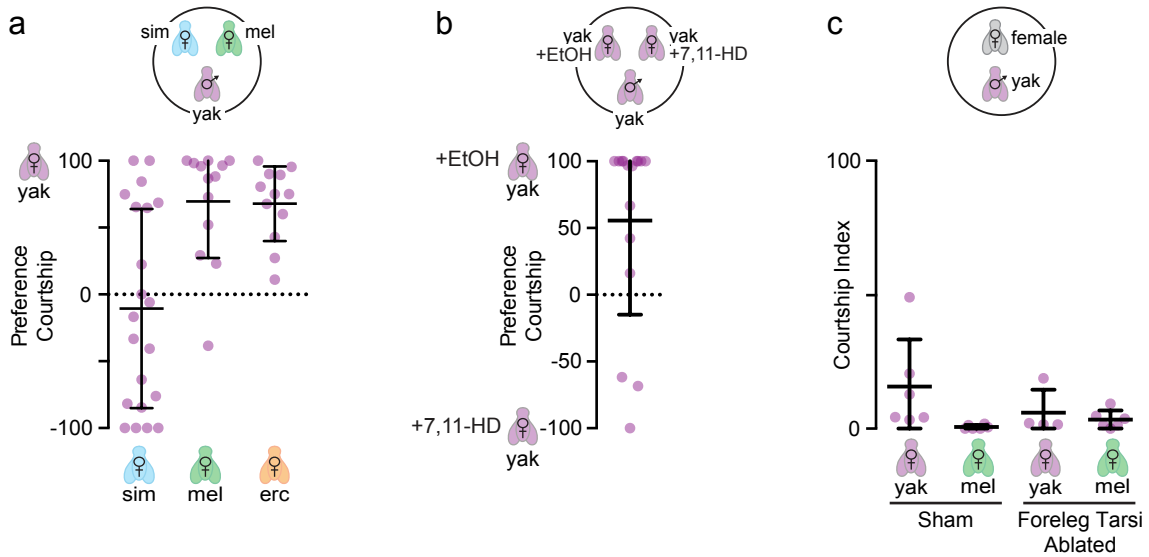
Figure 4.1: Courtship preferences of *D. yakuba* males. a, Courtship preferences of *D. yakuba* wild type males when presented with conspecific and heterospecific females (n=19-20). **b**, Courtship preferences of *D. yakuba* wild type males when presented with *D. yakuba* females prefumed with ethanol or 7,11-HD (n=19). **c**, Courtship index towards *D. yakuba* or *D. melanogaster* females by *D. yakuba* males with either their foreleg tarsi intact (sham) or ablated (ablated). Dots represent courtship by an individual and bars represent mean and s.d. Preferences were analyzed using a one-sample t-test with a Bonferroni correction where ns denotes that preference was not significantly different from zero.

suggests that foreleg tarsi are necessary for courtship suppression in *D. yakuba* males (Fig. 4.1 c), as observed in *D. simulans* males (Fig. 2.1 a). While *D. yakuba* males normally do not court *D. melanogaster* females, surgically ablating their foreleg tarsi modestly increases their courtship towards these inappropriate mates (Fig. 4.1 c). This is despite significant movement deficits caused by ablating foreleg tarsi in *D. yakuba*, which resulted in a decrease in conspecific courtship, unlike in *D. simulans* males. Together, these data suggest that in both *D. simulans* and *D. yakuba*, sensory neurons in the male's foreleg tarsi mediate courtship suppression and these sensory neurons potentially detect a broad range of diene hydrocarbons. We are currently generating sensory mutants to explore the role of ppk23 and Gr32a in regulating courtship and species discrimination.

Our initial analysis of pheromone processing circuitry has greatly benefitted from a transgenic line in *D. yakuba*[71] that labels the Fru+ neurons, which was recently generated by David Stern and Yun Ding (Janelia/HHMI). In *D. yakuba* males, Fru+ neurons appear largely morphologically conserved, allowing us to readily identify vAB3, mAL and P1 neurons (Fig. 4.2). The conservation of Fru+ anatomy between *D. yakuba*, *D. melanogaster* and *D. simulans* was striking considering these species diverged over 10-15 million years ago[103]. Distinct differences in the innervation patterns, however, exist. In future studies, it will be important to determine if these differences reflect true anatomical diversification between species. Alternatively, given that Gal4 was integrated into a different region of the *D. yakuba fru* locus in comparison to *D. simulans* and *D. melanogaster* alleles where Gal4 insertions were less than 100 base pairs apart, the observed differences may actually reflect differences in the neuronal populations labeled by Gal4.
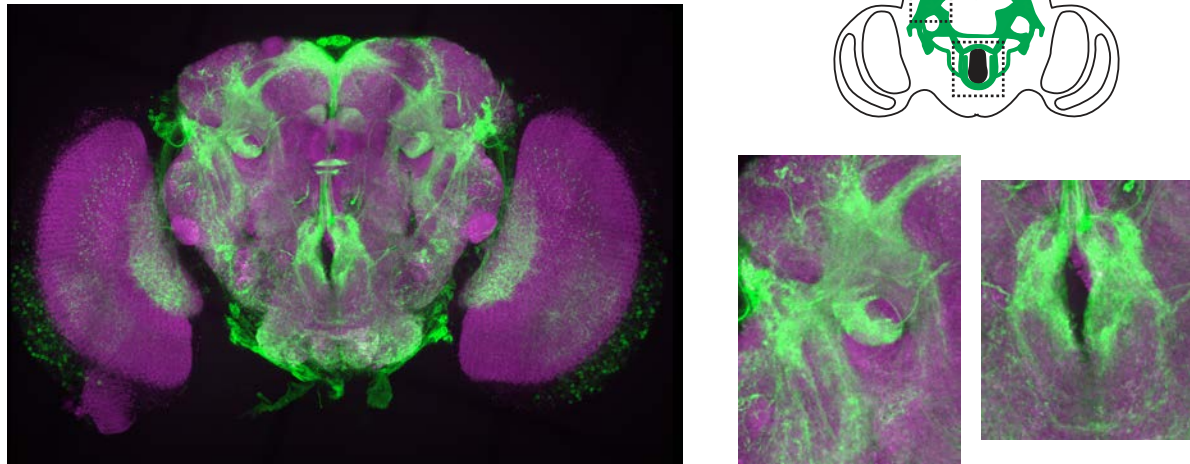
Figure 4.2: Anatomy of Fru+ neurons in *D. yakuba* males. *D. yakuba* adult male brain expression of Fru+ neurons (green) and neuropil counterstain (magenta). 2x zoomed in image of Fru+ neurons in the LPC (middle) and SEZ (right).

As observed in *D. melanogaster* and *D. simulans*, P1 neurons in *D. yakuba* are sufficient to drive courtship behavior[71]. Ding *et al* 2018 showed that while *D. yakuba* males normally do not court other males, optogenetic activation of P1 neurons is sufficient to drive courtship towards this inappropriate target. In preliminary experiments, we demonstrated that P1 neuron activation is also sufficient to override courtship suppression towards *D. melanogaster* females (data not shown). The conserved function of P1 neurons across diverse species implies that these neurons were potentially important in the ancestral state for male courtship behavior.

Given that P1 neurons retain a conserved behavioral role in promoting male courtship in *D. yakuba* males, we propose two general models for how *D. yakuba* males discriminate between *D. melanogaster* and *D. yakuba* females. These models mirror our original ideas for species discrimination by *D. simulans* males. The first model relies on a peripheral swap in the pheromones that activate conserved central circuits that promote and suppress courtship. In this model, 7,11-HD-responsive ppk23+ sensory neurons would no longer activate vAB3, but would instead directly activate mAL neurons to suppress P1 neurons (Fig. 4.3). The strongest support for this model would be that *D. melanogaster* female pheromones evoked responses in mAL neurons but not vAB3 neurons. This model would also permit, but not require, either 7-T-responsive ppk23+ sensory neurons or Gr32a+ sensory neurons to activate vAB3 and P1 neurons to drive courtship towards conspecific females. The second model relies on peripheral conservation of pheromone responses with changes in how central circuits process pheromones (Fig. 4.3), replicating what we observed in *D. simulans*. The strongest support for this model would be if we observed *D. melanogaster* female-evoked responses in vAB3 and mAL neurons

Model 1: Peripheral Evolution
-Dienes activate the subset of ppk23+/Gr32a+ sensory neurons that activate mAL
-7-T could lead to P1 activation
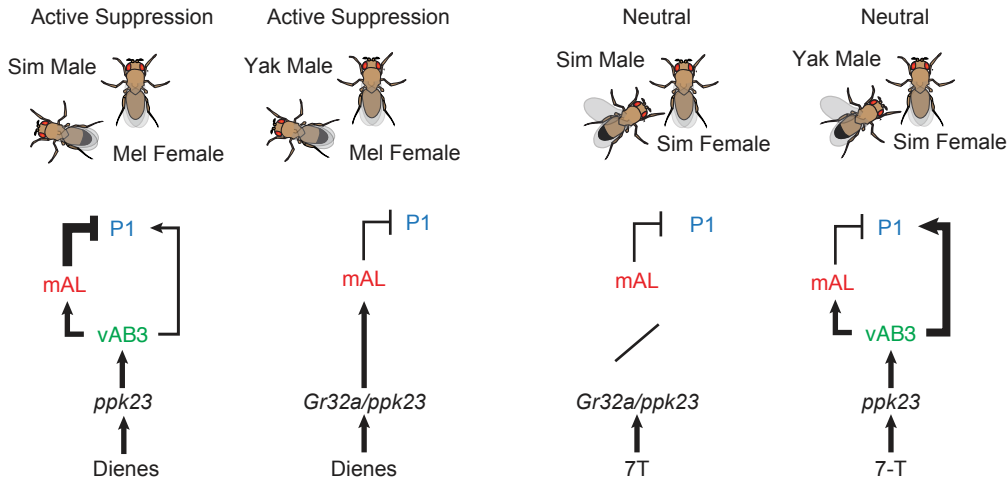
Model 2: Central Circuit Evolution
-Dienes activate a conserved subset of ppk23+ sensory neurons that activate vAB3
-7-T either no longer activates foreleg sensory neurons or these neurons do not activate mAL
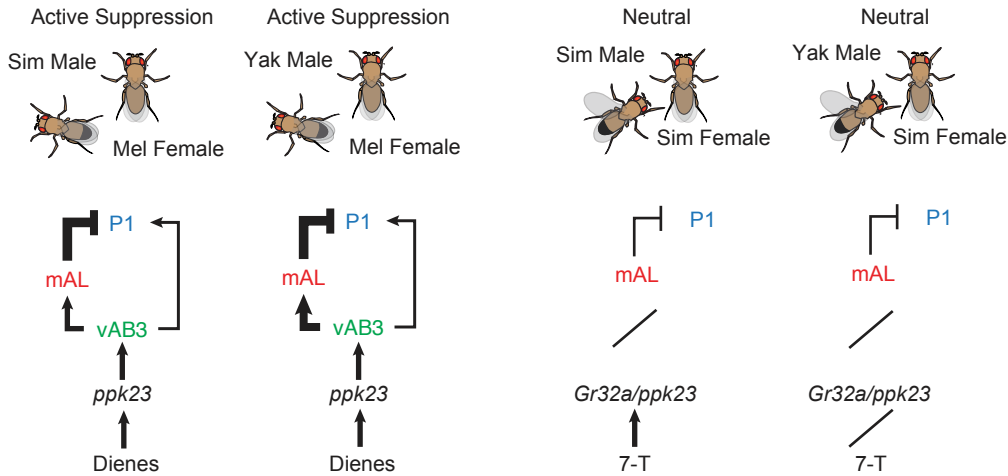
Figure 4.3: Potential models for species discrimination by *D. yakuba* males. Model 1: peripheral evoluiton where conserved central circuits are activated by different pheromone cues. Model 2: central circuit evolution where peripheral dection is conserved with central circuit diversification.

but not P1 neurons. Labeling the Fru+ neurons in *D. yakuba* provides genetic access to investigate species-specific differences in pheromone-processing pathways.

To gain initial insight into the neural circuitry that processes 7,11-HD in *D. yakuba*, we first assessed the pheromone tuning of the LPC. Using the same *in vivo* preparation described in Chapter 3, we tethered a *fru*^{Gal4}>*UAS-GCaMP D. yakuba* male under a two-photon microscope and imaged the LPC as we offered him female abdomens to tap (Fig. 4.4 a). The LPC of *D. yakuba* males could exhibit strong responses to the taste of a conspecific female, suggesting that conspecific female pheromones activate P1 neurons, as observed in *D. melanogaster* males. This would be a radical difference from what we observed functionally and behaviorally in *D. simulans* where conspecific female pheromones do not appear to play an important excitatory role. Alternatively, the LPC could be weakly tuned to the taste of a *D. melanogaster* female, as we previously observed in *D. simulans*.

Imaging the Fru+ neurons in the *D. yakuba* revealed neurons in the LPC are preferentially tuned to the taste of a *D. melanogaster* female with equivalently weak responses evoked by the taste of a *D. simulans* and *D. yakuba* female (Fig. 4.4). The responses evoked by the taste of a *D. melanogaster* female could reflect activation of mAL, vAB3 or potentially other neurons innervating this complex neuropil. Therefore, while we cannot distinguish between peripheral or central circuit changes mediating 7,11-HD courtship suppression, these data show that a larger portion of Fru+ neurons in this integrative node are dedicated to detecting 7,11-HD than the conspecific female pheromone 7-T. We, therefore, speculate that 7-T does not play a strong excitatory role in promoting courtship in *D. yakuba*.
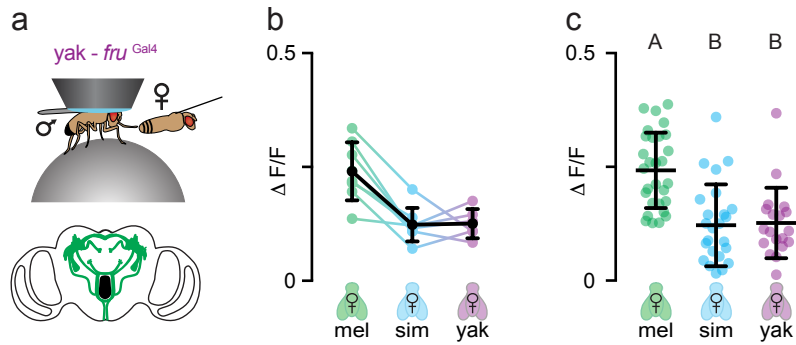
Figure 4.4: Pheromone responses in Fru+ LPC neurons of *D. yakuba* males. **a**, Schematic of *in vivo* preparation used to measure pheromone responses. **b**, Functional GCaMP responses visualized in Fru+ neurons in the LPC of *D. yakuba* males evoked as a male taps a female abdomen. Paired intra-animal averages with colored dots representing average individual responses and black bars and dots representing mean and s.d. **c**, Individual tap-evoked responses in Fru+ neurons in the LPC (n=20 taps per 6 individuals, Kruskal-Wallis test, P<0.0001 for both, different letters mark significant differences by Tukey's multiple comparisons test). Dots represent individual a tap-evoked GCaMP response and black bars represent mean and s.d.

To investigate if vAB3 remains functionally connected to mAL and P1 neurons in *D. yakuba*, we iontophoresed acetylcholine onto the spatially segregated ppk23 axons and vAB3 dendrites within the ventral nerve cord (VNC). Multi-plane functional imaging of Fru+ neurons in response to stimulation of vAB3 neurons revealed robust activation of mAL and vAB3 in the brain, as previously observed in *D. melanogaster* and *D. simulans* (Fig. 4.5)*.* When we imaged the LPC from the ventral side of the brain in response to vAB3 stimulation, we observed only sparse activity in the LPC, mirroring the patterns we observed in *D simulans* (Fig. 4.5). However, when we imaged the *D. yakuba* LPC from the dorsal side, we observed strong responses in the LPC, similar to what we observed in *D. melanogaster* (Fig. 4.5). This result was rather surprising because in *D. melanogaster* and *D. simulans*, responses were consistent irrespective of which side of the brain was imaged. We first considered whether the strong activity in the dorsal LPC reflected activation of P1 neurons. However, we observed no response to vAB3 stimulation in the fasciculated axon bundle of P1 neurons (Fig. 4.6 b). Since the robustly activated neural population in the dorsal LPC is unlikely to be P1 neurons, we hypothesize it could either be mAL, reflecting an increase in vAB3 to mAL signaling, or another uncharacterized neural population not present in *D. melanogaster* or *D. simulans.* Uncovering the identity of this neural population could provide tremendous insight into the neural circuitry underlying 7,11-HD suppression.
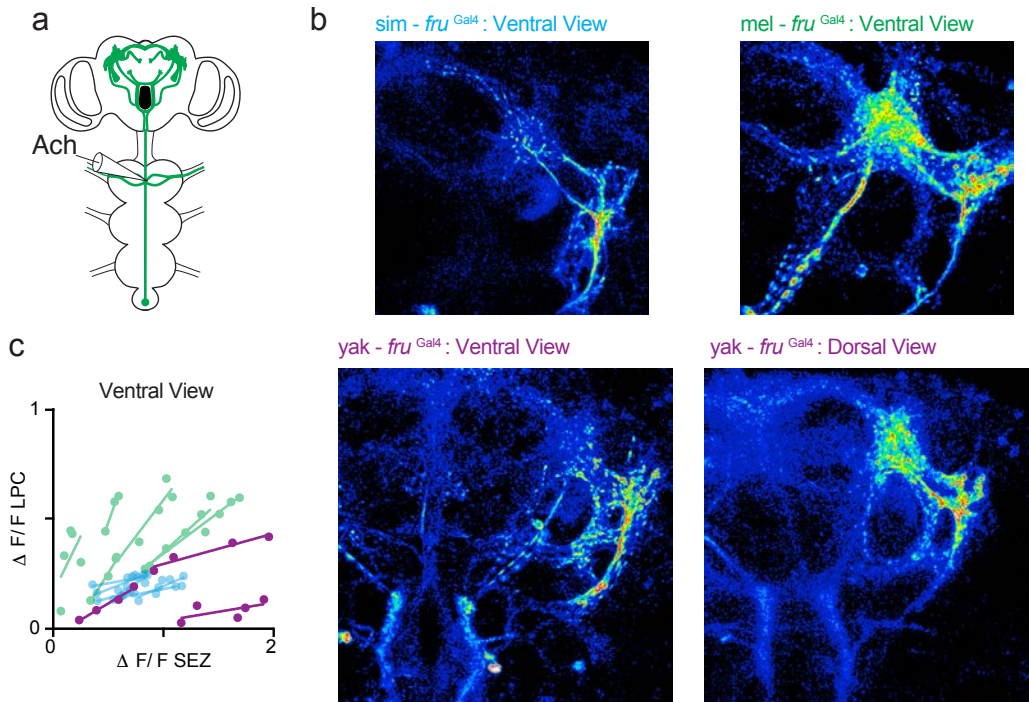
Figure 4.5: Propagation of vAB3 stimulation to LPC in *D. yakuba* males. a, Schematic depicting stimulation of vAB3 neurons by acetylcholine iontophoresis in the ventral nerve cord and activated Fru+ neurons in the central brain. **b**, Representative multi-plane image of GCaMP responses in Fru+ neurons in *D. melanogaster* (left) and *D. simulans* males (right). **c**, Graph (left) compares relationship between responses in the SEZ and LPC in *D. yakuba* males (purple) with *D. melanogaster* (green) and *D. simulans* (blue) males. Dots on graph represent different stimulation intensities and lines connect different individual males (n=6 animals). Representative multi-plane image of GCaMP responses in Fru+ neurons in *D. yakuba* male brains imaged from the ventral orientation or dorsal orientation.

Given that P1 neurons were not responsive to 7,11-HD stimulation, we considered whether vAB3 neurons were simply no longer functionally connected to P1 neurons or if mAL inhibition was capable of suppressing vAB3 excitation. By severing mAL axons in *D. simulans,* we previously revealed that mAL-mediated inhibition antagonizes vAB3 excitation to inhibit P1 neurons (Fig. 3.15). Similarly, after bilaterally severing mAL axons in *D. yakuba* we observed that activity in vAB3 neurons propagated to P1 neurons (Fig. 4.6 c, d). These data suggest two preliminary conclusions. First, despite last sharing a common ancestor 10-15 million years ago, the neural architecture of pheromone circuits in *D. melanogaster, D. simulans* and *D. yakuba* is largely conserved, where vAB3 and mAL neurons form a feed-forward inhibitory circuit onto P1 neurons. Second, it appears as though in both *D. yakuba* and *D. simulans* males*,* P1 neurons receive greater levels of mAL-mediated inhibition than vAB3-mediated excitation to suppress peripheral pheromone responses.

This raises the interesting possibility that a homologous 7,11-HD pheromone processing circuit consisting of vAB3, mAL and P1 neurons exists in *D. yakuba, D. simulans* and *D. melanogaster* males. Therefore, to transform an excitatory cue that promotes courtship into an inhibitory cue that suppresses courtship, *D. simulans* and *D. yakuba* would have independently derived changes at the same circuit node. In the future, it will be interesting to characterize the *in vivo* functional tuning and anatomy of the Fru+ neurons that process 7,11-HD in *D. yakuba*. In particular, characterizing the peripheral sensory neurons and understanding if 7,11-HD activates vAB3 neurons would help constrain models for circuit evolution. Additionally, it would be useful to more precisely characterize central circuits in *D. simulans* and *D. yakuba* males to understand the detailed molecular mechanisms of how different species discriminate between females carrying
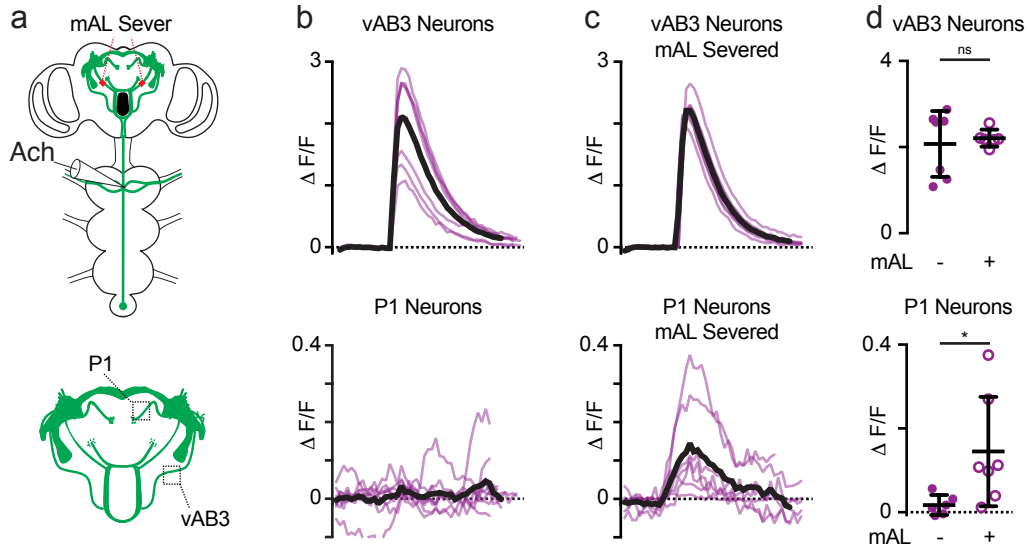
Figure 4.6: Propagation of vAB3 stimulation to P1 neurons in *D. yakuba* males. a, Schematic of vAB3 stimulation and regions imaged. **b-d** Response of *D. yakuba* vAB3 neurons and P1 neurons in the brain to vAB3 stimulation before (**b**) and after (**c**) mAL severing. Colored lines represent single stimulations and black line represents the average (n=6 stimulations). **d,** Peak Δ F/F plotted with colored dots representing a single stimulation and black bars representing mean and s.d. (n=3 animals with 2 stimulations, unpaired t-test vAB3:P = 0.6838 and P1:P = 0.0387).

monoene and diene pheromones. In *D. simulans*, we believe that changes in the strength of synaptic connections exist between either mAL or vAB3 neurons and P1 neurons. In *D. yakuba* changes could also occur at this node, or they could alternatively occur in the strength of vAB3 excitation onto mAL neurons or in peripheral detection. Since suppression of courtship towards diene-producing females was independently derived in *D. simulans* and *D. yakuba,* this comparison provides a rare opportunity to understand the neural mechanisms underlying parallel behavioral evolution.

4.3   Species discrimination in *D. erecta*

D. erecta males robustly prefer to court conspecific females over *D. melanogaster, D. yakuba* and *D. simulans* females (Fig. 4.7 a). Interestingly, however, when males were given a choice between two undesirable targets, *D. melanogaster* and *D. simulans* females, they preferred to court *D simulans* females (Fig. 4.7 a). This suggests that a potential hierarchy of inhibitory pheromones exists where 7,11-HD is more aversive than 7-T.

D. erecta is the only species we tested where males always selectively court their conspecific female. Selectivity could be achieved though a combination of courtship suppression by 7,11-HD or 7-T, courtship promotion by the conspecific female's unique species-specific dienes pheromones or by visual or behavioral discrimination. Given the importance of *ppk23* in detecting 7,11-HD to suppress courtship of *D. melanogaster* females*,* we generated *ppk23* sensory mutants in *D. erecta* to see if this receptor is necessary for species discrimination. To do so, we targeted a CRISPR guide RNA to the first exon of the *ppk23* locus and isolated a mutant with a frame shift mutation.
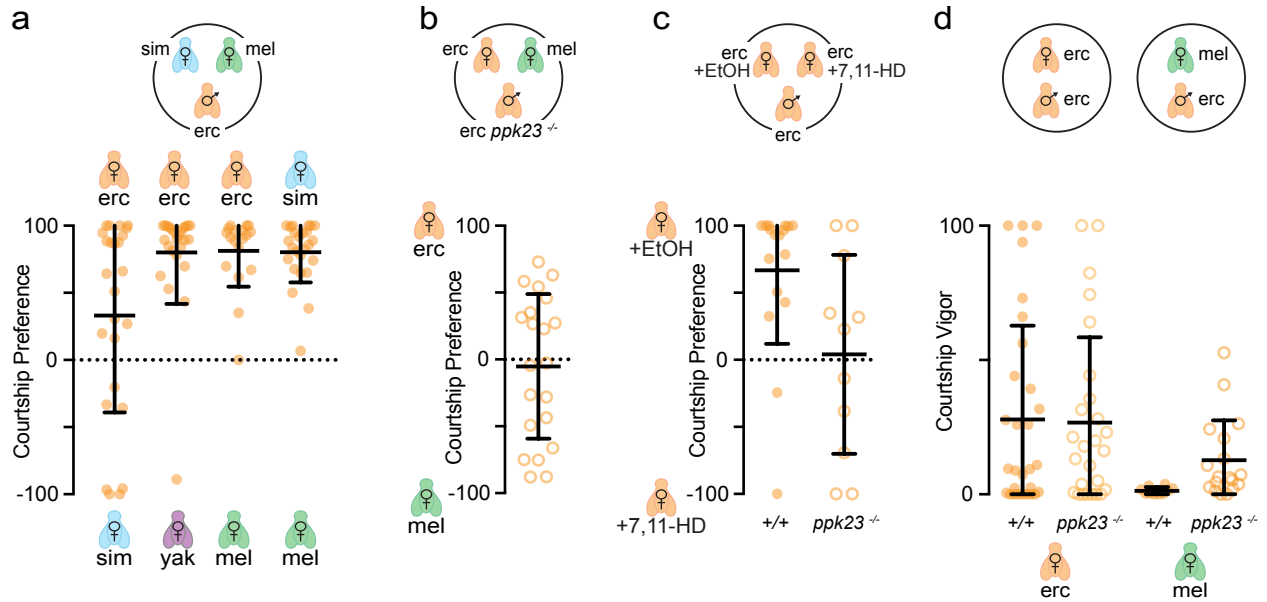
Figure 4.7: Courtship preferences of *D. erecta* males. a, Courtship preferences of *D. erecta* wild type males when presented with conspecific and heterospecific females (n=19-20). **b**, Courtship preferences of *D. erecta* wild type and *ppk23* mutant males when presented with *D. erecta* and *D. melanogaster* females (n=19). **c**, Courtship preferences of *D. erecta* wild type and *ppk23* mutant males when presented with *D. erecta* females prefumed with ethanol or 7,11-HD (n=19). **d**, Court-ship index towards *D. erecta* females and *D. melanogaster* females by *D. erecta* males with their foreleg tarsi intact or ablated. Dots represent courtship by an individual and bars represent mean and s.d.

In preference assays, *D. erecta ppk23* mutant males were unable to differentiate between *D. melanogaster* and *D. erecta* females, indicating this sensory pathway is essential for erecting a pre-mating barrier between species, as it is in *D. melanogaster* and *D. simulans* males (Fig. 4.7 b). To test whether the promiscuous courtship by *ppk23* mutants reflects an inability to detect 7,11-HD, we offered *D. erecta* males the choice of *D. erecta* females perfumed with 7,11-HD or ethanol (Fig. 4.7 c). Wild type males preferentially courted the ethanol-perfumed female, which suggests that 7,11-HD is sufficient to erect a species barrier. However, *ppk23* mutants pursued both females indiscriminately (Fig. 4.7 c). Thus, *D. simulans, D. melanogaster* and *D. erecta* males all rely on *ppk23* to detect 7,11-HD, but detection of this pheromone initiates opposing behaviors—promoting courtship in *D. melanogaster* while suppressing courtship in *D. simulans* and *D. erecta*.

In *D. simulans*, the *ppk23+* sensory neurons detect a diversity of diene hydrocarbons, including 7,11-HD and the *D. erecta* female pheromone 9,23-TTCD, to suppress courtship towards inappropriate mates. We suspect that the ppk23+ sensory neurons in *D. melanogaster* are also broadly tuned to diene hydrocarbons. Therefore, in addition to detecting 7,11-HD to suppress courtship, the *D. erecta ppk23* mutant male may have also lost their ability to detect other diene hydrocarbons, including the species-specific *D. erecta* diene compound that could promote courtship. However, both wild type and *ppk23* mutant males courted conspecific females equivalently (Fig. 4.7 d). While this observation suggests that *ppk23* is not necessary for detection of conspecific female dienes to promote courtship, it is possible that *D. erecta* female pheromones act redundantly with other sensory cues like vision. In *D. melanogaster*, *ppk23* mutant males exhibit reduced courtship of conspecific females only in the dark. Therefore, while

ppk23 is necessary to detect 7,11-HD in *D. erecta* males, further experimentation is needed to assess if *ppk23* also necessary to detect *D. erecta* female pheromones.

We have two general models for how *D. erecta* males can discriminate between conspecific and heterospecific females, both of which assume conservation of the functional architecture of ppk23, vAB3, mAL and P1 neurons. In the first model, species discrimination is achieved by peripheral diversification such that *D. erecta* female pheromones would activate vAB3 neurons to lead to net excitation of P1 neurons and drive courtship initiation (Fig. 4.8). To achieve this, the subset of *ppk23+* sensory neurons in *D. erecta* males that activates vAB3 neurons would be tuned specifically to *D. erecta* female pheromones, instead of 7,11-HD or dienes, as occurs in *D. melanogaster* and *D. simulans*. Additionally, the subset of *ppk23+* sensory neurons that activates mAL neurons would be tuned to 7,11-HD as opposed to cVA/7-T, as observed in *D. melangoster*. As a result, *D. erecta* males would prefer to court conspecific females over *D. simulans* females because the *D. erecta* specific dienes would promote courtship. They would, however, prefer to court *D. simulans* over *D. melanogaster* because 7,11-HD would be strongly inhibitory while 7-T would be neutral.

Alternatively, a second general model relies on diversification of both the sensory periphery and central circuitry (Fig. 4.8). In this model, a central circuit change would result in vAB3 neuron activation leading to greater mAL inhibitory input than vAB3 excitatory input onto P1 neurons, resulting in net inhibition of P1 neurons. As a result of peripheral evolution, the subset of *ppk23+* sensory neurons that activates vAB3 neurons would be selectively tuned to 7,11-HD such that *D. erecta* female pheromones do not activate this pathway to suppress courtship. *D. erecta* female

97

pheromones would themselves be neutral, neither promoting nor suppressing courtship, as we have observed in *D. simulans*. The neural circuitry that suppresses courtship in response to 7-T/cVA would be conserved between *D. melanogaster* and *D. erecta* males. As a consequence, inhibitory pheromones would bias courtship away from inappropriate mates either through direct or indirect activation of mAL. As in *D. simulans*, courtship of conspecific females would occur because they lack inhibitory pheromones.

We are currently generating reagents to label the Fru+, ppk23+, mAL and P1 neurons in *D. erecta* to understand their anatomy, functional connections and pheromonal tuning. While the evolution of species discrimination in *D. erecta* is most likely only due to a derivation or combination of the models described above, we believe they provide a useful starting point for guiding future experiments.

It is unclear if courtship suppression towards *D. melanogaster* females by *D. yakuba* and *D. erecta* males shares a common evolutionary origin or if these behaviors were independently derived. If the first model of peripheral diversification is closest to the truth, it is most parsimonious to assume *D. yakuba* and *D. erecta* independently derived their species-specific preferences. However, if the second model of central circuit changes is correct, then perhaps the last common ancestor of *D. yakuba* and *D. erecta* physically overlapped with an ancestral version of *D. melanogaster* or another extinct Drosophilid whose females expressed 7,11-HD. Thus, a selective pressure would drive the derivation of neural mechanisms for suppressing courtship towards females with 7,11-HD.

Model 1: Peripheral Evolution
-7,11-HD specifically activates the subset of ppk23+/Gr32a+ sensory neurons that activate mAL
-*D. erecta* female dienes activate the subset of ppk23+ sensory neurons that activate vAB3
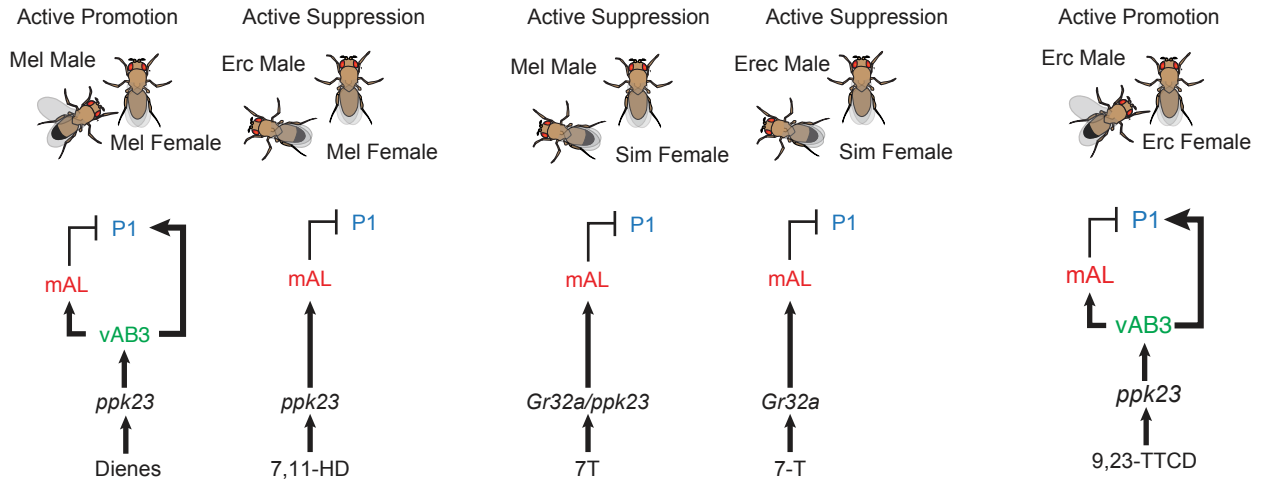
Model 2: Peripheral and Central Circuit Evolution
-7,11-HD activates a conserved subset of ppk23+ sensory neurons that activate vAB3
-These neurons no longer respond to *D. erecta* female dienes
-7-T receptor and circuitry is conserved between *D. erecta* and *D. melanogaster* male
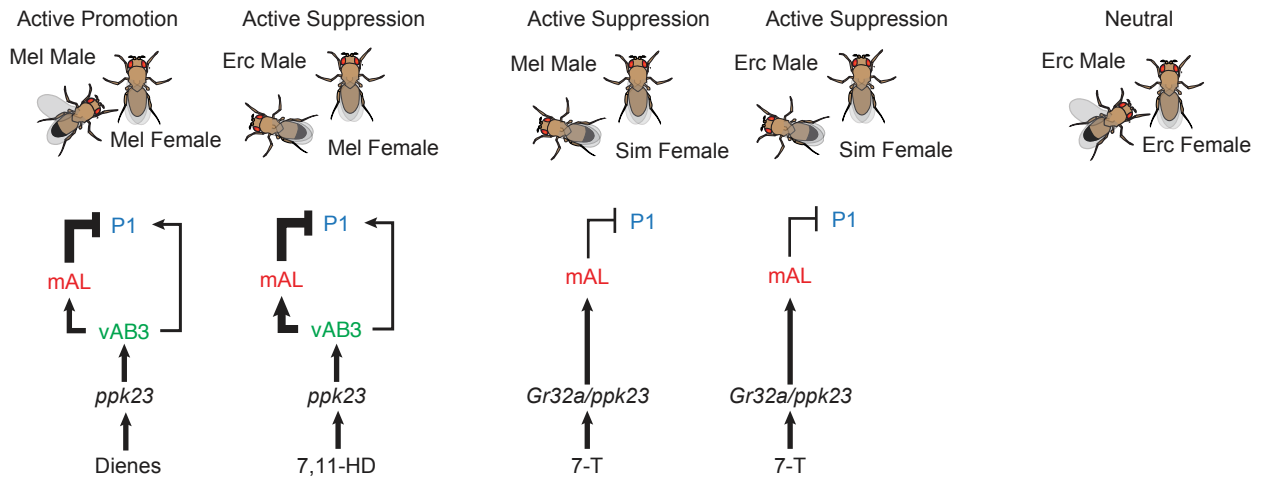
Figure 4.8: Potential models for species discrimination by *D. erecta* males. Model 1: peripheral evoluiton where conserved central circuits are activated by different pheromone cues. **b**, Model 2: peripheral and central circuit evolution where divergent central circuits are activated by divergent sensory neurons.

4.4 *D. ananassae* species discrimination

D. ananassae, which is part of the *D. ananassae* subgroup, is a cosmopolitan species that has an ancestral range in South East Asia and is distinct from the members of the *D. melanogaster* subgroup who originated in Africa. Both males and females produce the diene 5,25-hentriacontadiene as their major cuticular hydrocarbon. In very preliminary analysis of *D. ananassae* mate preferences, we found that males could robustly distinguish between conspecific females and *D. simulans* or *D. melanogaster* females (Fig. 4.9). The original study describing their cuticular pheromones demonstrated that while *D. anananasse* males do not court a freeze-killed fly lacking pheromones (a *D. melanogaster* male that went through three hexane washes), perfuming that male with the diene 5,25-hentriacontadiene stimulated robust courtship[121]. However, *D. ananassae* males would not court dummy flies perfumed with 5,27-tritriacontadiene, the hydrocarbon pheromone of its closest relative *D. pallidosa*[121]. *D. pallidosa* males exhibited the opposite mate preferences of *D. ananassae* males with the *D. pallidosa* female pheromone stimulating courtship[121]. Therefore, conspecific female pheromones could stimulate courtship in this monomorphic species and mediate species discrimination. It will be an interesting area of study to determine how more distantly related species discriminate between conspecific and heterospecific females and whether they rely on completely distinct neural changes than we propose in the *D. melanogaster* subgroup.
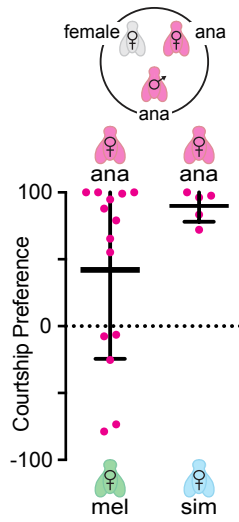
Figure 4.9: Courtship preferences of *D. ananassae* males. Courtship preferences of *D. ananassae* wild type males when presented with conspecific and heterospecific females (n=19-20). Dots represent courtship by an individual and bars represent mean and s.d. Preferences were analyzed using a one-sample t-test with a Bonferroni correction where ns denotes that preference was not significantly different from zero.

4.5   Discussion

Frequently, similar genetic changes underlie the parallel evolution of a phenotype[42,74,119,122]. For instance, both *D. simulans* and *D. yakuba* females independently lost the ability to produce diene hydrocarbons through distinct mutations in the cis-regulatory elements of the *desatF* gene[74] (Fig. 1.1a). In approximately 40 million years of *Drosophila* evolution, there have been 11 independent changes in the cis-regulatory elements of *desatF* that control its expression[74]. Given that a critical function of the waxy hydrocarbons that coat the fly's body is to prevent desiccation, as evidenced by the rapid death of flies lacking pheromones[77], limits likely exist on how much cuticular hydrocarbons can change due to very strong fitness costs[123]. *desatF*, therefore, may serve as a repeated target because changing its expression could have minimal pleiotropic effects while yielding an immediate adaptive phenotypic change[120] – an ability for males to discriminate between females using cuticular hydrocarbons.

As *D. simulans* and *D. yakuba* females independently lost an ability to produce diene hydrocarbons, males of both species had to independently evolve neural mechanisms to suppress courtship towards females carrying diene pheromones. Both *D. simulans* and *D. yakuba* males are strongly inhibited by the pheromone 7,11-HD[77], providing a model system to study the neural basis for parallel behavioral evolution. In *D. melanogaster*, *D. simulans,* and *D. yakuba,* vAB3 neurons drive activity in mAL and P1 neurons with mAL inhibiting P1 neurons. The balance of excitation and inhibition onto P1 neurons is such that activation of vAB3 drives net excitation of P1 neurons in *D. melanogaster* males*,* but not in *D. simulans* or *D. yakuba* males. It will be interesting if we observe in *D. yakuba* males that 7,11-HD drives net inhibition of P1 neurons though similar central circuit changes that we observed in *D. simulans*. This observation could

suggest that the vAB/mAL/P1 node is a particularly 'evolvable' substrate for switching the

behavioral valence of a conserved pheromone, just as *desatF* is an 'evolvable' gene for changing

a fly's pheromone profile.

5| Sex discrimination occurs though broad conservation of cVA pathways with diversification of 7-T pathway

5.1 Introduction

In chapters 2, 3 and 4, I primarily focused on species-specific behavioral changes elicited by the *D. melanogaster* female pheromone 7,11-HD. However, there are several additional pheromones known to regulate male courtship, including 7-T and *cis*-vaccenyl acetate (cVA). 7-T, the major cuticular hydrocarbon produced by *D. simulans* females and all males in the *D. melanogaster* subgroup, is aversive to *D. melanogaster* males[77,99]. Perfuming 7-T onto an otherwise attractive oneocyte-less female that lacks cuticular hydrocabons renders her unattractive to a *D. melanogaster* male[99]. Similarly, wild type *D. melanogaster* males exhibit increased courtship of males lacking oenocytes, but this is suppressed if the male is re-perfumed with 7-T[77]. Courtship by *D. simulans* males, however, is neither promoted nor inhibited by 7-T[79], potentially because both conspecific males and females produce this pheromone[73]. Therefore, differences must exist in the detection or processing of 7-T between *D. melanogaster* and *D. simulans* males such that this pheromone can be inhibitory in one species and neutral in another.

On the other hand, *cis*-vaccenyl acetate (cVA) appears to retain a conserved role in mediating courtship suppression across a broad range of species[124–127]. cVA is a volatile and contact pheromone that males produce in their ejaculatory bulb[95,127,128]. During copulation, males transfer cVA along with sperm and peptides to the female[124–127]. These peptides render a female unreceptive to further copulation attempts[129], which is probably why males have developed neural mechanisms to discriminate between mated and virgin females. Therefore, cVA marks

mates as inappropriate either because they are male or because they are females that recently mated.

In this chapter I will describe preliminary experiments to examine the divergent neural circuits that process 7-T and conserved neural circuits that process cVA in *D. simulans* and *D. melanogaster* males.

5.2   Divergent behavioral response to 7-T in *D. melanogaster* and *D. simulans* males

7-T is present on *D. simulans* females and inhibits courtship by *D. melanogaster* males, but not *D. simulans* males[77,79,99]. Therefore, both 7-T and 7,11-HD evoke species-specific responses that contribute to mate recognition. In the course of studying differential sensory processing of 7,11-HD in the two species, we have also made insights into the differential sensory processing of 7-T.

As described in Chapter 2, *D. melanogaster* males whose foreleg tarsi have been surgically ablated inappropriately court *D. simulans* females due, in part, to their inability to detect the inhibitory pheromone 7-T present on a *D. simulans* female. Both Gr32a+ sensory neurons and ppk23+ sensory neurons present in a male's foreleg are thought to detect 7-T, however, there are conflicting reports as to the behavioral role of these sensory neurons[93,95,99], as I discuss below. Given that ppk23+ sensory neurons detect both 7,11-HD and 7-T, it was not surprising that *D. melanogaster ppk23* mutants exhibited promiscuous courtship of conspecific and heterospecific females (Fig. 5.1 a). Therefore, as observed in *D. simulans* and *D. erecta*, ppk23+ sensory neurons are necessary for species discrimination.
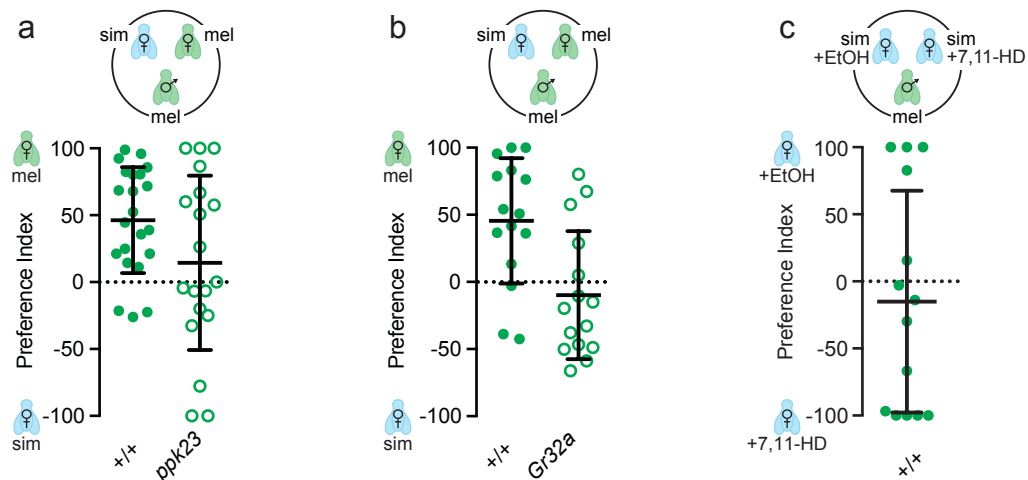
Figure 5.1: Courtship preferences of *D. melanogaster ppk23* and *Gr32a* mutant maless. a, Courtship preferences of *D. melanogaster* wild type (+/+) and *Gr32a* mutant males when presented with conspecific and heterospecific females (n=19-20). **b**, Courtship preferences of *D. melanogaster* wild type (+/+) and *ppk23* mutant males males when presented with conspecific and heterospecific females (n=19-20). **c**, Courtship preferences of *D. melanogaster* wild type (+/+) males when presented with *D. simulans* females prefumed with ethanol or 7,11-HD (n=19). Dots represent courtship by an individual and bars represent mean and s.d. Preferences were analyzed using a one-sample t-test with a Bonferroni correction where ns denotes that preference was not significantly different from zero.

We were surprised, however, that *Gr32a* mutant males also exhibited indiscriminate courtship of conspecific and heterospecific females (Fig. 5.1 b), implying that 7-T is necessary for species discrimination and 7,11-HD is insufficient to mediate discrimination, despite promoting courtship of conspecific *D. melanogaster* females. Indeed, when we offered wild type males the choice of courting a *D. simulans* female perfumed with either 7,11-HD or ethanol, they could not distinguish between these females (Fig. 5.1 c). Ideally, this experiment would be repeated with oenocyte-less females to test the sufficiency of 7,11-HD in the absence of 7-T. However, these behavioral manipulations ultimately suggest that detection of 7-T by *D. melanogaster* males is of central importance for erecting a reproductive barrier between species.

Similarly, in *D. simulans,* the inhibitory pheromone 7,11-HD appeared to be sufficient for species discrimination. We previously observed that *Gr32a* mutant males could not only robustly discriminate between conspecific and heterospecific females (Fig. 2.4 a), but also that both *Gr32a* and *ppk23* mutants did not exhibit any apparent courtship deficits towards conspecific *D. simulans* females (Fig. 2.3). Together, these data suggest that 7-T was transformed from an inhibitory pheromone that suppresses courtship in *D. melanogaster*, into a neutral pheromone in *D. simulans* that neither suppresses nor promotes courtship.

Males have to select mates not only based on species, but also based on sex. Given the importance of inhibiting courtship towards other males, we were surprised that *D. simulans Gr32a* and *ppk23* mutants exhibited no increase in male-male courtship compared to wild type males (Fig. 5.2). In contrast, previous studies have shown that *D. melanogaster* males mutant for
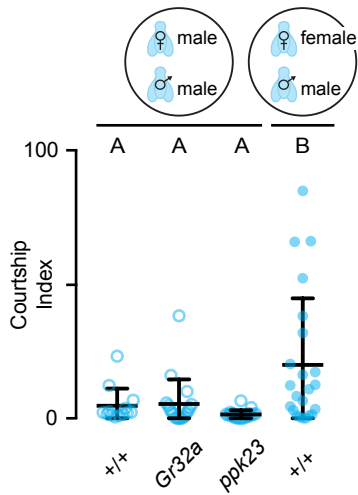
Figure 5.2: Male-male courtship by *D. simulans ppk23* and *Gr32a* mutant males. Courtship indices of *D. simulans* wild type (+/+), *Gr32a* and *ppk23* mutant males when paired with a *D. simulans* wild type. *D. simulans* wild type male paired with a female (n=13-23, Kruskal-Wallis test, P=0.0007, different letters mark significant differences in courtship by Dunn's multiple comparisons test). Dots represent courtship by an individual and bars represent mean and s.d.

either receptor exhibited elevated male-male courtship[93–95,99]. There are several potential explanations for this species difference. First, *D. simulans* Gr32a+ and "male" ppk23+ sensory neurons could no longer be tuned to 7-T and cVA or these sensory neurons could no longer activate downstream inhibitory circuitry. Second, olfactory detection of cVA could work redundantly with detection of gustatory pheromones. Surgically ablating the antenna of *D. simulans* wild type, *Gr32a,* or *ppk23* mutant males or generating a mutant for the olfactory cVA receptor, *Or67d,* could test if the cVA olfactory pathways exclusively mediate male-male courtship suppression or if the olfactory and gustatory pathways work redundantly together.

We first considered whether there were changes in the peripheral tuning of gustatory sensory neurons. The absence of a behavioral phenotype in *D. simulans Gr32a* and *ppk23* mutants towards conspecific females and males could be due to these sensory neurons losing sensitivity to 7-T. While we do not have the genetic tools to examine the functional tuning of the Fru-Gr32a+ sensory neurons, we did observe equivalent functional responses to the taste of a *D. simulans* female in the ppk23+ sensory neurons in both species (Fig. 2.10 a). These responses were significantly decreased in *ppk23* mutants (Fig. 2.8 d, e), suggesting that *ppk23* is necessary for detection of *D. simulans* pheromones in both species.

We also wished to investigate if 7-T pheromone signals were differentially propagated to neurons in the higher brain of *D. melanogaster* and *D. simulans* males. Courtship-suppressing mAL neurons are poised to receive direct input by Gr32a+ sensory neurons and a small subset of Fru- ppk23+ sensory neurons whose axons ascend directly to the SEZ and terminate there[130]. While Gr32a+ sensory neurons have been shown to innervate the *D. simulans* male foreleg[131],

there have been no reports of their projections to the VNC or brain. However, the *D. simulans* and *D. melanogaster* Gr32a promoters drive similar expression patterns in *D. melanogaster* males (data not shown). The ascending projections of Fru- ppk23+ sensory neurons are conserved in males of both species (Fig. 2.9 d). Therefore, both neural populations appear poised to synapse onto mAL in both species.

We, thus, wished to characterize the *in vivo* functional tuning of mAL neurons in the lateral protocerebral complex by expressing GCaMP under the control of 25E04-Gal4 and stimulating the foreleg with *D. melanogaster* females, *D. simulans* females and males (Fig. 5.3 a). We previously found that mAL neurons were equivalently responsive to the taste of a *D. melanogaster* female (Fig. 5.3 b). However, the taste of a *D. simulans* female evokes significantly stronger activity in the mAL neurons of *D. melanogaster* males than *D. simulans* males (Fig. 5.3 c), supporting behavioral observations that *D. melangoaster* foreleg tarsi detect 7-T to suppress courtship[98,99] (Fig. 2.1 a). We were surprised that responses in *D. simulans* mAL neurons were only reduced and not abolished, given that 7-T does not appear to suppress courtship in *D. simulans* males. In the future, it will be interesting to determine if the modest amount of mAL activation we observe is behaviorally significant as it could help explain why *D. simulans* males tend to be less vigorous than *D. melanogaster* males when courting conspecific females. Unexpectedly, we observed that the taste of a male activated mAL neurons in *D. simulans* males significantly more than in *D. melanogaster* males (Fig. 5.3 d). These data suggest that in *D. simulans*, foreleg sensory neurons detect male pheromones to strongly activate inhibitory neural pathways to suppress male-male courtship. Additionally, since males and *D. simulans* females activate mAL neurons equivalently in *D. melanogaster* males, but not in *D.*
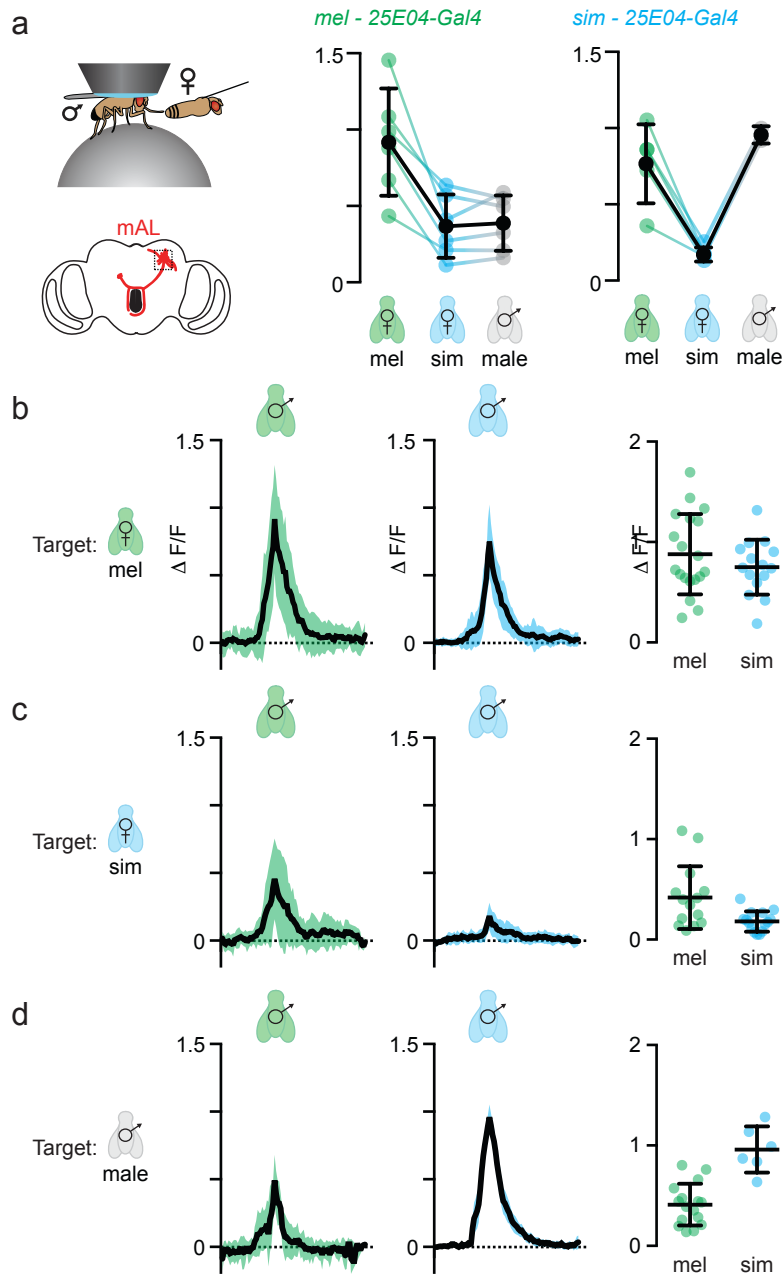
Figure 5.3: Divergent functional tuning of mAL neurons in *D. melanogaster* and *D. simulans* males. **a**, Schematic of *in vivo* GCaMP imaging preparation (left) with paired intra-individual responses in mAL neurons to the taste of a *D. melanogaster* female, *D. simulans* female or male target fly using *25E04-Gal4 > UAS-GCaMP* in *D. melanogaster* (middle) and *D. simulans* (right) males **b-d**, Aligned responses in mAL neurons of *D. melanogaster* (left) and *D. simulans* (right) males. Black line represents the mean and the colored area represents s.d. for each aligned frame. Recordings were captured at a constant frequency. Peak ΔF/F plotted when a male taps the abdoment of a *D. melanogaster* female (**b**), *D. simulans* female (**c**) or male (**d**) target fly with colored dots representing a tap-evoked response and black bars representing mean and s.d.

simulans males, peripheral evolution of either the Gr32a+ or "male" ppk23+ sensory neurons must have occurred to either increased sensitivity to cVA or decreased sensitivity to 7-T. Alternatively, a distinct sensory neuron population in the foreleg may have evolved to detect male pheromones and provide additional excitatory input to mAL neurons in *D. simulans* males. In the future, it will be interesting to further probe the pheromone tuning of Gr32a+ sensory neurons and ppk23+ sensory neurons and image mAL neurons in *Gr32a* and *ppk23* mutants of both species.

The pheromone tuning of mAL neurons implies that P1 neurons are inhibited by the taste of a male in both *D. melanogaster* and *D. simulans* males. While we had previously shown that optogenetic activation of P1 neurons was sufficient to overcome inhibition by heterospecific females, we had not tested male-male courtship. When we placed eight males that express CsChrimson in their P1 neurons in a dish together, we saw extremely robust male-male courtship upon optogenetic stimulation (Fig. 5.4). While we have not quantified this observation, we have replicated this experiment numerous times using both R71G01-Gal4 as a P1 neural driver and another transgene we integrated into the *D. simulans* genome, R15A01-Gal4. R15A01-Gal4 expresses in P1 neurons of both species, but has a more restricted expression pattern than R71G01-Gal4, which gave us additional confidence in our analysis of optogenetic activation of P1 neurons. This observation suggests that sensory cues that suppress male-male courtship potentially converge on P1 neurons. In the future, it will be interesting to determine the relative contributions of olfactory and gustatory pheromones to P1 neuron suppression towards other males.

pre-stim = -10 sec   stim = +30 sec   stim = +60 sec

stim = +80 sec   stim = +120 sec   stim = +130 sec

stim = +240 sec   post-stim = +30 sec   post-stim = +90 sec
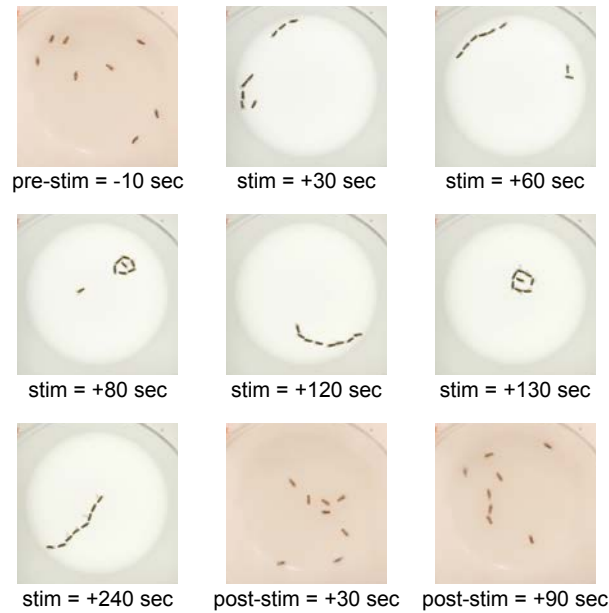
Figure 5.4: P1 neuron activation drives male-male courtship in *D. simulans* males. Anectodal example of a male chaining behavior after P1 neuron activation, which is robust behavior we consistently observed numerous times in R71G01>UAS-CsChrimson (shown here) and R15A01-Gal4>UAS-CsChrimson (not shown). Prior to light stimulation male-male courtship and chaining is very low. After light stimulation males start courting each other which can manifest as lines or circles of male-male courtship. Robust courtship lasts for the duration of the 5 minute light stimulus. After the light stimulus is turned off robust courtship ceases, but males still show brief bouts of male-male courtship.

5.3 Conservation of cVA pheromone circuitry

The male-specific olfactory pheromone *cis*-vaccenyl acetate (cVA) is transferred to females during copulation, suppressing further courtship by males towards mated females[124–127]. *D. melanogaster* and *D. simulans* males can discriminate between conspecific females perfumed with cVA or a control solvent (Fig. 5.5 b), revealing a strong aversion to courting females scented with cVA, as was previously observed in *D. melanogaster*[126]. In fact, cVA appears to be a broadly conserved pheromone that serves as a potent antiaphrodisiac for many species including, but not limited to, *D. melanogaster*, *D. simulans*, *D. yakuba*, *D. pseudoobscura* and *D. ananassae* (Fig. 5.5 c). Interestingly, cVA is also broadly conserved as an aggregation pheromone in these species, highlighting another strong selective pressure for maintenance of this circuitry[132,133].

Since all species in the *D. melanogaster* subgroup produce cVA and respond to it, we believe that their last common ancestor also produced cVA. Thus, all existing neural circuitry that processes this pheromone most likely has a common evolutionary origin, making this an interesting model system to study how functional conservation of circuitry underlies a conserved behavior. Comparing the cVA-responsive neural pathways across species could reveal near perfect conservation of anatomy and function, which would then provide a useful system for studying how circuitry in maintained. Alternatively, cross-species comparisons of the cVA circuit could reveal anatomical or functional changes, which would then provide a useful system for studying the persistence of behavioral integrity despite perturbations in circuitry, or in other words circuit robustness.
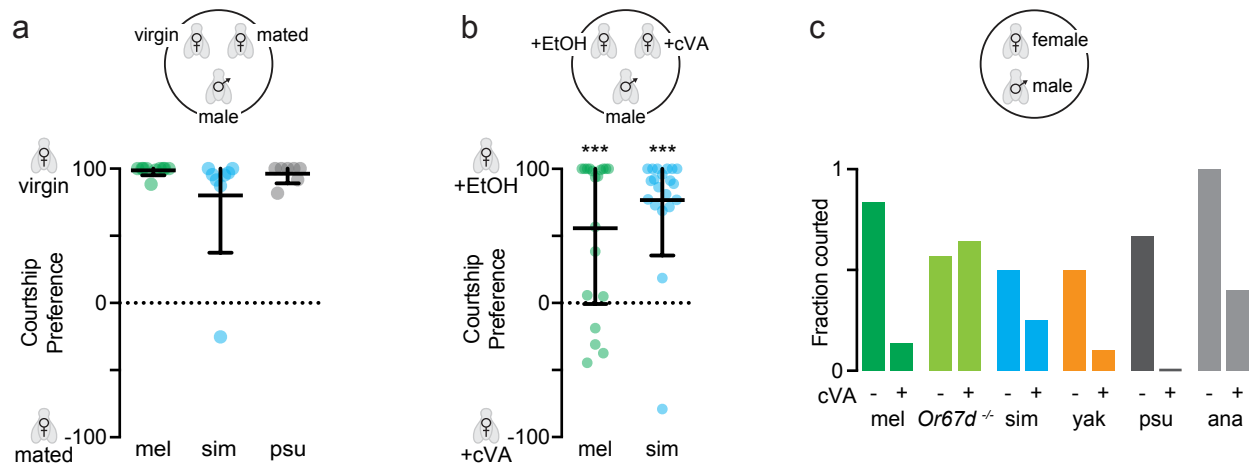
Figure 5.5: cVA suppresses courtship in many species. a, Courtship preference of *D. melanogaster*, *D. simulans* and *D. pseudoobscrua* males between two conspecific females - one virgin and one recently mated female. **b**, Courtship preference of *D. melanogaster* and *D. simulans* males when offered a choice between conspecific females perfumed with ethanol (control) or cVA (one-sample t-test with Bonferroni correction. mel P=0.004 and sim P<0.0001). **c**, Fraction of males who initiated courtship in single pair assays towards a conspecific female perfumed with cVA or ethanol.
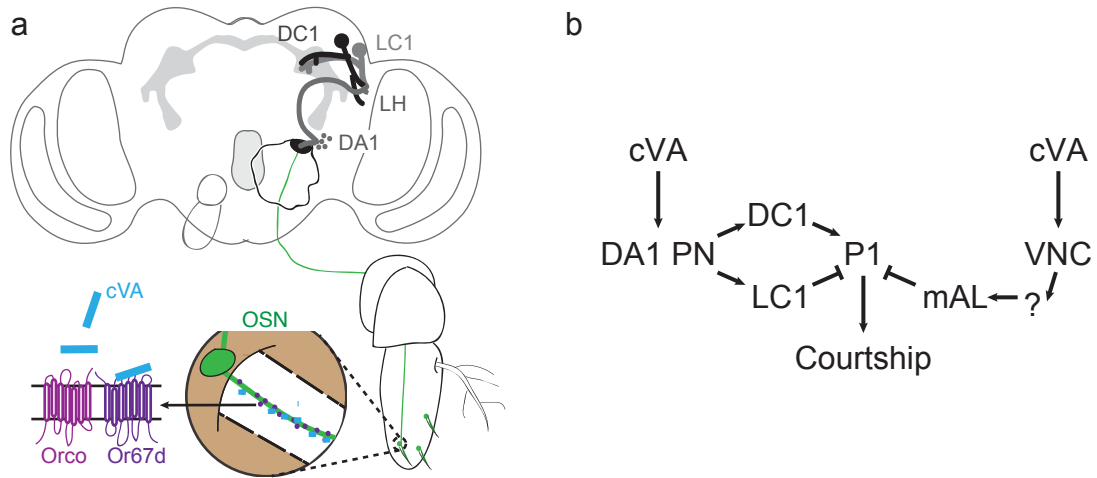
Figure 5.6: Olfactory and gustatory pathways that process cVA. a, Schematic of olfactory architecture that processes cVA. **b**, Schematic of olfactory and gustatory pathways that process cVA, both of which converge onto P1 neurons.

cVA, in addition to activating the foreleg-mediated gustatory pathway described above, also activates an antennae-mediated olfactory pathway (Fig. 5.6). In the olfactory system, cVA is detected by Or67d, an olfactory receptor (OR) expressed in olfactory sensory neurons (OSN) whose dendrites innervate the T1 tricoid sensilla, one of the few mono-innervated sensilla of the antenna (Fig. 5.6)[128,134,135]. Fru+ Or67d^{+} OSNs project to the DA1 olfactory glomerulus, which is dedicated to cVA processing[128]. The *fru+* DA1 excitatory projection neurons (PNs) extend sexually dimorphic axonal arbors into the lateral horn, an area associated with driving innate olfactory behaviors[136,137]. In males, the axons of DA1 PNs form connections with excitatory dorsal (DC1) and GABAergic lateral (LC1) neuronal clusters in the lateral horn (Fig. 5.6)[137]. Both the DC1 and LC1 neuronal populations transmit cVA signals to the lateral protocerebral complex, where they are thought to provide excitatory and inhibitory input onto P1 neurons resulting in net-inhibition when a male detects cVA[102,116]. In females, the DC1 neurons do not appear to innervate the lateral horn and LC1 neurons exhibit sexually dimorphic morphology[137,138].

Taking advantage of the readily identifiable position and size of the DA1 glomerulus[136–138], we dye-filled DA1 PNs in males of several other *Drosophila* species and found that all have projection neurons that innervate the ventral lateral horn (Fig. 5.7). However, there were reproducible differences in the distinct patterns of axonal arbors across species, with the arborizations being more similar between closely related species. It is unclear if these differences reflect adaptive or meaningful changes in circuit function or, rather, if they simply reflect anatomical drift over millennia. Maintenance of circuit function despite anatomical drift would suggest robustness in the circuit.
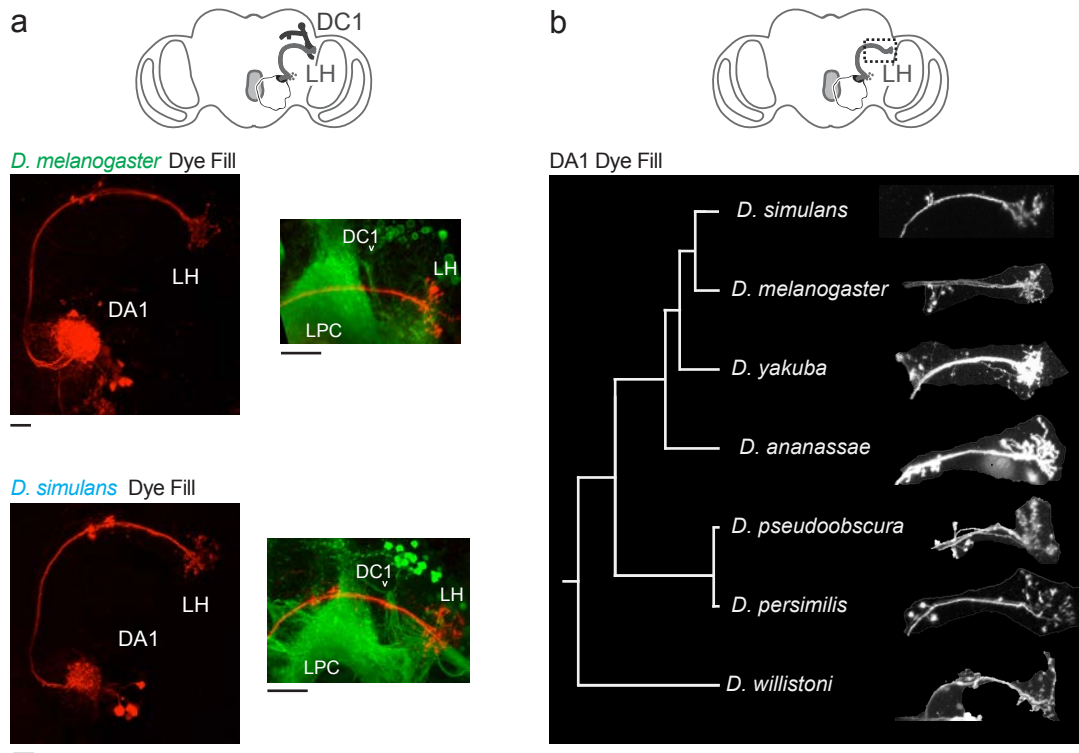
Figure 5.7: Conservation of components of the cVA-responsive olfactory pathways. a, Anatomic conservation of neurons in the cVA-processing pathway in *D. melanogaster* (top) and *D. simulans* (bottom) males. In both species, Texas-Red dextran dye-fill of the DA1 glomerulus (left) demonstrates that the DA1 projection neurons extend projections into mushroom body calyx and lateral horn. DA1 dye-fill with Fru+ neuropil (green) zoomed in on the lateral horn (LH) and lateral protocerebral complex (LPC) shows DC1 interneurons (arrow) innervating both the LH and LPC (right). **b**, Anatomy of DA1 PNs axons in the lateral horn of several species. Scale bars represent 10 μm.

In both *D. melanogaster* and *D. simulans*, the DA1 PNs also revealed a conserved anatomy where they projected to the lateral horn (Fig. 5.7 a). Likewise, the DC1 interneurons are Fru+ and exhibit a conserved, identifiable anatomy in both species. LC1 neurons have a more diffuse arborization pattern within the lateral horn and cannot be as readily distinguished from other Fru+ projections. Given the similar anatomical organization of the DA1 projection neurons and DC1 interneurons, we wanted to explore if there was also functional conservation of this pathway. Iontophoresis of acetylcholine into DA1 drove strong activity in DA1 PNs and DC1 neurons in *D. melanogaster*, *D. simulans* and *D. yakuba*, suggesting that in addition to retaining anatomical conservation, they also remain functionally connected (Fig. 5.8).

To test if cVA was still sufficient to evoke responses in these neural populations, we stimulated the antenna of a tethered male walking on an air-supported foam ball with cVA. In both DA1 and DC1 neurons, cVA evokes equivalent responses in *D. melanogaster* and *D. simulans* males (Fig. 5.9)[136,137]. We observe strong responses in the Fru+ neurons of the LPC in *D. melanogaster*, *D. simulans* and *D. yakuba* males when bringing a target male's abdomen within one body length of the male we were imaging, but not allowing contact to occur, potentially reflecting activation of cVA olfactory circuits (data not shown). In contrast, we did not observe responses in the Fru+ LPC to any olfactory pheromones present on virgin females (data not shown). Furthermore, a male stimulus only evoked responses in mAL neurons when contact chemosensation occurred during tapping, and not via olfactory stimulation by volatile cVA (data not shown). Therefore, while we observed differential activation of the LPC in response to 7,11-HD, a cuticular pheromone that drives species-specific behaviors, differences were not apparent in response to cVA, an olfactory cue that plays a conserved role in shaping mating preferences.
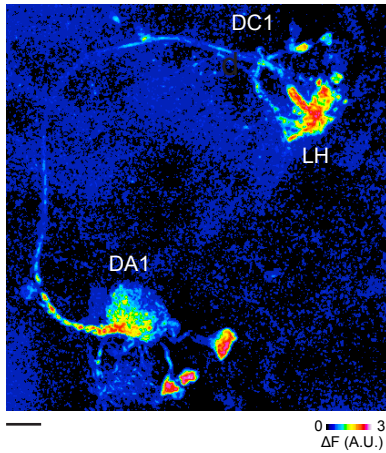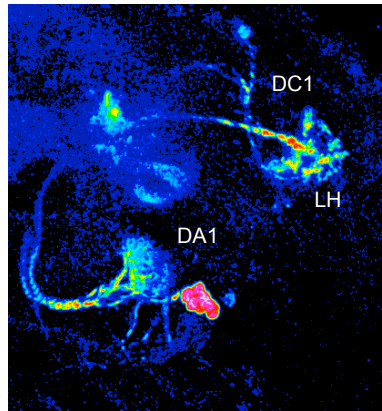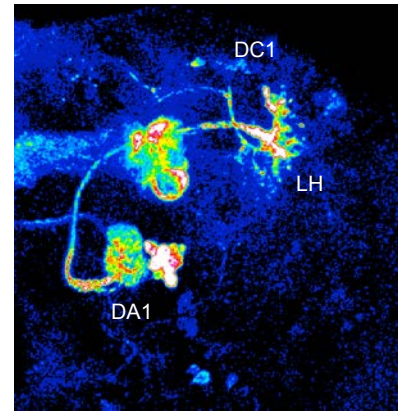
Figure 5.8: Conservation of a cVA-responsive circuit across species. Representative multi-plane image of GCaMP responses in Fru+ neurons of the central brain in response to acetylcholine iontophoresis in the DA1 glomerulus in *D. melanogaster*, *D. simulans* and *D. yakuba* males. DC1 neurons, DA1 neurons and the lateral horn (LH) are noted. Scale bar represents 10 μm.
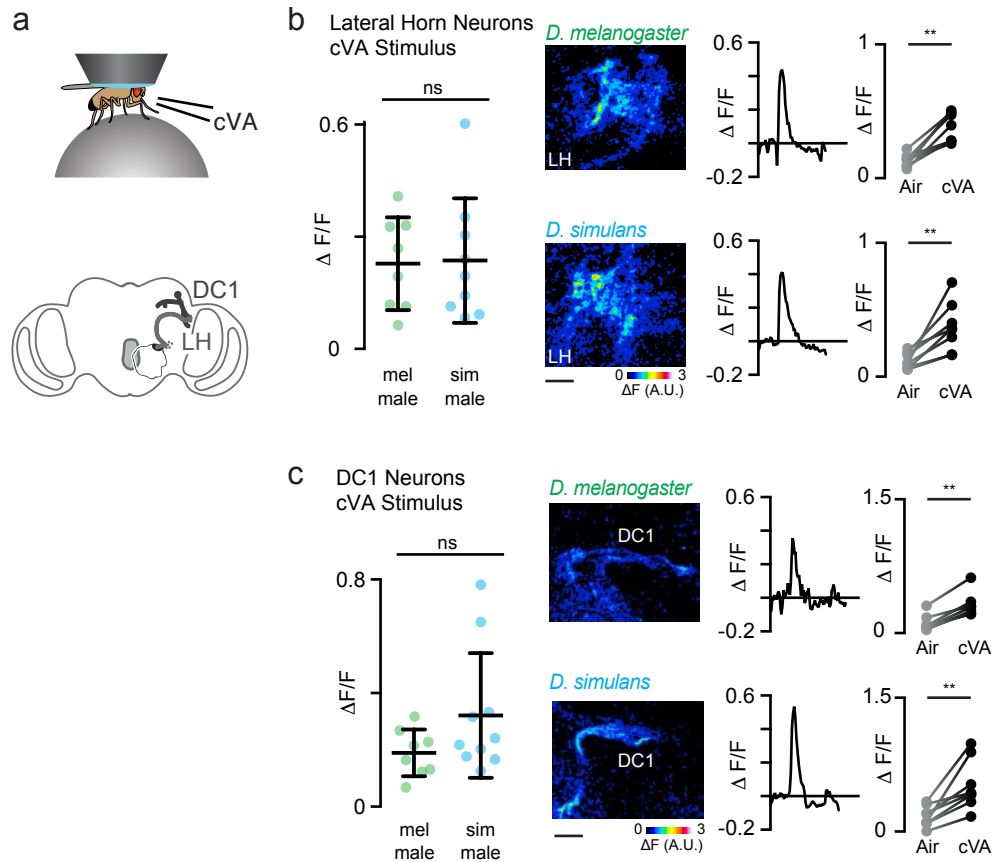
Figure 5.9: Conservation of *in vivo* cVA responses. **a**, Cartoon of the anatomic relationship between DC1 and lateral horn (top) and experimental set-up of *in vivo* cVA stimulation (bottom). **b**, **c**, *In vivo* GCaMP imaging of Fru+ lateral horn neuropil (**b**) and DC1 interneurons (**c**) in response to volatile cVA. Comparison of peak responses (left) in *D. melanogaster* and *D. simulans* males to cVA in the LH (**b**, n=8-9, Mann-Whitney test, P=0.9410) and DC1 interneuorns (**c**, n=9-10, Mann-Whitney test P=0.1699). Dots represent average individual responses. Black bars represent mean and s.d. Representative images depict heat map of fluorescence increase (ΔF, middle). Graph summarizes paired intra-animal averages for cVA (black) and ethanol control (grey) responses (Right, Wilcoxon matched-pairs test. n=8-10, P<0.001). Scale bars represent 10 μm.

5.4   Role of *D. melanogaster* foreleg sensory neurons in suppressing courtship towards males and *D. simulans* females

In *D. melanogaster*, past work has suggested that Gr32a+ sensory neurons detect 7-T and cVA in order to suppress courtship towards both males[99,139] and heterospecific females[99]. "Male" ppk23+ sensory neurons have also been proposed to detect 7-T and cVA, but somehow only mediate courtship suppression towards males[94,95,99] and not *D. simulans* females[99]. Activation of either neural populations is sufficient to reduce male courtship behavior[97,99]. Below I will address my attempts at resolving the inconsistences of these observations.

First, I considered how both *Gr32a* and *ppk23* could be necessary for courtship suppression. One possibility is that these receptors are expressed in an overlapping sensory neuron population with mutation of either disrupting sensory transduction. To explore this hypothesis, I co-expressed Gr32a-Gal4>UAS-GFP and ppk23-LexA>LexAOp-Tomato in the same males. While we observed overlap of Gr32a+ sensory neurons and the subset of Fru- "male" ppk23+ sensory neurons in both the VNC and brain, we could not confidently assess if they were expressed in the same soma due to weak expression of Tomato. I next tried an alternative approach and used the ppk23 promoter to suppress Gal4 (through expression of Gal80) in any Gr32a+ sensory neurons that also express the ppk23 promoter. However, in Gr32a-Gal4>UAS-GFP, ppk23-LexA>LexAOp-Gal80 males, I always observed GFP expression in the same number of Gr32a+ sensory neurons, implying Gr32a and ppk23 likely label distinct populations.

Second, it is confusing how Gr32a+ and ppk23+ sensory neurons both detect 7-T in *D. melanogaster* males, yet only *Gr32a* mutant males court *D. simulans* females. Some insight was

gained from imaging the aggregate responses of "male" ppk23+ sensory neurons in the VNC, which implied that these neurons might be more responsive to the taste of a male than a *D. simulans* female, suggesting they are preferentially tuned to other male pheromones than 7-T. The literature speculates that the Gr32a+ and the Fru- ppk23+ sensory neurons that ascend directly from the VNC to the SEZ directly activate mAL to suppress courtship[130]. Given that mAL neurons respond to the taste of both males and *D. simulans* females, it will be informative to understand how the *ppk23* and *Gr32a* sensory mutants impact signal transduction from the foreleg to mAL neurons.

Understanding the redundant roles of Or67d+ olfactory neurons, "male" ppk23+ sensory neurons and Gr32a+ sensory neuron in detecting inhibitory cues to suppress courtship will provide a more holistic view of how sensory cues converge onto P1 neurons to regulate courtship.

5.5   Discussion

The olfactory pathway that processes cVA appears to be conserved between *D. simulans* and *D. melanogaster*. However, while 7-T suppresses courtship in *D. melanogaster*, it does not appear to impart strong excitation or inhibition in *D. simulans*. Indeed, *D. simulans* hydrocarbon pheromones are sexually monomorphic and thus offer ambiguous signals for mate recognition. While both *D. melanogaster* and *D. simulans* ppk23+ sensory neurons responded equivalently weakly to the taste of a *D. simulans* female (Fig. 2.10 a), this signal is only strongly propagated to mAL neurons in *D. melanogaster* males to suppress heterospecific courtship (Fig. 5.3). Therefore, in *D. simulans,* there appears to be a peripheral modification in the detection of 7-T

that prevents propagation of this signal to mAL neurons. In contrast, the taste of a male evoked stronger responses in *D. simulans* mAL neurons than *D. melanogaster* mAL neurons.

Both Gr32a+ and "male" ppk23+ sensory neurons have been suggested to detect cVA and 7-T in *D. melanogaster*. Perhaps, in *D. simulans*, either one or both sensory neuron populations have become exclusively tuned to cVA or the '7-T-responsive' sensory neurons no longer activate mAL. Either way, there is strong evidence that an additional modification occurred in *D. simulans*, potentially peripherally, to prevent 7-T from suppressing courtship towards a conspecific female mate. As a result of these peripheral and central changes, mAL neurons in *D. simulans* and *D. melanogaster* males are equivalently activated in response to two target flies a male does not court: other males and heterospecific females. In the future, it will be informative to better understand whether changes to peripheral detection of 7-T or central circuit changes to how this signal is conveyed to mAL neurons have occurred. It will also be illuminating to study this circuit in *D. yakuba*, a species that is also monomophic in its pheromone production and thus needs to interpret 7-T as neutral or attractive.

6 | Discussion and Outlook

The work I have presented represents one of the first systematic cross-species comparisons of sensory circuits in *Drosophila.* Through the development of neurogenetic reagents in *D. simulans*, *D. yakuba* and *D. erecta*, we were able to directly compare homologous neural populations to understand conservation and divergence in pheromone processing circuits across species. In *D. simulans* and *D. melanogaster*, the comparison of three, inter-related neural pathways that process male and female pheromones have revealed that circuits mediating divergent behaviors can emerge through both modifications in peripheral detection and central processing and that circuits mediating shared behaviors across species remain functionally conserved.

6.1   Major Conclusions

Our comparison of homologous neural circuits across closely related species has yielded several insights:

1 | Evolution of a central neural circuit underlies the divergent pheromone preferences of *D. melanogaster* and *D. simulans* males to mediate mate discrimination.

2 | In *D. melanogaster*, *D. simulans, D. erecta* and, likely, *D. yakuba* males, recognition of *D. melanogaster* female pheromones requires the ppk23 receptor. Comparing pheromone-processing circuitry in these species provides a rare opportunity to investigate the neural basis of parallel behavioral evolution.

3 | A functionally homologous neural circuit exists in *D. simulans*, *D. melanogaster,* and *D. yakuba* males where neurons that look homologous to vAB3 and mAL neurons provide feed-forward inhibition onto P1 neurons. This inherently flexible circuit architecture, where pheromone signals are transmitted through parallel excitatory and inhibitory branches, could represent an 'evolvable' node of the nervous system.

4 | Male-male courtship is suppressed in both *D. simulans* and *D. melanogaster*. *D. melanogaster* males use gustatory detection of cVA and 7-T and olfactory detection of cVA to inhibit male-male courtship. However, while *D. simulans* males use conserved cVA pathways to suppress male-male courtship, a peripheral modification of 7-T detection potentially rendered this inhibitory pathway non-functional in order to permit attraction to conspecific females.

5 | Studying the neuronal basis of behavioral evolution though systematic comparisons of homologous circuits can uncover novel mechanisms for how behaviors diverge and, thus, should be a complementary approach to studying the genetic basis for behavioral evolution.

6.2   General Trends in Sex and Species Discrimination in *Drosophila*

6.2.1   *Gustatory Pheromones Are Not Necessary for Courtship*

Our observation that *D. simulans* female pheromones are not necessary for male courtship was incongruent with the long-held assumption that female pheromones play an essential role in promoting a male's arousal in *Drosophila*. However, multiple lines of behavioral and functional evidence suggest that males in the *D. melanogaster* subgroup do not rely on the pheromones of their conspecific female to initiate or maintain courtship in the light.

Most compellingly, perhaps, is the striking observation that *D. melanogaster*, *D. simulans*, *D. yakuba,* and *D. erecta* males vigorously court *D. melanogaster* oenocyte-less females that carry no hydrocarbon pheromones on their cuticle[115]. Furthermore, we replicate prior work demonstrating that tarsi-ablated *D. simulans* and *D. melanogaster* males will still vigorously court despite their inability to detect any excitatory cues with their forelegs[99]. Finally, we show that *D. simulans* ppk23 mutant males exhibit fervent courtship towards diene-producing females as distantly related as *D. ananassae*. This mirrors the fervent courtship *D. melanogaster ppk23* mutant males exhibit towards their conspecific females.

In both *D. simulans* wild type males and *D. melanogaster* ppk23 mutant males, conspecific female pheromones do not excite the P1 neurons or any other Fru+ neural population in the LPC, yet males of both species remain capable of courtship. Together, these data demonstrate that *Drosophila* males can be aroused in the absence of any species-specific excitatory pheromone cue implying that other sensory inputs control the initiation of courtship. Given that vision is obligatory for robust courtship in *D. simulans* males[91] and *D. melanogaster ppk23* mutant males[93], we speculate that visual cues may serve to promote their sexual arousal. In future work, it will be fascinating to explore how visual signals promote courtship behavior in these species, and whether *D. simulans* and other males that lack a female-specific cuticular pheromone rely more extensively on visual cues.

6.2.2 Pheromones Are Necessary and Sufficient for Sex and Species Discrimination in Drosophila

While species-specific pheromones are dispensable for courtship, they are essential for species discrimination. *D. simulans*, *D. yakuba* and *D. erecta* males will vigorously court *D. melanogaster* females whose oenocytes have been genetically ablated, but suppression of heterospecific courtship is restored if the oenocyte-less females are perfumed with 7,11-HD[115]. In addition, we have demonstrated that *D. simulans, D. yakuba* and *D. erecta* males can discriminate between conspecific females perfumed with 7,11-HD or ethanol. In *D. simulans* and *D. erecta,* we further demonstrated that ppk23+ sensory neurons are necessary for detection of inhibitory pheromones like 7,11-HD to mediate species discrimination. Therefore, the detection of inhibitory pheromones is sufficient to both suppress courtship towards inappropriate mates and mediate species discrimination.

Somewhat surprisingly, courtship discrimination by *D. melanogaster* males appears to also mainly depend on detection of the inhibitory pheromone 7-T and not the excitatory pheromone 7,11-HD. *D. melanogaster Gr32a* mutant males, which are thought to only have deficits in detecting gustatory 7-T and cVA signals[98,99], indiscriminately court *D. melanogaster* and *D. simulans* females. Thus, in the light, the excitatory signal from 7,11-HD does not bias a *D. melanogaster* male to pursue only his conspecific female. Indeed, 7,11-HD is not even essential to promote courtship[77] in the light as *D. melanogaster* males find oenocyte-less and wild type females equally attractive. In the future, it will be interesting to replicate these experiments in the dark, where I predict 7,11-HD will be sufficient to mediate species discrimination.

Discrimination between mated and virgin females is mediated by the presence of the inhibitory pheromones, like cVA, that get transferred to females during copulation. While inhibitory pheromones serve a central role in assessment of females, it is not known if sex discrimination is entirely mediated by inhibitory pheromones or if males can also use morphological or behavioral differences between males and females to bias their courtship. Understanding the necessity and sufficiency of different cues will help further our understanding of the multimodal sensory signals integrated by P1 and other neurons that control courtship.

6.2.3 Speculative Role for Learning in Species Discrimination

During my Ph.D., I specifically studied the genetically hardwired neural circuitry a male uses to discriminate between species and sexes. As such, my behavior experiments were designed to test innate preferences. Courtship experiences like sexual satiety are known to regulate the excitability of P1 neurons to modulate courtship behavior in an individual[117]. Similarly, prior courtship experiences like encountering an unreceptive heterospecific female are also thought to modulate a male's courtship behavior[140]. If true, it will be interesting to see if learning to avoid interspecific courtship is also regulated by alterations in P1 neurons. However, it remains an open question if learning to discriminate between receptive conspecific females and unreceptive heterospecific females is a general strategy for species discrimination. Just as phenotypic plasticity can reflect the 'evolvability' of a genetic locus[120], behavioral plasticity could also reflect the 'evolvability' of a circuit node and possibility even facilitate behavioral evolution.

6.3 Evolution of the 'Process-of-Elimination' Strategy for Species Discrimination by *Drosophila* males

To find an appropriate mate, males in the *D. melanogaster* subgroup use a process-of-elimination strategy where they inhibit courtship of heterospecific females rather than promoting courtship towards conspecific females. This strategy appears to be atypical in other insects, where appropriate mates are mainly recognized using inter-specific communication[141]. Indeed, even females in the *D. melanogaster* subgroup appear to use species-specific cues to positively regulate mating with conspecific males. When considering how the process-of-elimination strategy may have evolved, it is important to remember that biological systems and species do not evolve to be perfect; they simply have to be good enough to pass on their hereditary material. Moreover, natural selection is not a goal-directed process, but rather a process that selects for adaptive changes and against maladaptive changes from an ancestral form. With these two ideas in mind, I will speculate on the selective pressures that could have shaped the evolution of this strategy.

One critical constraint that likely shaped the evolution of *Drosophila* mate selection is the limited evolution of hydrocarbon pheromones. While hydrocarbon profiles have diversified between species, very few species produce unique hydrocarbons. Prior work has suggested that inter-species communication is likely a secondary role of hydrocarbons, with their primary role being to prevent desiccation[123,142]. Flies that lack oenocytes and do not produce hydrocarbons are much more susceptible to dessication[77]. Therefore, any modification to hydrocarbons on the fly's cuticle could have a lethal effect[123,142].

Frequently mechanisms for long-range olfactory or auditory recognition of conspecific cues develop to facilitate finding a mate. However, *Drosophila* mating and courtship naturally occur on the species' preferred food substance, which males and females find through long range attraction to food odor and aggregation pheromones. Therefore, since ancestral mechanisms were already in place to facilitate males and females finding each other, there was potentially no selective pressure for the development of long-range conspecific olfactory pheromones.

Interestingly, considering that flies of many species will aggregate on a food source[81], a male's process-of-elimination strategy may actually be the most efficient way to find a conspecific female. General excitation by the presence of flies motivates a male to begin investigating females. If the male then tastes an inhibitory pheromone, he will terminate courtship and reinitiate towards another female. If that female does not have an inhibitory pheromone, he will continue courting her. While excitatory pheromones could have potentially evolved to motivate a fly to continue courting a conspecific female, there could be limitations in how the central brain is wired such that pheromonal excitation of P1 neurons may not greatly contribute to putative visual excitation of the P1 population. This would explain the observation that excitatory pheromones act redundantly with vision in *D. melanogaster* and why 7,11-HD does not mediate species discrimination. Therefore, a male's process-of-elimination strategy could have evolved both because there are limitations on pheromone diversity and because the ancestral neural circuits were organized in such a way that excitatory pheromones are not necessary for a male that is visually excited.

It should be noted that while this process-of-elimination strategy may be uncommon, as we learn more about species-discrimination in other genera, we may find that it is not unique. Rigorously demonstrating that heterospecific pheromones are inhibitory rather than neutral is difficult since in both cases lack of attraction may appear the same behaviorally. One must be able to test the necessity and sufficiency of an inhibitory cue to suppress courtship of an otherwise attractive mate, which is difficult if the cue and its receptor are not known.

6.4   Neural Circuit Diversification in *D. simulans* and *D. melanogaster*

As *D. melanogaster* and *D. simulans* diverged, their reproductive isolation was likely strengthened by the ability of both species to detect the same pheromonal cues, but assign them different meaning. Central circuit modifications altered the valence of 7,11-HD and peripheral modifications altered the valence of 7-T. However, neural circuits that process the male-specific pheromone cVA to mediate courtship suppression were most likely conserved between these species. While it is difficult to know the order of evolutionary processes, considering *D. simulans* females lost the ability to produce 7,11-HD[74], I speculate that the neural changes in *D. simulans* represent a derived state.

One mechanism for reinforcing species barriers between *D. melanogaster* and *D. simulans* is a differential interpretation of the valance of 7-T. In the ancestral state, males most likely had neural mechanisms to suppress courtship towards 7-T since it was a male-specific pheromone. Considering that *D. melanogaster* is dimorphic in its pheromone production, this species potentially represents the ancestral state. *D. melanogaster* male mAL neurons are strongly activated by the taste of both males and *D. simulans* females, which suppresses P1 neurons to

inhibit courtship. However, when female production of 7-T was derived in *D. simulans*, the neural mechanisms that detect 7-T to inhibit courtship were likely selected against. As a result, while 7-T inhibits *D. melanogaster* male courtship, it does not appear to inhibit *D. simulans* courtship. Interestingly, *D. simulans* mAL neurons have strong responses to the taste of male pheromones but weak responses to the taste of *D. simulans* female pheromones, as compared to *D. melanogaster*. Considering that mAL activation suppresses courtship in *D. simulans*, we predict that peripheral sensory neurons that detect both cVA and 7-T have altered pheromone tuning such that they now detect only cVA.

Another mechanism for reinforcing species barriers between *D. melanogaster* and *D. simulans* is a differential interpretation of the valance of the *D. melanogaster* female pheromone 7,11-HD. In *D. melanogaster* and *D. simulans* males, 7,11-HD is detected by the same peripheral sensory neurons and equivalently activates the same downstream excitatory and feed-forward inhibitory neural populations, which converge on the courtship-promoting P1 neurons. In *D. melanogaster*, the balance of excitation and inhibition is such that detection of 7,11-HD drives net excitation of the P1 neurons. In *D. simulans*, however, there has been a reweighting of synaptic connections such that 7,11-HD drives net inhibition of P1 neurons to suppress courtship. This central circuit change might have been selected for both because this region of the pathway is potentially highly 'evolvable' but also because a peripheral swap in the tuning of sensory neurons that directly activate vAB3 and mAL could have unintended pleiotropic effects. For instance, either losing gustatory detection of cVA to inhibit courtship or, even worse, if cVA activated P1 neurons to drive male-male courtship.

Finally, in both *D. melanogaster* and *D. simulans* males, the neural circuitry that processes the olfactory pheromone cVA is conserved in both peripheral detection by the Or67d sensory neurons and the propagation of this signal to DA1 projection neurons and the DC1 neurons in the LPC. However, further characterization of the neural circuits that process gustatory cVA signals is necessary before we reach any conclusions about conservation of cVA pathways. In particular, we need to better understand the relative contributions of the olfactory and gustatory input pathways to P1 neurons that mediate suppression across the two species.

6.5   Genetic "Tool kits" and Neuronal "Blue prints"

In developmental biology, conserved 'tool kit' genes underlie the development of specific aspects of morphologically dissimilar body types[3]. A major mechanism by which animal bodies diversify is though changes in the timing or expression of these 'tool kit' genes. Similarly, highly conserved molecules like the transcription factors Fruitless and FoxP2 or the neuromodulators dopamine and vasopressin orchestrate similar aspects of animal behavior across different species[12]. Just as identification of morphological 'tool kit' genes has facilitated our understanding of how they change to underlie morphological evolution, identification of behavioral 'tool kit' genes can provide genetic traction for studying the neuronal basis of behavioral evolution.

In my Ph.D., labeling neurons that express Fruitless in multiple species has provided genetic access to the circuits that control male courtship behaviors, allowing me to probe patterns of circuit conservation and diversification. Prior to this analysis, it was unclear whether we could identify conserved neural populations even between the recently diverged sister species, *D.*

simulans and *D. melanogaster,* but instead we identified the same circuits in *D. yakuba* (Fig. 2.6). In the three pheromone-processing circuits we studied, two mediating divergent responses to female pheromones (7,11-HD and 7-T) and one mediating a conserved response to a male pheromone (cVA), we found 'neuronal blueprints' of functionally conserved circuitry. Evolution did not generate entirely new pathways, but seems to have reused the same core neural pathways. In particular, conservation of the feed-forward inhibitory circuit of vAB3 and mAL neurons onto P1 neurons is surprising to find in species that last shared a common ancestor 10-15 million years ago. The existence of functionally conserved 'blueprint' circuitry may actually be common since large structural reorganizations of the brain are rare through an evolutionary lineage, suggesting they may be even more rare among closely related species. Therefore, a conceptual framework for future studies of behavioral evolution could be to first identify a 'tool kit' gene that mediates a divergent behavior and, second, label its expression pattern in the brain to uncover a 'blue print' of the relevant neural populations to systematically compare.

6.6   Evolvability and Parallel Evolution

Evolvability reflects the capacity of a phenotype to have heritable variation that can be selected upon[143]. Certain genetic sequences, gene regulatory networks, neurons, or behaviors are more tolerant of maintaining variation within a population, which can make those elements more 'evolvable'. As such, similar genetic changes frequently underlie the parallel evolution of a phenotype[42,74,119,122], potentially due to the fact that these genetic changes have minimal pleiotropic effects while yielding an adaptive phenotypic change[46,120].

It has been proposed that the sensory periphery and neuromodulators are the most 'evolvable' aspects of the nervous system[46]. In addition to this rich body of literature, we would like to propose that altering synaptic weights could also be an 'evolvable' area of the nervous system. Interestingly, experience-dependent changes[111,117] and evolutionary adaptations may both be acting on P1 neurons. Therefore, plasticity in P1 neurons may actually facilitate behavioral evolution similar to how phenotypic plasticity may facilitate morphological evolution[144].

Just as synaptic weight changes are an important mechanism for changing the valance of an odor during learning, reweighting of functional connections could be an extremely 'evolvable' aspect of circuits that differentially interpret the valence of an ethologically important cue. We will be able to test this idea when comparing the neural circuit changes that independently resulted in a strong aversion to 7,11-HD in both *D. simulans* and *D. yakuba* males. Further, this comparison will allow us to think about parallel behavioral evolution at the level of the circuit, synapse, neuron and even gene. It will be interesting to understand neural circuit 'evolvability' at several levels.

7 | Methods

Flies stocks and husbandry

Flies were housed under standard conditions at 25 °C under a 12 hr light: 12 hr dark cycle. Strains and sources: *Drosophila melanogaster* Canton S, *20xUAS-IVS-GCaMP6s* (Bloomington #42746, #42749), *UAS-mCD8::GFP* (#5130, #5137), *LexAop-GCaMP6s* (#53747), *10xUAS-IVS-myr::tdTomato* (#32222), *R71G01-Gal4* (#39599), *AbdB-Gal4* (#55848) *R25E04-Gal4* (#49125) and *20xUAS-IVS-CsChrimson.mVenus* (#55134) were obtained from the Bloomington Stock Center. The following were gifts, obtained as indicated: *D. simulans* attP2039 [145] (Yun Ding and David Stern, Janelia Research Campus); SplitP1-Gal4 [111] (David Anderson, Caltech); *fru^LexA* [146] and *fru^Gal4* [18] (Barry Dickson, HHMI/Janelia Farm Research Campus); *D. melanogaster* ppk23-Gal4 [95] (Kristin Scott, UC Berkeley); UAS-C3PA [137]. All experimental animals are male and all stimulus animals are virgin females unless noted.

Courtship behavior assays and analysis. To standardize fly size and life history across trials, all flies used for behavioral assays were reared in food vials at a low density (3 females and 3 males as parents). Males for all assays were collected as virgins, placed in individual food vials (d = 3 cm, h = 9.5 cm) and housed in isolation for 3-6 days. Males were added to behavioral assays by direct aspiration from the food vial without ice or CO_2 anesthetization, except for the tarsi ablation experiments in which males were ice-anesthetized. Virgin females were group-housed in food vials and aged 3-6 days. All behavior experiments were conducted with the experimenter blinded to the genotype of any male or female fly that was a variable in a given experiment. The experimenter was unblinded only after analysis of the assay. All behavioral assays were conducted at *zeitgeber* 0 to 3 hrs except for assays using flies reared in the dark. All

behavioral assays were conducted in a heated, humidified room (25 °C, 46% RH) on a back-lite surface (Slim Edge-Light Pad A-5A, 5400K, 6 kLux) to maximize courtship indices. For all statistical comparisons of behavior, an equal sample size per condition per day was used to control for potential variations in experimental conditions across days. For all preference assays, only males who spent more than 5% of the time courting (>30 s of total courtship) were included in the analysis. Courtship behaviors included in analysis were singing, tapping, licking, orienting, abdomen bending and chasing.

For all preference assays, a male and two female flies were placed into a 38 mm diameter, 3 mm height circular chamber with sloping walls (courtship arena)[92]. The experimenter, who was blinded to the female, kept track of them during the assay either by noting which female was introduced first to the courtship arena or by painting a small white dot on the thorax of the female 16-20 hrs prior to the start of the experiment under ice anesthesia. Results were not affected by the method used to differentiate between females and the experimenter was unblinded only after analysis. The preference index, expressed as a percentage, reflects the amount of time the male spent courting one female subtracted from the amount of time spent courting the other female divided by the total time spent courting within a 10 min assay. When males displayed no preference for females it was because, on average, the population courted the two females an equal amount of time. The wide spread of the data reflects the fact that individual males will sometimes continue to pursue a single female throughout the assay even if both females are equivalent.

For the tarsi ablation assays, males were ice-anesthetized 16-20 hrs prior to the start of the experiment and had either the distal three tarsal segments on both forelegs removed or a sham treatment that left their appendages intact. For single-choice assays, the rear leg tarsi were ablated as a control. Males were then returned to a food vial to recover in isolation.

In *D. simulans* single pair courtship assays, a single virgin female and a *D. simulans* male were loaded into a courtship arena. Courtship index (time spent courting divided by total time together, expressed as a percentage) was measured for the 10 min after the male was introduced into the chamber.

For the chaining assay, eight males were loaded into a courtship arena and chaining index (time where at least three of the males were simultaneously courting each other) was measured for 10 min after the males were introduced into the chamber.

For the preference assays with perfumed females, we provided a male the choice between a *D. simulans* virgin female perfumed with pheromone (cVA or 7,11-HD) or the solvent for the pheromone. The solvent for cVA was ethanol and the solvent for 7,11-HD was hexane. We perfumed females with 7,11-HD (7(Z), 11(Z)-heptacosadiene, 10 mg/mL Cayman Chemicals #100462-58-6) or cVA ((11Z)-11-octadecen-1-ol acetate 10 mg/mL Cayman Chemicals #10010101) using a previously published protocol[115]. Briefly, the pheromone was added to a volume of solvent greater than 100uL on ice that was in a small glass vial. All solvent was rapidly evaporated using nitrogen gas. Seven ice anesthetized female flies were aspirated into the treated glass vials and gently vortexed three times for 30 s. Flies were then moved to food vials

where they were allowed to recover for exactly 1 hr. After perfuming, separate aspirators were used to handle the flies in order to avoid pheromone contamination.

To evaluate the behavioral efficicacy of cVA in many species, a male was placed in a small petri dish (35mm x 3 mm) filled with food and given the choice between courting a virgin female perfumed with hexane (the control solvent) versus a virgin female perfumed with cVA. The courtship chambers were designed to promote reliance on olfactory cues and stimulate courtship. We kept binary records of which female(s) each male courted in the 15 min assay.

For fru^{Gal4} optogenetic stimulation experiments, $fru^{Gal4}>UAS\text{-}CsChrimson\text{-}tdTomato$ or fru^{Gal4} parental controls were reared in the dark for 3-7 days after eclosion. Male flies were transferred to food containing 400 µM all-trans-retinal (Sigma R2500-10MG) 16-20 hrs before the assays[111]. Single male flies were loaded into a courtship arena and allowed to acclimate for 1 min. Flies were subsequently recorded for 7 min, alternating between 1 min dim white light followed by 1 min with constant LED stimulation (530 nm Precision LED Spotlight with Uniform Illumination–PLS-0530-030-S, Mightex Systems at an intensity of 0.02 mW/mm^2). The experimenter was blinded to the genotype of the flies until after the experiment. Genotypes were established using PCR sequencing of the UAS transgene. We quantified a courtship behavior index, which represented the percentage of time a male spent performing courtship behaviors, with or without LED stimulation.

For $ppk23$-Gal4 and 25E04-Gal4 optogenetic stimulation experiments, we used $D.\ simulans\ w^+$ $25E04\text{-}Gal4$, $ppk23\text{-}Gal4$ and $UAS\text{-}CsChrimson.tdTomato$ parental stocks and $D.\ melanogaster$

w⁻ ppk23-Gal4 and *UAS-CsChrimson* parental stocks lacking balancer chromosomes. The original *D. simulans 25E04-Gal4*, *ppk23-Gal4* and *UAS-CsChrimson.tdTomato* parental stocks were in a background mutant for *white* (*w⁻*), which exhibited extremely low courtship indices (~5% on average) presumably due to their low visual acuity, in contrast to *D. melanogaster w⁻* transgenic lines that maintained robust courtship even in a *white* mutant background (data not shown). We therefore backcrossed *D. simulans* stocks to wild type flies to generate *w⁺* strains and confirmed their genotype by PCR. Generating stable *w⁺* stocks was prohibitively difficult since neither 3xp3::DsRed nor mini-white are easily detectable in red-eyed flies. All crosses were reared in the dark. Virgin male progeny were reared in isolation in the dark for 3-7 days after eclosion and then transferred to food containing 400 µM all-trans-retinal 16-20 hrs before the assays[111]. We found that *D. simulans* courtship was less robust under single wavelength LED illumination or dim white light illumination so we conducted our assays using the same lighting conditions used for the non-optogenetic courtship assays (Slim Edge-Light Pad A-5A, 5400K, 6 kLux). Single male flies were loaded into a courtship arena that contained a conspecific virgin female and courtship index was assayed over a 10 min period after the male was introduced. For both crosses, progeny were a mix of wild type, parental controls, and experimental flies. The experimenter was blinded to the genotype of the flies until after the experiment. Genotypes were established using PCR sequencing of the Gal4 and UAS transgenes. Males of all genotypes exhibited similar levels of locomotion when they were not courting.

For optogenetic stimulation of P1 neurons in *D. simulans*, we used R*71G01-Gal4>UAS-CsChrimson.mVenus* males that carried a wild type (*w⁺*) X chromosome. As in other behavioral experiments, P1 neuron-elicited courtship pursuit was far weaker in males mutant for *white* (data

not shown). For optogenetic stimulation of P1 neurons in *D. yakuba* and *D. melanogaster w*⁻*;*

71G01-Gal4>UAS-CsChrimson-mVenus males lacking balancer chromosomes were used. We

found a high degree of lethality in both the *D. melanogaster* and *D. simulans R71G01-*

Gal4>UAS-Chrimson crosses grown on standard fly food containing cornmeal (presumably due

to the low levels of retinal metabolized from vitamin A). We therefore we grew these crosses on

sugar-yeast food in the dark (Per 1L of water: 100g Brewer's Yeast, 50g sucrose, 15g agar, 3mL

Propionic acid, 3g p-Hydroxy-benzoic acid methyl ester). Progeny of parental crosses were

group housed in the dark for 3-7 days after eclosion before males were transferred to food

containing 400 µM all-trans-retinal 48 hrs before the assays[111]. Single male flies were loaded

into a courtship arena that contained either a virgin *D. simulans* female, virgin *D. melanogaster*

female or a magnet (radius=1mm, height=1mm) rotating in a circle at 9mm/sec[102]. Upon loading

the male fly into the chamber with the target, we alternated between 2 min of dim light (10 Lux)

and 2 min of bright light (6 kLux) in a 14 min assay. Dim light was used because it was

sufficient to allow males to visually track a target object but insufficient to optogentically

activate the P1 neurons, as evidenced by the lack of courtship towards a magnet or *D.*

melanogaster female prior to bright illumination. Assays were filmed (Sony alpha6) and later

scored for courtship behavior, binned in 1-second intervals. We calculated "fraction courting" as

a function of time by dividing the number of males courting during a one-second interval

(aligned from the start of the assay) by the total males tested. Courtship indices were also

calculated for each individual at different times relative to the optogenetic stimulation: "pre"

represents the courtship index of the 2 min prior to the first bright light stimulus, "stimulus"

represents an average of the courtship indices during bright light illumination period and "post"

represents an average of the courtship index after the bright light illumination. For the parental

controls, we used *w+;UAS-CsChrimson.mVenus* males grown in an identical way as the experimental animals and similarly placed on retinal for 48 hours. For the non-retinal controls, *w+;71G01-Gal4>UAS-CsChrimson-mVenus* males were placed in a new vial of SY food for 48 hours prior to the experiment. To characterize evoked courtship as a function of light intensity, each experiment was initiated by illuminating for two minutes with dim light (10 Lux) to establish a baseline and then adding increasing intensity 627nm illumination from an LED, with two minutes at each intensity, and finally ending with two minutes of bright white light illumination. A power meter (Coherent PowerMax-USD light sensor) was used to measure the intensity of 627nm illumination in the behavioral chamber during the assay. To examine how elicited courtship depends on the speed of the magnet, each male was given the opportunity to court a magnet moving at 0, 3, 6, 10 and 20 mm/s during bright white light illumination. Magnet speed order was randomized and there were one-minute periods in between stimulus trials were the light was off and the magnet was stationary.

Methods to Develop CRISPR/Cas9 genome editing in *D. simulans*

To assess the feasibility of CRISPR/Cas9 to create double stranded breaks in *D. simulans*, I first designed three CRISPR guide RNAs (gRNAs) that targeted distinct regions of *white*, a gene located on the X chromosome that encodes a protein necessary for red eye pigmentation. I found that the three gRNAs (w1, w2 and w3) produced a low, medium and high percentage of males with mosaic white eyes, which correspond to disrupted function of *white*. To qualitatively assess the efficiency of CRISPR/Cas9-mediated cleavage, I settled on the T7 endonuclease 1 (T7E1) assay as a rapid, facile and cost-effective molecular readout[147]. In this assay, a PCR product is created with the CRISPR target site off center. The PCR product is then denatured and

143

reannealed to mix the strands before T7E1 is added. The nuclease T7E1 cleaves at the site of mismatched base pairs, which can be produced by natural polymorphisms or CRISPR-induced insertions and deletions. The entire reaction is then run on a polyacrylamide gel, a modification of published protocols that allows for greater sensitivity and resolution. Naturally occurring polymorphisms, which cause smearing on the gel, should not differ between the control flies and the CRISPR-injected flies. However, if the gRNA had high cutting activity, two novel bands should appear in the CRISPR-injected flies representing the asymmetrically cut PCR product. Only in w3 did I observe novel bands at the predicted cleavage size. Successfully targeting *white* validated the feasibility of using CRISPR/Cas9 in *D. simulans*.

Targeted mutagenesis and transformation in *D. simulans*

The protocols described below combine methods for CRISPR mutagenesis[148–150]. See last section of the methods for sgRNA sequences, sgRNA primers and sequencing primers.

CRISPR guide RNAs had an 18-20 nucleotide target sequence and were flanked by a 3' PAM sequence ('NGG') and a 5' T7 RNA polymerase recognition sequence ('GG'). Before designing sgRNAs, Sanger sequencing was carried out across target genomic sites to identify single nucleotide polymorphisms. Guide RNA template was amplified using KOD HotStart (Millipore #71086-3) and 0.5 μM forward and reverse primers as templates for each other. Reactions were cycled on an Eppendorf MasterCycler (98 °C 30 s, 35 cycles of [98 °C 10 s, 60 °C 30 s, 72 °C 15 s], 72 °C 10 min, 4 °C hold) and then purified (PCR purification kit, QIAGEN). *In vitro* transcription of 300 ng of sgRNA template DNA using T7 MEGAscript kit (Ambion) was carried out at 37 °C for 16-20 hrs. Turbo DNAse was added for an additional 15 min at 37 °C

before adding a 10% ammonium acetate stop solution. The RNA was isolated using a phenol/chloroform reaction and was precipitated by adding isopropanol and placing the reaction at -20 $^{\circ}$C for 16-20 hrs. The precipitated reaction was purified with 70% ethanol, re-suspended with RNAse-free water, and frozen in small aliquots at -80 $^{\circ}$C for long-term storage. Before injection, the sgRNA was thawed on ice and purified using sodium acetate and ethanol before being re-suspended in RNAse free water.

CRISPR injection mixtures contained 300 ng/μL recombinant Cas9 protein (CP01, PNA Bio), 40 ng/μL sgRNA (per guide) and 125 ng/μL single stranded DNA oligonucleotide. CRISPR injection mixture was combined on ice and placed at -80 to -20 $^{\circ}$C until the injection. PhiC-31 mediated recombination injection mixtures contained donor plasmid (1 μg/μL) and helper plasmid (1 μg/μL), both of which were purified using endotoxin-free plasmid prep kits (Qiagen). Rainbow Transgenic Flies, Inc performed all injections.

Mutating *ppk23* and *Gr32a* in *D. simulans* and *D. erecta*

To generate mutant alleles of *ppk23* and *Gr32a*, we designed sgRNAs targeting three regions spanning 200 bp of the first exon for each gene. These sgRNAs were combined into a single cocktail and injected into ~200 wild type *D. simulans* eggs. Only CRISPR guide sequences that generated the mutations are listed in Table 1. The adult G0 flies were individually crossed to wild type male or virgin female flies. For each G0 cross, we PCR screened 8-16 progeny (F1s) for the presence of an insertion or deletion. Genomic DNA was extracted from the F1 flies by placing a midleg, hindleg or wing into a well of a 96-well plate containing 20 μL of lysis buffer (10 mM Tris pH 8.2, 1 mM EDTA pH 8.0, 25 mM NaCl, 400 μg/ml Proteinase K). The fly was

then placed in the corresponding well of a 96-well deep well plate (Brandtech VWR #80087-070) filled halfway with fly food and capped with cotton. The 96-well plate of lysis buffer and fly legs was then heated at 37 °C for 1 hr followed by a 2 min heat inactivation at 95 °C. 3.2 µL of genomic DNA from the leg was used as the PCR template for a 20 µL reaction of Apex Taq Red Master Mix (Genesee Scientific #42-138) for 35 cycles. The PCR screening primers spanned an approximately 400 bp region encompassing the three sgRNA target sites. In order to maximize resolution of heterozygous indels, we ran the entire PCR reaction on a 2% agarose gel at 70 V. Using these specifications, the smallest indel we detected was ~20 bp. We backcrossed any flies that had a heterozygous mutation to wild type flies and then homozygosed their progeny. Flies were Sanger sequenced to determine if an in-frame stop codon was introduced. Homozygous stocks were genotyped and Sanger sequenced for three generations to ensure that the population was pure.

We wanted to explore the behavioral role of *ppk25* by using CRISPR/Cas9 to generate sensory mutants. However, despite the successful generation of several *ppk25* mutant lines with large (~500 bp) and small (4bp) deletions, we could not propagate the line. *ppk25* homozygous mutant parents would mate, but we never observed progeny. This is most likely because mutations in *ppk25* could also effect an essential gene *missing-in-metastasis* (*mim*), which is necessary for proper development of cells that facilitate egg fertilization[151], since the two share a genomic position. Indeed, *D. melanogaster ppk25* mutants are maintained using the second chromosome balancer *cyo*, with most flies in the stock being heterozygous. We do not yet have X chromosome or 2nd chromosome balancers in *D. simulans*.

Targeting Fru in *D. simulans*

For recombination into the *fru* locus, we prescreened sgRNAs to identify those that mediate efficient cutting. Nine sgRNAs were designed, six which targeted the intronic region upstream of the first exon and three which targeted the first exon. Pools of three sgRNAs were injected into 100 embryos and genomic DNA was extracted from surviving flies. We first used the T7 endonuclease1 (T7E1) assay for preliminary qualitative analysis of cutting propensity (http://www.crisprflydesign.org/t7-endo-i-assay/). Two positive hits from the T7E1 assays were analyzed using MiSeq analysis[148], which revealed that over 95% of the reads in PCR product were mutated. We only used these two sgRNAs (listed in Table 1), one targeted to the exon and one targeted to the intron, for generating mutant flies.

To generate *fru^attP^* flies, we integrated in a 200 bp single stranded oligonucleotide designed to have the minimal 51 bp attP sequence[152], a diagnostic restriction digest site and ~70 bp arms of homology that flanked the CRISPR target site into the *fru* intron. To generate *fru^-/-^* flies, we integrated in a similar attP-containing oligo into the first exon of the FruM coding sequence, but also used this oligo to replace the ATGATG start site with TTGTTG, as has been previously generated in *D. melanogaster*[18]. The sgRNA, attP-oligo and Cas9 protein were injected into ~200 embryos. G0s were singly crossed to wild type virgin flies. F1s with successful integration of the attP site were identified by PCR genotyping, isolated, and sequenced using methods described above. *fru^attP^* and *fru^-/-^* F1s were backcrossed to wild type flies and then homozygosed. Homozygous stocks were genotyped for three generations to ensure that the population was pure.

We used PhiC31-mediated recombination to integrate attB plasmids containing larger transgenes into the intronic *fru^attP^* locus. We chose not to use eye color visual markers to avoid complications of the white mutation on behavior. To determine if the transgene was homozygous, we screened F1s using the protocol described above for the binary presence of a PCR product using one primer pair that spanned the transgene and one that spanned the genomic locus. To create a stable stock of flies, we crossed homozygous virgin females to *D. simulans* males with a balancer allele on their 3rd chromosome (In(3R)Ubx, Flybase ID FBab0023784, UCSD Stock Center #14021-0251.098). Progeny with the TM2 visible mutation were crossed together and subsequent progeny were genotyped.

Plasmid design and construction

attB-SAS-GFP was made by amplifying eGFP from pUAST-mCD8GFP using primers that attached a splice acceptor site[153] and kozak sequence onto the 5' end of the GFP and an SV40 termination sequence onto the 3' end. A nested-PCR was performed to attach Gibson-assembly adaptors onto the GFP PCR product, which was then combined with PCR-linearized pHD-DsRed-attP using Gibson assembly (NEB). The plasmid was then digested with EcoRI and NotI to insert a 51 bp attB oligo with flanking EcoRI and NotI sites. The double stranded oligo was made by annealing two single-stranded oligos together.

attB-SAS-Gal4 was made by integrating attB-SAS and Gal4 DNA fragments into pHD-DsRed cut with EcoRI and SpeI using Gibson Assembly (NEB). The attB-SAS fragment was amplified from attB-SAS-GFP and the Gal4 fragment was amplified from pBPGUw. The digestion removed 3xP3-DsRed.

We generated an *attP* landing site with an inactivated *EYFP* gene using CRISPR-Cas9 mutagenesis. We co-injected embryos of *D. simulans* strains carrying an *attP* landing site marked with *3XP3::EYFP* with p{CFD4-EYFP-3xP3::DsRed}[145] and *Cas9* mRNA and sib-mated surviving adults. We screened for progeny with reduced or no *EYFP* expression in the eyes. Flies with *EYFP-* were bred to homozygosity and the *3XP3::EYFP* transgene in each strain was re-sequenced to confirm the presence of the mutation and to confirm that the mutation did not disrupt the *attP* landing site. To generated flies expressing GCaMP6s under UAS control, we co-injected p{GP-JFRC7-20XUAS-IVS-GCaMP3 K78H T302L R303P D380Y T381R S383T R392G.15.641}[154] and pBS130 (containing phiC-31 integrase under control of a heat-shock promoter) into the *attP, EYFP-* strain and screened for *w+* integrants. We generated one *D. simulans* UAS-CsChrimson transgenetic line by co-injecting p{20XUAS-IVS-CsChrimson.tdTomato}[155] and pBS130 into the *attP, EYFP-* strain and screening for *w+* integrants. We generated a second *D. simulans* UAS-CsChrimson transgenetic line by co-injecting a piggyBac vector pBac(20xUAS-CsChrimson.mVenus, 3xp3::dsRed)2 and a piggyback transposase helper plasmid into wild type flies and screened for dsRed expression in the eye.

The *D. melanogaster* ppk23-LexA and *D. simulans* ppk23-Gal4 plasmids were cloned by amplifying the homologous 2.695 kb fragment upstream of the *D. melanogaster* and *D. simulans* *ppk23* promoter, analogous to previously published methods[95], and TOPO-cloning the PCR product into the pDONR-Topo vector. Using a BP-clonase Gateway reaction, the sim-*ppk23* promoter was recombined into pBPGUw (addgene #17575) and the mel-*ppk23* promoter was

recombined into pBPnlsLexA-GADUw. PhiC31-mediated recombination was used to integrate mel-ppk23-LexA and sim-*ppk23*-Gal4 into *D. melanogaster* attP40 and sim-ppk23-Gal4 into *D. simulans* attp2034[145], R25E04-Gal4, 3xp3::DsRed in *D. simulans* attP2176[145] and pBPGuW R71G01-Gal4 in *D. simulans* attP2176[145].

Immunohistochemistry

To visualize *D. simulans fru* ^{GFP}, *D. melanogaster fru*^{Gal4}>*UAS-GCaMP*, *D. yakuba fru*^{Gal4}>*UAS-GCaMP D. simulans ppk23*^{Gal4}>*UAS GCaMP* and *R25E04-Gal4*>*UAS-GCaMP*, 1-3 day old adult brains were dissected in Schneider's Medium for 1 hr then immediately transferred to cold 1% PFA (Electron Microscopy Sciences) and fixed for 16-20 hrs at 4 ^{o}C. Samples were then washed in PAT3 Buffer (0.5% BSA/0.5% Triton/1X PBS pH 7.4) 3 times, with last two washes incubated for 1 hr on nutator at room temperature. Brains were blocked in 3% Normal Goat Serum for 90 min at room temperature. Primary antibodies in 3% Normal Goat Serum were incubated 3 hrs at room temperatures then left at 4 °C for 16-20 hrs. Primary antibodies used were 1:20 Mouse nc82 (Developmental Studies Hybridoma Bank), 1:1000 Sheep anti-GFP (Sim *fru*^{GFP}, mel *fru*^{Gal4}>*UAS-GCaMP* and sim *ppk23-Gal4*>*UAS GCaMP*. Bio-Rad #4745-1051) and 1:100 rabbit anti-GABA antibody (*D. simulans fru*^{GFP}, *D. melanogaster fru*^{Gal4}>*UAS-GCaMP* and R*25E04-Gal4*). Catalog #A2052; Sigma, St. Louis, MO). Brains were then washed in PAT3 Buffer. Secondary antibody was incubated 3 hr at room temperature then for 5-7 days at 4 °C. Secondary antibodies used were 1:500 Anti-sheep Alexa Fluor 488, Anti-mouse Alexa Fluor 647 and Anti-mouse Alexa Fluor 555 (ThermoFischer Scientific). Brains were washed in PAT3 buffer three times then once in 1X PBS, nutating at room temperature for 5 min. Samples were mounted in Vectashield (Vector Laboratories) in 5/8th inch hole

reinforcements placed on glass slides. Images were captured on a Zeiss LSM 880 using a 40X objective.

To visualize *sim-ppk23-Gal4>UAS-GFP/mel-ppk23-LexA>LexAOp-Tomato* and *mel-ppk23-Gal4>UAS-GFP*, a similar protocol was used except that the brains were transferred to cold 4% PFA after dissection, fixed for 25 min, washed 3x in PBST for 5 min and then blocked with NGS for 60 min. Primary antibody in 4% Normal Goat Serum was incubated 48 hrs at 4 °C. Primary antibodies used were 1:1000 Chicken anti-GFP (*mel-ppk23-Gal4>UAS-GFP*. Abcam #ab13970), 1:500 Rabbit anti-DsRed (*mel-ppk23-LexA>LexAOp-Tomato*. Clontech #632496 #A2052) and 1:1000 Sheep anti-GFP (*sim-ppk23-Gal4>UAS-GFP*. Bio-Rad #4745-1051). Brains were washed 3 times for 10 min in PBST, rotating. Secondary antibody in 4% Normal Goat Serum was incubated for 48 hours at 4°C. Secondary antibodies used were 1:1000 Anti-sheep Alexa Fluor 488, 1:1000 Anti-rabbit Alexa Fluor 568 and 546, Anti-chicken Alexa Fluor 633 and Anti-mouse Alexa Fluor 546 (ThermoFischer Scientific). Brains were washed 4 times for 15 min in PBST, rotating. Images were captured on a Leica TCS using a 10X or 40X objective.

Two-photon functional imaging

All imaging experiments were performed on an Ultima two-photon laser scanning microscope (Bruker Nanosystems) equipped with galvanometers driving a Chameleon Ultra II Ti:Sapphire laser. Emitted fluorescence was detected with either photomultiplier-tube or GaAsP photodiode (Hamamatsu) detectors. Images for *ex vivo* experiments were acquired with an Olympus 60×, 1 numerical aperture objective and *in vivo* experiments were acquired with an Olympus 40x 0.8 numerical aperture objective (LUMPLFLN). All images were collected at 512 pixel × 512 pixel

resolution with a frame rate from 0.2-0.4 Hz when imaging an ROI and 0.7-0.8 Hz when imaging the whole field of view. Saline (108 mM NaCl, 5 mM KCl, 2 mM $CaCl_2$, 8.2 mM $MgCl_2$, 4 mM $NaHCO_3$, 1 mM NaH_2PO_4, 5 mM trehalose, 10 mM sucrose, 5 mM HEPES pH7.5, osmolarity adjusted to 275 mOsm) was used to bath the brain for all imaging experiments unless otherwise noted.

To prepare flies for *in vivo* imaging of Fru+ and ppk23+ sensory afferents in the ventral nerve cord, the wings and all legs except one foreleg were removed from a 4-7 day old CO_2-anesthetized male. The single-legged male was tethered to a piece of clear packing tape covering a hole in the bottom of the modified 35 mm petri dish using a hair placed across his cervical connectives. The body was oriented such that the ventral side faced the inside of the dish. A rectangular hole the length and width of the male fly's body was cut from the tape and the fly was positioned such that the ventral half of the body was placed above the plane of the tape. Great care was taken to ensure that the foreleg was extended so the tibia and femur did not cover the thorax. Small dots of UV-curable glue were used to secure the eyes, part of the thorax and the tip of the abdomen to the tape. The dish was then filled with saline and the cuticle covering the first thoracic ganglion was gently removed, taking care to not damage the foreleg nerve. The preparation was positioned on the two-photon microscope and an ROI was centered on the most ventral portion of the VNC corresponding to the intact leg. To prepare stimulating females, a pin was attached to the dorsal thorax of virgin female *D. melanogaster* or *D. simulans* fly with their head, wings and legs removed so that the abdomen could make contact with the distal tarsal segments of the male fly's foreleg. To guide stimulation, an 850 nm IR light was used to illuminate the chamber and the fly was imaged from the side using a Point Grey Firefly camera

mounted with a 1x-at-94 mm Infinistix lens fitted with a shortpass IR filter (850 nm OD 4, Edmund Optics) to block 925 nm two-photon laser illumination. After recording a 10 s baseline, the experimenter gently tapped the female abdomen onto the tarsi of the experimental fly once every 10 s for 6-8 bouts. Three replicates per preparation (total 18-24 tapping bouts) were conducted with *D. simulans* and *D. melanogaster* stimuli interweaved.

Images and quantification of ppk23+ soma in the male's foreleg were completed using a Zeiss Axioplan 2 scope under Nomarski optics and widefield fluorescence at 40x or 63x. Images were acquired through a Zeiss AxioCam and the Axiovision software. Somata were counted only in the first three tarsal segments of the foreleg.

We modified published methods from the Scott lab[95,97] for *in vivo* imaging of ppk23+ soma in the foreleg. Male *ppk23-Gal4>UAS-GCaMP* flies were isolated as virgins and aged 3-6 days, CO_2-anesthetized, decapitated, and immobilized by folding a piece of parafilm over the body such that the first five tarsal segments extended out of the parafilm. The immobilized animal was placed on a glass coverslip for imaging using a monochromatic camera (Point Grey Research, Flir Chameleon 3). Pheromone was presented as follows: 1 μL of 7,11-Heptacosadiene or ethanol was pipetted onto a paper wick (Hampton Research) that had been trimmed such that one constituent fiber was exposed at the tip. Using a micromanupulator, the wick was brought into contact with one chemosensory sensillum on the 3rd tarsal segment of the foreleg. GCaMP responses were visualized using a 50x air objective using 488 nm LED illumination on a bright field microscope (Scientifica). DeltaF/F values were calculated using ImageJ as the maximum signal in the 30 s following pheromone presentation in accord with published

methods[95,97]. Without more precise genetic tools in *D. simulans*, we defined soma A as the soma that responded more strongly to 7,11-HD presentation, in accord with previous work[95]. To demonstrate that the response of soma A was specific to the pheromone, we also presented the ethanol vehicle in which ethanol alone was adsorbed to a wick. The range of our maximum DeltaF/F values for 7,11-HD stimulation are consistent with previously published results in *D. melanogaster*[95–97].

To prepare flies for *in vivo* imaging of the central brain using both *fru*[Gal4] and R*25E04-Gal4* neural drivers, CO_2-anesthetized 4-7 day old males were affixed to a plate using UV-curable glue around their head and thorax[156]. Glue was cured in short bursts to minimize exothermic damage to the preparation and flies whose legs touched the glue were discarded. The proboscis was glued to the head, carefully avoiding the antennae, to minimize movement of the brain during imaging. Flies were given an hour to recover and were only used if they displayed vigorous activity post-tether. A small hole in the head was opened under external saline using sharp forceps. Muscle 16, obstructing trachea, and fat were removed. The imaging plate had magnets inside to allow facile positioning under the 40x objective in the two-photon microscope. Using a micromanipulator, a styrofoam ball[157] floating on an air stream was positioned under the fly so that he had a surface to stand and walk on. Only animals that exhibited robust walking or grooming behavior following dissection were used for further experimentation. A *D. melanogaster* or *D. simulans* virgin female tethered to a pin (see above for tethering detail) was positioned in front of the tethered male using a micromanipulator. To stimulate tapping events, the female was moved in front of the male fly who freely tapped on her abdomen with his foreleg tarsi. The male fly was imaged from the side (see above methods) to facilitate positioning the

ball and the stimulus during the experiment. After 4 to 5 s of baseline recording, the stimulus fly was presented to the tethered male for 2-5 s allowing multiple taps before being withdrawn. This was repeated 9 times for each fly stimulus with *D. melanogaster* and *D. simulans* stimuli interweaved. An ROI was centered on the LPC or on the fasciculated projections from P1 neuron cell bodies to the LPC. We vetted our ability to reproducibly identify P1's characteristic processes by first imaging them using R71G01-Gal4>UAS-GCaMP in *D. melanogaster* males. When imaging the fasciculated projections of P1 neurons, our field of view contained both the LPC and the P1 projections so we were capable of aligning responses in the LPC with P1 neurons when the male tapped a female. We attempted to use the R71G01-Gal4 driver for functional imaging of the P1 neurons in *D. simulans,* but we observed no response to the taste of either a *D. melanogaster* or *D. simulans* female. While this is consistent with the lack of pheromone responses we observed when imaging all Fru+ neurons in the LPC or Fru+ P1 neurons, we could not rule out that the last of responses was due to weak expression of GCaMP. Notably, we observed pheromone responses using similarly weak driver lines like R25E04-Gal4 in both *D. melanogaster* and *D. simulans*.

For experiments with picrotoxin, *in vivo* responses were recorded in the LPC before and after iontophoresis of picrotoxin unilaterally into the LPC (1 mM in water, 3-5 pulses, 100 ms at 20 V). Local injection of picrotoxin had no noticeable effect on the male fly's behavior or baseline fluorescence of the LPC, in contrast to bath application of picrotoxin (10 μM and 100 μM), which caused seizures in the fly and a dramatic, fluctuating increase in baseline fluorescence of the LPC (Data not shown). Iontophoresis of saline had no effect on pheromone-evoked responses in either species (data not shown). Picrotoxin iontophoresis was based on previously published

methods[158,159]. We did not attempt picrotoxin iontophoresis with *D. simulans* 71G01-Gal4 because we could not confidently identify the LPC due to weak expression of GCaMP.

For *in vivo* odor stimulation, the fly was tethered and positioned under the microscope onto an air-supported ball as described above. Odor stimulation was achieved by directing a continuous stream (400-500 mL/min) of clean air through a clean glass pasture pipette positioned with a micromanipulator 1 cm from the fly's antenna[102,160]. 50% of the total airstream was diverted through a teflon tube containing a thin strip of filter paper with 2 μL of either 100% ethanol or pure cVA. For each preparation, functional responses were monitored in the DA1 projections in the lateral horn and DC1 lateral horn neurons. Baseline fluorescence was recorded for 4 s before a 1 s odor stimulus was delivered. Trials were repeated three times for each brain region and then ΔF/F responses were averaged.

To prepare flies for *in vivo* imaging of vAB3, 2-5 day old male flies were briefly anesthetized using CO_2 (for <30 s) and then tethered used a previously described preparation[57] in which the male was affixed to a piece of tape covering a hole in the bottom of a modified 35 mm petri dish using human hair placed across the cervical connectives. A small strip of tape was placed over they fly's proboscis and two pieces of putty were placed next to the fly's thorax to prevent the legs from getting stuck onto the tape. A small hole above the head was precisely cut into the tape and the head was secured using two small dots of UV-curable glue that bridged the eyes and the tape. The dish was filled with external saline and the head capsule was opened by carefully tearing off the flap of cuticle covering the dorsal portion of the head and removing any obstructing trachea and fat. The dish was placed under the microscope and vAB3's axonal tract

projecting from the SEZ to the LPC was identified. We vetted our ability to reproducibly identify vAB3's characteristic morphology by first imaging the vAB3 axonal tract using *AbdB-Gal4>UAS-GCaMP* in *D. melanogaster* males. Baseline fluorescence was recorded for 4 s before a female abdomen was presented to the male for him to tap (see above for methods). Trials were repeated three times for each female region and then ΔF/F responses were averaged.

Ex vivo stimulation of vAB3 and DA1 was preformed as previously described[102,137]. A Grass stimulator was used to iontophorese acetylcholine (10 V, 200 ms) through a fine glass electrode positioned on the axons of the ppk23+ sensory neurons in the ventral nerve cord or in the DA1 glomerulus. The stimulating electrode was filled with 10 mM acetylcholine, 10 mM glutamate or external saline and Texas-Red Dextran BSA to facilitate positioning the electrode in the Fru+ neuropil. The local nature of the stimulation combined with the anatomically segregated sensory innervation of DA1 and the ppk23+ sensory neurons in the ventral nerve cord facilitated restricted and reproducible stimulation. To functionally visualize responsive neurons in the brain, we imaged a Z-plane every 5 μm and combined these to build a volume of the anterior ~100 μm of the brain. For quantitative comparisons of specific neural populations across individuals, single Z-planes were recorded using a 40x objective at 2x zoom with an ROI of 300 x 300 pixels. Given that P1 soma and fasiculated processes reside on the posterior side of the brain, when imaging P1 and vAB3 neurons in response to vAB3 stimulation, we rotated the brain 180° around the cervical connectives.

For two-photon severing of mAL, the brain was pinned ventral side up and we focused 925 nm light on a small ROI encompassing only the mAL axon tract at 8X optical zoom. The mAL axon

tract could be readily identified by its characteristic morphology. For two-photon severing of vAB3 or a mock Fru+ neuron, the VNC and brain were pinned ventral side up. We validated that vAB3 axons could be reproducibly identified within the ventral nerve cord by performing initial experiments in *AbdB-Gal>UAS-Tomato/Fru-LexA>LexAOP-GCaMP D. melanogaster* males in which vAB3 neurons are anatomically marked. We found that vAB3 axons were always robustly activated by acetylcholine iontophoresis and have a characteristic position within the ventral cord that allowed for their identification even in the absence of an anatomical marker. We focused 925 nm light on a small ROI encompassing either the vAB3 axon tract or the tract of a Fru+ neuron more lateral than vAB3. We then switched the laser wavelength to 850 nm and imaged using short (<1s) pulses until a cavitation bubble was observed. After switching back to 925 nm and zooming out, if the axon tract was successfully severed, we observed a striking increase in baseline fluorescence due to Ca^{2+} rushing into the neurons and activating GCaMP. Since vAB3 neurons project bilaterally, we also severed the corresponding axon tract on the opposite side of the brain. To image P1 neurons after severing mAL, we re-pinned the brain such that the dorsal side of the brain and the ventral side of the VNC were facing up, inserted the stimulating electrode in the VNC and recorded activity in P1 neurons and vAB3 neurons. vAB3 activation was not affected by mAL severing (data not shown).

Dye-filling of neural tracts using Texas-Red Dextran (100 mg/mL, Invitrogen) was performed as previously described[137]. For dye-filling we targeted the fasciculated bundle of P1 neurons projecting from the somata, the segregated vAB3 terminals in the VNC, the characteristic mAL axonal bundle projecting between the SEZ and LPC and the DA1 glomerulus. To photolabel neurons, we located the neural structure of interest using 925 nm laser illumination, a wavelength

that does not cause significant photoconversion, defined an ROI in PrairieView Software in a single Z-plane, and exposed the target area to 710 nm light (~10-30 mW at the back aperture of the objective) 100-300 times. After diffusion of the photoconverted fluorophores throughout the targeted neurons for 30-60 min, we imaged at 925 nm. All anatomical images are maximum projections of z-stacks with 1μm steps. Autofluorescence from the glial sheath and basal fluorescence from non-dye-filled structures were masked for clarity.

Unless stated, anatomical images were acquired on the 2P microscope using standard techniques.

Imaging and Statistical Analysis

To compare responses across animals, we calculated ΔF/F for each frame of calcium imaging time courses using the second to sixth frames as the baseline. Unless otherwise noted, we used the maximum ΔF/F value within the time during which the stimulus was presented and then averaged individual responses to each stimulus type. For *in vivo* tapping assays, each pair of dots connected by a line represents responses to *D. melanogaster* female (green) and *D. simulans* female (blue) for a given individual. To represent responses graphically, we show heatmaps (ΔF): the maximum projection of two frames of baseline subtracted from the maximum projection of the two frames with peak fluorescence in response to a stimulus (FIJI). The arbitrary units (A.U.) correspond to $1/100^{th}$ of the "minimum displayed value" and "maximum displayed value" when we set the display range in FIJI.

We used the PRISM software package to graph and statistically analyze data. Prior to statistical analysis, we tested if the values were normally distributed using D'Agostion-Pearson ombibus

and Shapiro-Wilk normality tests. When data were normally distributed, we used parametric tests. When data was not normally distributed, we used non-parametric tests.

Statistics

Fig. 1.2   Courtship preferences of *D. melanogaster*, *D. simulans*, *D. sechellia* and *D. mauritiana*   16

Figure	Panel	Male	Comparison	n	Test	P value
1.2	a	Mel	Mel v Sech	21	One-sample t-test	0.5312
			Mel v Erc	19		0.0177
			Mel v Sim	20		0.0002
			Mel v Maur	30		<0.0001
			Sech v Sim	6		n too small
1.2	b	Sech	Sech v Mel	22	One-sample t-test	0.2046
			Sech v Sim	14		<0.0001
			Mel v Sim	10		0.0223
1.2	c	Sim	Sim v Yak	20	One-sample t-test	0.1941
			Sim v Mel	17		<0.0001
			Sim v Sech	19		<0.0001
			Sim v Erc	17		<0.0001
1.2	d	Maur	Maur v Sim	27	One-sample t-test	0.1596
			Maur v Mel	30		0.0024

Fig. 2.4   Courtship preferences of *D. simulans ppk23* and *Gr32a* mutant males   27

Figure	Panel	Male	Comparison	n	Test	P value
2.4	a	WT	Sim v Mel	19	One-sample t-test	<0.0001
		Gr32a	Sim v Mel	20		<0.0001
		ppk23	Sim v Mel	20		0.9931
2.4	b	WT	Sim 7,11-HD vs EtOH	19	One-sample t-test	<0.0001
		ppk23	Sim 7,11-HD vs EtOH	19		0.534

Fig. 2.8   Conserved pheromonal tuning of ppk23+ Fruitless+ foreleg sensory neurons   34

Figure	Panel	Species	Genotype	n	Test	P value
2.8	b	Mel	WT	12	Wilcoxin matched-	0.0002

160

		ppk23	6	pairs test	>0.9999
c	Sim	WT	14	Wilcoxin matched-	0.005
		ppk23	6	pairs test	0.6875

CRISPR and genotyping primers:

Sim Gr32a CRISPR

CrSim_Gr32a-F: gaaattaatacgactcactataGGCGAGATTCTTCGCGGATAgttttagagctagaaatagc

Genotype sim Gr32a mutant

SimSeq_Gr32a-F: CCCGAACACTTGGGTAATTG

SimSeq_Gr32a-R: CGATCCACTGGTTCACATTG

Sim ppk23 CRISPR

CrSim_ppk23-F: gaaattaatacgactcactataGGTCTGGAACTTCTCCCAGgttttagagctagaaatagc

Genotype sim ppk23 mutant

SimSeq_ppk23-F: CGCAGCCTCATCTACCAGAC

SimSeq_ppk23-R: TTGCATCCAATCTATAAGATACAATAA

Fru Intron CRISPR

CrSim_FruIntron-F:

gaaattaatacgactcactataGGTCCGCGGAAAAGGGCGTAgttttagagctagaaatagc

Fru Intron attP oligo

161

GCTTTGGGCGTTTGATTCTCGACGCTTAGCGCTCGGAATTCAGTGCTCAGTTCAGTA

GGTGACACCATTGCGCTACGCCCCCAACTGAGAGAACTCAAAGGTTACCCCAGTTG

GGGCACTACGCGGCCGCCGTAGGTGTTTTGGTCGGCCCACGACGTCTGGCCTATATT

GCCACATATGGCAGTATATGCAACTCCTCCCG

Genotype sim Fru-attP Intron

Sim_FruIntron-ExF: GCTTTGGGCGTTTGATTCT

Sim_FruIntron-ExR: GCACAACCCACATAAATCTCAA

Genotype sim Fru-GFP

Sim_FruGFP-InR: TTGGGACAACTCCAGTGAAA

Genotype Fru-GAL4

Sim_FruGAL4-InR: TCGGTTTTTCTTTGGAGCAC

Fru Exon CRISPR

CrSim_FruExon-F:

gaaattaatacgactcactataGGTCCGCGGAAAAGGGCGTAgttttagagctagaaatagc

Fru Exon attP oligo

GCTTTCAGCCAGAGCCAAATTGTTGGCGACGTCACAGGATTATTTTGGCAATCCATA

CGCCCTTTTCCGCGGCTACGCCCCCAACTGAGAGAACTCAAAGGTTACCCCAGTTGG

162

GGCACTACgaattcACCGCCCACAACACTGCGGCCACGCGAGTCGCCGCTGGGCGTGGG
CCACCCTCACGGCCATGGGCACCTGCA

Genotype sim Fru-attP Exon

Sim_FruExon-F: GAGGCAATCGGTGGCTATAA

Sim_FruExon-R: GGAGGCTTACCTAGGGGATG

attB-SAS-GFP Plasmid:

Forward primer for eGFP with SAS+Kozak sequences and reverse primer for eGFP with SV40

termination sequence

SAS-Kozak-GFP-F:

cggccgcggacatatgcaCACCTGCgatcgtagtgccccaactggggtaacctttgaAAAAGCAGGCTTCAGTCG

ATCCAACATGGCGACTTGTCCCATCCCCGGCATGTTTAAATATACTAATTATTCTTGA

ACTAATTTTAATCAACCGATTTATCTCTCTTCCGCAGCAAAATGAGTAAAGGAGAAG

AACTTTTCAC

GFP-SV40-R:

tacgcccccaacGGGGACCACTTTGTACAAGAAAGCTGGGTGATCCAGACATGATAAGAT

ACATTGATGAGTTTGGACAAACCACAACTAGAATGCAGTGAAAAAAATGCTTTATTT

GTGAAATTTGTGATGCTATTGCTTTATTTGTAACCATTATAAGCTGCAATAAACAAG

TTCAGTTCCATAGGTTGGAATCTAAA

Nested PCR primers to add on gibson overhangs to GFP PCR product

Gib-GFP-pHDattP-F:

acacctgcgatcgtagtgccccaactggggtaacctttgaAAAAGCAGGCTTCAGTCGAT

Gib-GFP-pHDattP-R:

tatagcatacattatacgaagttatctacgcccccaacGGGGACCACTTTGTACAAGAAA

Linearize pHD-DsRed-attP plasmid

Gib-Linear-pHDattP-F: gttgggggcgtagataacttc

Gib-Linear-pHDattP-R: tcaaaggttaccccagttgg

oligo for inserting attB

EcoRI-attB:

AATTcGGAGTACGCGCCCGGGGAGCCCAAGGGCACGCCCTGGCACCCGCACCGCGG

gc

attB-NotI:

ggccgcCCGCGGTGCGGGTGCCAGGGCGTGCCCTTGGGCTCCCCGGGCGCGTACTCCg

Sequencing primers for attB-SAS-GFP insertion

DsRed-GFP-Seq-LeftF: CATGCCGAACTCAGAAGTGA

DsRed-GFP-Seq-LeftR: TTGGGACAACTCCAGTGAAA

pHD-GFP-Seq-RightF: TCCAACCTATGGAACTGAACTTG

pHD-GFP-Seq-RightR: CGACGTGTTCACTTTGCTTG

attB-SAS-Gal4 Plasmid:

164

Forward and reverse primer for Gal4 with Gibson assembly overhang

Gibson-Gal4-F

ATTTATCTCTCTTCCGCAGCAAAGAAAGATGAAGCTACTGTCTTCTATCG

Gibson-Gal4-R

GATCCACTAGTTCTAGAGCGGCGCATAGGCCACTAGTtaaagatc

Forward primer for attB-SAS with Gibson assembly overhang

Gibson-attBSAS-F:

TGGGGTGTCGCCCTTCGCTGAAGCAGGTGgAGCAGGTGgAATTcGGAGTA

Gibson-attBSAS-R:

GCATGCTTGTTCGATAGAAGACAGTAGCTTCATCTTTCTTTGCTGCGGAAGAGAGAT

8 | References

1.   Shubin, N., Tabin, C. & Carroll, S. B. Fossil, genes and the evolution of animal limbs. *Nature* **388,** 639–648 (1997).

2.   Wagner, G. The developmental genetics of homology. *Nat. Rev. Genet.* **8,** 191–206 (2007).

3.   Carroll, S. B. Evo-Devo and an Expanding Evolutionary Synthesis: A Genetic Theory of Morphological Evolution. *Cell* **134,** 25–36 (2008).

4.   King, M. & Wilson, A. C. Humans and chimpanzes. *Science (80-.).* **188,** 107–116 (1975).

5.   Stern, D. L. Perspective: Evolutionary Developmental Biology and the Problem of Variation. *Evolution (N. Y).* **54,** 1079–1091 (2000).

6.   Hoekstra, H. E. & Coyne, J. A. The locus of evolution: Evo devo and the genetics of adaptation. *Evolution (N. Y).* **61,** 995–1016 (2007).

7.   Wray, G. A. The evolutionary significance of cis-regulatory mutations. *Nat Rev Genet* **8,** 206–216 (2007).

8.   Graham, A., Papalopulu, N. & Krumlauf, R. The murine and Drosophila homeobox gene complexes have common features of organization and expression. *Cell* **57,** 367–378 (1989).

9.   Gellon, G. & William McGinnis. Shaping animal body plans in development and evolution by modulation of Hox expression patterns. *BioEssays* **20,** 116–125 (1998).

10.   Pichaud, F. & Desplan, C. Pax genes and eye organogenesis. *Curr. Opin. Genet. Dev.* **12,** 430–434 (2002).

11.   Toth, A. L. & Robinson, G. E. Evo-devo and the evolution of social behavior. *Trends Genet.* **23,** 334–341 (2007).

12.   Rittschof, C. C. & Robinson, G. E. *Behavioral Genetic Toolkits: Toward the Evolutionary Origins of Complex Phenotypes*. *Current Topics in Developmental Biology* **119,** (Elsevier Inc., 2016).

13.   Ben-Shahar, Y., Robichon, A., Sokolowski, M. B. & Robinson, G. E. Influence of Gene Action Across Different Time Scales on Behavior.pdf. *Science (80-.).* **296,** 741–744 (2002).

14.   Lai, C. S. L., Fisher, S. E., Hurst, J. A., Vargha-Khadem, F. & Monaco, A. P. A forkhead-domain gene is mutated in a severe speech and language disorder. *Nature* **413,** 519–523 (2001).

15.   Haesler, S. FoxP2 Expression in Avian Vocal Learners and Non-Learners. *J. Neurosci.* **24,** 3164–3175 (2004).

16.   Teramitsu, I. Parallel FoxP1 and FoxP2 Expression in Songbird and Human Brain Predicts Functional Interaction. *J. Neurosci.* **24,** 3152–3163 (2004).

17.   Stockinger, P., Kvitsiani, D., Rotkopf, S., Tirián, L. & Dickson, B. J. Neural circuitry that governs Drosophila male courtship behavior. *Cell* **121,** 795–807 (2005).

18.   Manoli, D. S. *et al.* Male-specific fruitless specifies the neural substrates of Drosophila courtship behaviour. *Nature* **436,** 395–400 (2005).

19.   Clynen, E., Ciudad, L., Bellés, X. & Piulachs, M. D. Conservation of fruitless' role as master regulator of male courtship behaviour from cockroaches to flies. *Dev. Genes Evol.* **221,** 43–48 (2011).

20.   Usui-Aoki, K., Mikawa, Y. & Yamamoto, D. Species-specific patterns of sexual dimorphism in the expression of Fruitless protein, a neural musculinizing factor in Drosophila. *J. Neurogenet.* **19,** 109–121 (2005).

21.   Cande, J., Stern, D. L., Morita, T., Prud'homme, B. & Gompel, N. Looking under the lamp post: neither fruitless nor doublesex has evolved to generate divergent male courtship in Drosophila. *Cell Rep.* **8,** 363–370 (2014).

22.   Katz, P. S. & Lillvis, J. L. Reconciling the deep homology of neuromodulation with the evolution of behavior. *Curr. Opin. Neurobiol.* **29,** 39–47 (2014).

23.   Beets, I., Temmerman, L., Janssen, T. & Schoofs, L. Ancient neuromodulation by vasopressin/oxytocin-related peptides. *Worm* **2,** e24246 (2013).

24.   Beninger, R. The role of dopamine in locomotor activity and learning. *Brain Res.* **287,** 1983 (1983).

25.   Garrison, J. L. *et al.* Oxytocin/Vasopressin-Related Peptides Have an Ancient Role in Reproductive Behavior. *Science (80-.).* **338,** 540–543 (2012).

26.   Shapiro, M. D. *et al.* Genetic and developmental basis of evolutionary pelvic reduction in threespine sticklebacks. *Nature* **428,** 717–723 (2004).

27.   Chan, Y. F. *et al.* Adaptive evolution of pelvic reduction of a *Pitx1* enhancer. *Science (80-.).* **327,** 302–305 (2010).

28.   Wittkopp, P. J., True, J. R. & Carroll, S. B. Reciprocal functions of the Drosophila yellow and ebony proteins in the development and evolution of pigment patterns. *Development* **129,** 1849–1858 (2002).

29.   Gompel, N., Prud'homme, B., Wittkopp, P. J., Kassner, V. A. & Carroll, S. B. Chance caught on the wing: cis-regulatory evolution and the origin of pigment patterns in

Drosophila. *Nature* **433,** 481–487 (2005).

30. Arnoult, L. *et al.* a Gene Regulatory Module. **8016,** 2011–2014 (2013).

31. Sucena, E. & Stern, D. L. Divergence of larval morphology between Drosophila sechellia and its sibling species caused by cis-regulatory evolution of ovo/shaven-baby. *Proc. Natl. Acad. Sci. USA* **97,** 4530–4534 (2000).

32. Cande, J., Prud'homme, B. & Gompel, N. Smells like evolution: The role of chemoreceptor evolution in behavioral change. *Curr. Opin. Neurobiol.* **23,** 152–158 (2013).

33. Bear, D. M., Lassance, J.-M., Hoekstra, H. E. & Datta, S. R. The evolving neural and genetic architecture of vertebrate olfaction. *Curr. Biol.* **26,** R1039–R1049 (2016).

34. Ramdya, P. & Benton, R. Evolving olfactory systems on the fly. *Trends Genet.* **26,** 307–316 (2010).

35. de Bruyne, M., Smart, R., Zammit, E. & Warr, C. G. Functional and molecular evolution of olfactory neurons and receptors for aliphatic esters across the Drosophila genus. *J. Comp. Physiol. A Neuroethol. Sensory, Neural, Behav. Physiol.* **196,** 97–109 (2010).

36. Tierney, A. J. Evolutionary implications of neural circuit structure and function. *Behav. Processes* **35,** 173–182 (1995).

37. Lerat, E. & Moran, N. A. The Evolutionary History of Quorum-Sensing Systems in Bacteria. *Mol. Biol. Evol.* **21,** 903–913 (2004).

38. Ng, W.-L. & Bassler, B. L. Bacterial Quorum-Sensing Network Architectures. *Annu. Rev. Genet.* **43,** 197–222 (2009).

39. Leary, G. P. *et al.* Single mutation to a sex pheromone receptor provides adaptive speci fi city between closely related moth species. *Proc. Natl. Acad. Sci.* **109,** 14081–14086 (2012).

40. Prieto-Godino, L. L. *et al.* Evolution of Acid-Sensing Olfactory Circuits in Drosophilids. *Neuron* **93,** 661–676.e6 (2017).

41. McBride, C. S. *et al.* Evolution of mosquito preference for humans linked to an odorant receptor. *Nature* **515,** 222–227 (2014).

42. McGrath, P. T. *et al.* Parallel evolution of domesticated Caenorhabditis species targets pheromone receptor genes. *Nature* **477,** 321–325 (2011).

43. Li, R. *et al.* The sequence and de novo assembly of the giant panda genome. *Nature* **463,** 311–317 (2010).

44. Jiang, P. *et al.* Major taste loss in carnivorous mammals. *Proc. Natl. Acad. Sci.* **109,** 4956–

4961 (2012).

45. Katz, P. S. & Harris-Warrick, R. M. The evolution of neuronal circuits underlying species-specific behavior. *Curr. Opin. Neurobiol.* **9,** 628–633 (1999).

46. Bendesky, A. & Bargmann, C. I. Genetic contributions to behavioural diversity at the gene–environment interface. *Nat. Rev. Genet.* **12,** 809–820 (2011).

47. Katz, P. S. Neural mechanisms underlying the evolvability of behaviour. *Philos. Trans. R. Soc. B Biol. Sci.* **366,** 2086–2099 (2011).

48. Young, L. J., Nilsen, R., Waymire, K. G., Macgregor, G. R. & Insel, T. R. Increased affliative response to vasopressin in mice expressing the V 1a receptor from a monogamous vole. *Nature* **400,** 1998–2000 (1999).

49. Bendesky, A. *et al.* The genetic basis of parental care evolution in monogamous mice. *Nature* **544,** 434–439 (2017).

50. Macosko, E. Z. *et al.* A hub-and-spoke circuit drives pheromone attraction and social behaviour in C. elegans. *Nature* **458,** 1171–5 (2009).

51. Flint, J., Valdar, W., Shifman, S. & Mott, R. Strategies for mapping and cloning quantitative trait genes in rodents. *Nat. Rev. Genet.* **6,** 271–286 (2005).

52. Flint, J. Analysis of quantitative trait loci that influence animal behavior. *J. Neurobiol.* **54,** 46–77 (2003).

53. Churchill, G. A. *et al.* The Collaborative Cross, a community resource for the genetic analysis of complex traits. *Nat. Genet.* **36,** 1133–1137 (2004).

54. Pasaniuc, B. & Price, A. L. Dissecting the genetics of complex traits using summary association statistics. *Nat. Rev. Genet.* **18,** 117–127 (2017).

55. McBride, C. S. & Arguello, J. R. Five Drosophila genomes reveal nonneutral evolution and the signature of host specialization in the chemoreceptor superfamily. *Genetics* **177,** 1395–1416 (2007).

56. McBride, C. S. Rapid evolution of smell and taste receptor genes during host specialization in Drosophila sechellia. *Proc. Natl. Acad. Sci. U. S. A.* **104,** 4996–5001 (2007).

57. Newcomb, J. M., Sakurai, a., Lillvis, J. L., Gunaratne, C. a. & Katz, P. S. Homology and homoplasy of swimming behaviors and neural circuits in the Nudipleura (Mollusca, Gastropoda, Opisthobranchia). *Proc. Natl. Acad. Sci.* **109,** 10669–10676 (2012).

58. Chiang, J.-T. A., Steciuk, M., Shtonda, B. & Avery, L. Evolution of pharyngeal behaviors and neuronal functions in free-living soil nematodes. *J. Exp. Biol.* **209,** 1859–1873 (2006).

59. Sun, X. J., Tolbert, L. P. & Hildebrand, J. G. Ramification pattern and ultrastructural characteristics of the serotonin-immunoreactive neuron in the antennal lobe of the moth Manduca sexta: a laser scanning confocal and electron microscopic study. *J. Comp. Neurol.* **338,** 5–16 (1993).

60. Bumbarger, D. J., Riebesell, M., Rödelsperger, C. & Sommer, R. J. System-wide rewiring underlies behavioral differences in predatory and bacterial-feeding nematodes. *Cell* **152,** 109–119 (2013).

61. Baltzley, M. J., Gaudry, Q. & Kristan, W. B. Species-specific behavioral patterns correlate with differences in synaptic connections between homologous mechanosensory neurons. *J. Comp. Physiol. A Neuroethol. Sensory, Neural, Behav. Physiol.* **196,** 181–197 (2010).

62. Sakurai, A., Newcomb, J. M., Lillvis, J. L. & Katz, P. S. Different roles for homologous interneurons in species exhibiting similar rhythmic behaviors. *Curr. Biol.* **21,** 1036–1043 (2011).

63. Coyne, J. A. & Orr, H. A. Patterns of speciation in Drosophila. *Evolution (N. Y).* **43,** 362–381 (1988).

64. Lachaise, D. *et al.* Historical biogeography of the D. melanogaster species subgroup. *Evol. Biol.* 159–226 (1988).

65. Pool, J. E. & Aquadro, C. F. History and structure of sub-saharan populations of Drosophila melanogaster. *Genetics* **174,** 915–929 (2006).

66. Kopp, A. & True, J. R. Evolution of male sexual characters in the oriental Drosophila melanogaster species group. *Evol. Dev.* **4,** 278–91 (2002).

67. Spieth, H. T. Courtship Behavior in Drosophila. *Annu. Rev. Entomol.* 385–405 (1974).

68. Ewing, A. W. & Bennet-Clark, H. C. The Courtship Songs of Drosophila. *Behaviour* **31,** 288–301 (1968).

69. Gleason, J. M. & Ritchie, M. G. Do Quantitative Trait Loci (QTL) for a Courtship Song Difference between Drosophila simulans and D. sechellia Coincide with Candidate Genes and Intraspecific QTL? *Genetics* **166,** 1303–1311 (2004).

70. Demetriades, M. C., Thackeray, J. R. & Kyriacou, C. P. Courtship song rhythms in Drosophila yakuba. *Anim. Behav.* **57,** 3790386 (1999).

71. Ding, Y. *et al.* Neural Changes Underlying Rapid Fly Song Evolution. *bioRxiv* (2017).

72. Ding, Y., Berrocal, A., Morita, T., Longden, K. D. & Stern, D. L. Natural courtship song variation caused by an intronic retroelement in an ion channel gene. *Nature* **536,** 329–332 (2016).

73. Jallon, J.-M. & David, J. R. Variation in cuticular hydrocarbons among the eight species

of the Drosophila melanogaster subgroup. *Evolution (N. Y).* **41,** 294–302 (1987).

74.   Shirangi, T. R., Dufour, H. D., Williams, T. M. & Carroll, S. B. Rapid evolution of sex pheromone-producing enzyme expression in Drosophila. *PLoS Biol.* **7,** 1–14 (2009).

75.   Legendre, A., Miao, X. X., Da Lage, J. L. & Wicker-Thomas, C. Evolution of a desaturase involved in female pheromonal cuticular hydrocarbon biosynthesis and courtship behavior in Drosophila. *Insect Biochem. Mol. Biol.* **38,** 244–255 (2008).

76.   Jallon, J.-M. A few chemical words exchanged by Drosophila. *Behav. Genet.* **14,** 441–478 (1985).

77.   Billeter, J.-C., Atallah, J., Krupp, J. J., Millar, J. G. & Levine, J. D. Specialized cells tag sexual and species identity in Drosophila melanogaster. *Nature* **461,** 987–991 (2009).

78.   Marcillac, F., Houot, B. & Ferveur, J. F. Revisited roles of Drosophila female pheromones. *Chem. Senses* **30 SUPPL.,** 273–274 (2005).

79.   Coyne, J. A., Crittenden, A. P., Mah, K. & Maht, K. Genetics of a pheromonal difference contributing to reproductive isolation in Drosophila. *Science (80-.).* **265,** 1461–1464 (1994).

80.   Grillet, M., Dartevelle, L. & Ferveur, J.-F. A Drosophila male pheromone affects female sexual receptivity. *Proc. R. Soc. B Biol. Sci.* **273,** 315–323 (2006).

81.   Markow, T. A. The secret lives of Drosophila flies. *Elife* **4,** 1–9 (2015).

82.   Vosshall, L. B., Amrein, H., Morozov, P. S., Rzhetsky, A. & Axel, R. A spatial map of olfactory receptor expression in the Drosophila antenna. *Cell* **96,** 725–736 (1999).

83.   Zhou, X. *et al.* Chemoreceptor evolution in hymenoptera and its implications for the evolution of eusociality. *Genome Biol. Evol.* **7,** 2407–16 (2015).

84.   Mackinnon, R., Cohen, S. L., Kuo, A., Lee, A. & Chait, B. T. Structural Conservation in Prokaryotic and Eukaryotic Potassium Channels. *Science (80-.).* **280,** 106–110 (1998).

85.   Vosshall, L. B., Wong, A. M. & Axel, R. An olfactory sensory map in the fly brain. *Cell* **102,** 147^160 (2000).

86.   Ressler, K. J., Sullivan, S. L. & Buck, L. B. A zonal organization of odorant receptor gene expression in the olfactory epithelium. *Cell* **73,** 597–609 (1993).

87.   Ressler, K. J., Sullivan, S. L. & Buck, L. B. Information coding in the olfactory system: evidence for a stereotyped and highly organized epitope map in the olfactory bulb. *Cell* 1245–1255 (1994).

88.   Andersson, M. N., Löfstedt, C., Newcomb, R. D. & Hill, S. R. Insect olfaction and the evolution of receptor tuning. *Front. Ecol. Evol.* **3,** 1–14 (2015).

89.   Groot, A. T., Dekker, T. & Heckel, D. G. The genetic basis of pheromone evolution in moths. *Annu. Rev. Entomol.* **61,** 99–117 (2016).

90.   Bastock, M. & Manning, A. The courtship of Drosophila melanogaster. *Behaviour* **8,** 85–111 (1955).

91.   Spieth, H. T. & Hsu, T. C. The influence of light on the mating behavior of seven species of the Drosophila melanogaster species group. *Evolution (N. Y).* **4,** 316–325 (1950).

92.   Agrawal, S., Safarik, S. & Dickinson, M. The relative roles of vision and chemosensation in mate recognition of Drosophila melanogaster. *J. Exp. Biol.* **217,** 2796–805 (2014).

93.   Lu, B., LaMora, A., Sun, Y., Welsh, M. J. & Ben-Shahar, Y. Ppk23-dependent chemosensory functions contribute to courtship behavior in Drosophila melanogaster. *PLoS Genet.* **8,** 1–13 (2012).

94.   Toda, H., Zhao, X. & Dickson, B. J. The Drosophila female aphrodisiac pheromone activates ppk23+ sensory neurons to elicit male courtship behavior. *Cell Rep.* **1,** 599–607 (2012).

95.   Thistle, R., Cameron, P., Ghorayshi, A., Dennison, L. & Scott, K. Contact chemoreceptors mediate male-male repulsion and male-female attraction during Drosophila courtship. *Cell* **149,** 1140–1151 (2012).

96.   Vijayan, V., Thistle, R., Liu, T., Starostina, E. & Pikielny, C. W. Drosophila pheromone-sensing neurons expressing the ppk25 ion channel subunit stimulate male courtship and female receptivity. *PLoS Genet.* **10,** 1–11 (2014).

97.   Kallman, B. R., Kim, H. & Scott, K. Excitation and inhibition onto central courtship neurons biases Drosophila mate choice. *Elife* **4,** 1–18 (2015).

98.   Miyamoto, T. & Amrein, H. Suppression of male courtship by a Drosophila pheromone receptor. *Nat. Neurosci.* **11,** 874–876 (2008).

99.   Fan, P. *et al.* Genetic and neural mechanisms that inhibit Drosophila from mating with other species. *Cell* **154,** 89–102 (2013).

100.   Demir, E. & Dickson, B. J. fruitless splicing specifies male courtship behavior in Drosophila. *Cell* **121,** 785–794 (2005).

101.   Lee, G. *et al.* Spatial, temporal, and sexually dimorphic expression patterns of the fruitless gene in the Drosophila central nervous system. *J. Neurobiol.* **43,** 404–426 (2000).

102.   Clowney, E. J., Iguchi, S., Bussell, J. J., Scheer, E. & Ruta, V. Multimodal chemosensory circuits controlling male courtship in Drosophila. *Neuron* **87,** 1036–1049 (2015).

103.   Tanaka, R., Higuchi, T., Kohatsu, S., Sato, K. & Yamamoto, D. Optogenetic activation of the fruitless -labeled circuitry in Drosophila subobscura males induces mating motor acts.

J. Neurosci. **37,** 11662–11674 (2017).

104. Pan, Y., Robinett, C. C. & Baker, B. S. Turning males on: Activation of male courtship behavior in Drosophila melanogaster. *PLoS One* **6,** (2011).

105. Bellocchio, E. E., Reimer, R. J., Fremeau, J. & Edwards, R. H. Uptake of glutamate into synaptic vesicles by an inorganic phosphate transporter. *Science (80-.).* **289,** 957–960 (2000).

106. Takamori, S., Rhec, J. S., Rosenmund, C. & Jahn, R. Identification of a vesicular glutamate transporter that defines a glutamatergic phenotype in neurons. *Nature* **407,** 189–194 (2000).

107. Lin, H., Mann, K. J., Starostina, E., Kinser, R. D. & Pikielny, C. W. A Drosophila DEG/ENaC channel subunit is required for male response to female pheromones. *Proc. Natl. Acad. Sci. U. S. A.* **102,** 12831–12836 (2005).

108. Philipsborn, A. C. Von *et al.* Article Cellular and Behavioral Functions of fruitless Isoforms in Drosophila Courtship. 242–251 (2014). doi:10.1016/j.cub.2013.12.015

109. von Philipsborn, A. C. *et al.* Neuronal control of Drosophila courtship song. *Neuron* **69,** 509–522 (2011).

110. Pan, Y., Meissner, G. W. & Baker, B. S. Joint control of Drosophila male courtship behavior by motion cues and activation of male-specific P1 neurons. *Proc. Natl. Acad. Sci.* **109,** 10065–10070 (2012).

111. Inagaki, H. K. *et al.* Optogenetic control of Drosophila using a red-shifted channelrhodopsin reveals experience-dependent influences on courtship. *Nat. Methods* **11,** 325–32 (2014).

112. Kohatsu, S., Koganezawa, M. & Yamamoto, D. Female contact activates male-specific interneurons that trigger stereotypic courtship behavior in Drosophila. *Neuron* **69,** 498–508 (2011).

113. Kohatsu, S. & Yamamoto, D. Visually induced initiation of Drosophila innate courtship-like following pursuit is mediated by central excitatory state. *Nat. Commun.* **6,** 6457 (2015).

114. Coen, P. *et al.* Dynamic sensory cues shape song structure in Drosophila. *Nature* **507,** 233–237 (2014).

115. Billeter, J.-C., Atallah, J., Krupp, J. J., Millar, J. G. & Levine, J. D. Specialized cells tag sexual and species identity in Drosophila melanogaster. *Nature* **461,** 987–991 (2009).

116. Koganezawa, M., Kimura, K. ichi & Yamamoto, D. The Neural Circuitry that Functions as a Switch for Courtship versus Aggression in Drosophila Males. *Curr. Biol.* **26,** 1395–1403 (2016).

117.	Zhang, S. X., Rogulja, D. & Crickmore, M. A. Dopaminergic circuitry underlying mating drive. *Neuron* **91,** 168–181 (2016).

118.	Yang, H. H. *et al.* Subcellular imaging of voltage and calcium signals reveals neural processing in vivo. *Cell* **166,** 245–257 (2016).

119.	Prud'homme, B. *et al.* Repeated morphological evolution through cis-regulatory changes in a pleiotropic gene. *Nature* **440,** 1050–1053 (2006).

120.	Stern, D. L. The genetic causes of convergent evolution. *Nat. Rev. Genet.* **14,** 751–764 (2013).

121.	Doi, M. Behavioral response of males to major sex pheromone component, (Z,Z)-5,25-hentriacontadiene, of Drosophila ananassae females. *J. Chem. Ecol.* **23,** 2067–2078 (1997).

122.	Martin, A. & Orgogozo, V. The loci of repeated evolution: A catalog of genetic hotspots of phenotypic variation. *Evolution (N. Y).* **67,** 1235–1250 (2013).

123.	Chung, H. & Carroll, S. B. Wax, sex and the origin of species: Dual roles of insect cuticular hydrocarbons in adaptation and mating. *BioEssays* **37,** 822–830 (2015).

124.	Ejima, A. *et al.* Generalization of Courtship Learning in Drosophila Is Mediated by cis-Vaccenyl Acetate. *Curr. Biol.* **17,** 599–605 (2007).

125.	MANE, S. D., TOMPKINS, L. & RICHMOND, R. C. Male Esterase 6 Catalyzes the Synthesis of a Sex Pheromone in Drosophila melanogaster Females. *Science (80-.).* **222,** 419–421 (1983).

126.	Laturney, M. & Billeter, J. C. Drosophila melanogaster females restore their attractiveness after mating by removing male anti-aphrodisiac pheromones. *Nat. Commun.* **7,** 1–11 (2016).

127.	Zawistowski, S. & Richmond, R. C. Inhibition of courtship and mating of Drosophila melanogaster by the male-produced lipid, cis-vaccenyl acetate. *J. Insect Physiol.* **32,** 189–192 (1986).

128.	Kurtovic, A., Widmer, A. & Dickson, B. J. A single class of olfactory neurons mediates behavioural responses to a Drosophila sex pheromone. *Nature* **446,** 542–546 (2007).

129.	Wolfner, M. F. The gifts that keep on giving: Physiological functions and evolutionary dynamics of male seminal proteins in Drosophila. *Heredity (Edinb).* **88,** 85–93 (2002).

130.	Koganezawa, M., Haba, D., Matsuo, T. & Yamamoto, D. The Shaping of Male Courtship Posture by Lateralized Gustatory Inputs to Male-Specific Interneurons. *Curr. Biol.* **20,** 1–8 (2010).

131.	Ahmed, O. M. *et al.* Evolution of mechanisms that control mating in Drosophila males.

bioRxiv 1–40 (2017).

132. Bartelt, R. J., Schaner, A. M. & Jackson, L. L. cis-Vaccenyl acetate as an aggregation pheromone inDrosophila melanogaster. *J. Chem. Ecol.* **11,** 1747–1756 (1985).

133. Symonds, M. R. E. & Wertheim, B. The mode of evolution of aggregation pheromones in Drosophila species. *J. Evol. Biol.* **18,** 1253–1263 (2005).

134. Clyne, P., Grant, A., O'Connell, R. & Carlson, J. R. Odorant response of individual sensilla on the Drosophila antenna. *Invertebr. Neurosci.* **3,** 127–135 (1997).

135. Shanbhag, S. ., Müller, B. & Steinbrecht, R. . Atlas of olfactory organs of Drosophila melanogaster. *Arthropod Struct. Dev.* **29,** 211–229 (2000).

136. Datta, S. R. *et al.* The Drosophila pheromone cVA activates a sexually dimorphic neural circuit. *Nature* **452,** 473–477 (2008).

137. Ruta, V. *et al.* A dimorphic pheromone circuit in Drosophila from sensory input to descending output. *Nature* **468,** 686–690 (2010).

138. Kohl, J., Ostrovsky, A. D., Frechter, S. & Jefferis, G. S. X. E. A bidirectional circuit switch reroutes pheromone signals in male and female brains. *Cell* **155,** 1610–1623 (2013).

139. Wang, L. *et al.* Hierarchical chemosensory regulation of male-male social interactions in Drosophila. *Nat. Neurosci.* **14,** 757–762 (2011).

140. Dukas, R. Male fruit flies learn to avoid interspecific courtship. *Behav. Ecol.* **15,** 695–698 (2004).

141. Zhang, J., Walker, W. B. & Wang, G. *Pheromone reception in moths: from molecules to behaviors. Progress in Molecular Biology and Translational Science* **130,** (Elsevier Inc., 2015).

142. Chung, H. *et al.* A single gene affects both ecologial divergence and mate choice in Drosophila. *Science (80-.).* **343,** 1148–1151 (2014).

143. Kirschner, M. & Gerhart, J. Evolvability. *Proc. Natl. Acad. Sci.* **95,** 8420–8427 (1998).

144. West-Eberhard, M. J. Developmental plasticity and the origin of species differences. *Proc. Natl. Acad. Sci.* **102,** 6543–6549 (2005).

145. Stern, D. L. *et al.* Genetic and Transgenic Reagents for Drosophila simulans. *G3 Genes| Genomes| Genet.* **7,** 1339–1347 (2017).

146. Mellert, D. J., Knapp, J.-M., Manoli, D. S., Meissner, G. W. & Baker, B. S. Midline crossing by gustatory receptor neuron axons is regulated by fruitless, doublesex and the Roundabout receptors. *Development* **137,** 323–332 (2010).

147. Yu, C., Zhang, Y., Yao, S. & Wei, Y. A PCR based protocol for detecting indel mutations induced by TALENs and CRISPR/Cas9 in zebrafish. *PLoS One* **9,** (2014).

148. Kistler, K. E., Vosshall, L. B. & Matthews, B. J. Genome engineering with CRISPR-Cas9 in the mosquito aedes aegypti. *Cell Rep.* **11,** 51–60 (2015).

149. Gratz, S. J. *et al.* Highly specific and efficient CRISPR/Cas9-catalyzed homology-directed repair in Drosophila. *Genetics* **196,** 961–971 (2014).

150. Bassett, A. R., Tibbit, C., Ponting, C. P. & Liu, J. L. Highly Efficient Targeted Mutagenesis of Drosophila with the CRISPR/Cas9 System. *Cell Rep.* **4,** 220–228 (2013).

151. Quinones, G. A., Jin, J. & Oro, A. E. I-BAR protein antagonism of endocytosis mediates directional sensing during guided cell migration. *J. Cell Biol.* **189,** 353–367 (2010).

152. Thorpe, H. M., Wilson, S. E. & Smith, M. C. M. Control of directionality in the site-specific recombination system of the streptomyces phage phiC31. *Mol. Microbiol.* **38,** 232–241 (2000).

153. Venken, K. J. T. & Bellen, H. J. Transgenesis upgrades for Drosophila melanogaster. *Development* **134,** 3571–84 (2007).

154. Chen, T.-W. *et al.* Ultrasensitive fluorescent proteins for imaging neuronal activity. *Nature* **499,** 295–300 (2013).

155. Klapoetke, N. C. *et al.* Independent optical excitation of distinct neural populations. *Nat. Methods* **11,** 338–46 (2014).

156. Maimon, G., Straw, A. D. & Dickinson, M. H. Active flight increases the gain of visual motion processing in Drosophila. *Nat. Neurosci.* **13,** 393–399 (2010).

157. Seelig, J. D. *et al.* Two-photon calcium imaging from head-fixed Drosophila during optomotor walking behavior. *Nat. Methods* **7,** 535–540 (2010).

158. Hill, R. G., Simmonds, M. A. & Straughan, D. W. Antagonism of GABA by picrotoxin in the feline cerebral cortex. *Br. J. Pharmacol.* **44,** 807–809 (1972).

159. Crossman, A. R., Walker, R. J. & Woodruff, G. N. Picrotoxin antagonism of y aminobutyric acid inhibitory responses and synaptic inhibition in the rat substantia nigra. *Br. J. Pharmacol.* **49,** 696–698 (1973).

160. Cohn, R., Morantte, I. & Ruta, V. Coordinated and compartmentalized neuromodulation shapes sensory processing in Drosophila. *Cell* **163,** 1742–1755 (2015).